ADDIS ABABA UNIVERSITY
SCHOOL OF GRADUATE STUDIES
Institute of Technology
School of Mechanical and Industrial Engineering
Thermal Engineering Stream

DESIGN OF FLUIDIZED BED BAGASSE GASIFIER

(A case study for Fincha Sugar Factory)

A Thesis submitted to the School of Graduate Studies of Addis Ababa University in partial fulfilment of the requirements for the Degree of Master of Science in Mechanical Engineering

By:

ABDULEHAK ALEMU ASFAW

Advisor: Dr. Tesfaye Dama

Co-Advisor: Ato Desta Lema (MSc)

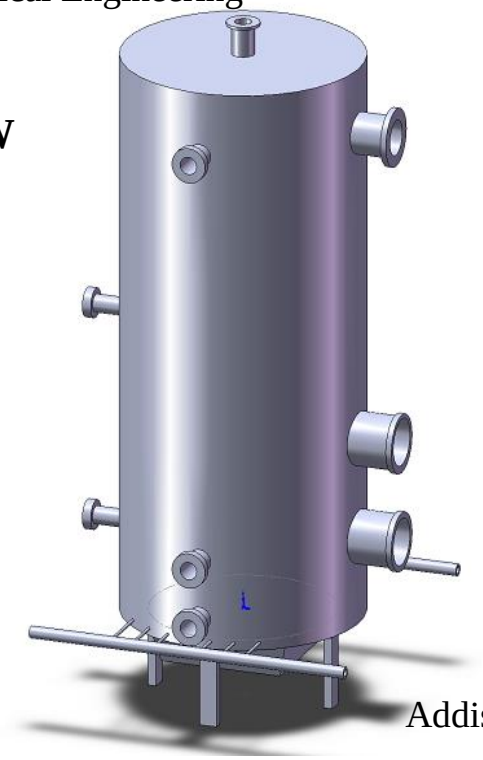

April 2013

Addis Ababa

DESIGN OF FLUIDIZED BED BAGASSE GASIFIER

By

ABDULEHAK ALEMU ASFAW

Approved by Board of Examiners

Dr. Ing. Demiss Alemu	_____	_____
Chairman,		
Department Graduate Committee	Signature	Date
Dr. Tesfaye Dama	_____	_____
Advisor	Signature	Date
Dr.Ing Abebayehu Assefa	_____	_____
Internal Examiner	Signature	Date
Dr. Ing. Demiss Alemu	_____	_____
External Examiner	Signature	Date
Dr. Daneil Tilahun	----------	----------
Head of The school	Signature	Date

DECLARATION

I, the undersigned, declare that this thesis is my original work and has not been presented for a degree in any University, and that all the source of materials used for the thesis has been duly acknowledged.

Declared by:
Name: Abdulehak Alemu Asfaw

Signature: _____

Date: _____

Confirmed by:
Name: Tesfaye Dama (Dr.)

Signature: _____

Date: _____

Abstract

With increasing demand of energy and global issue of sustainable energy resource of the world, energy from Biomass is attracting the attention of many researchers as a source of energy in the world.

Currently in Ethiopia about nine new sugar factories are being installed requiring adequate amount of electrification and energy. The demand of these industries can be met from different sources of energy. Gasification can be considered one of these sources.

In this work an attempt has been made to develop a procedure for designing a fluidized bed reactor that can handle $60{,}900\,\frac{kg}{day}$ bagasse as a feedstock. By using an appropriate design procedure a complete design of a gasification reactor was studied deeply. The design procedure followed in this thesis is presented in Appendix III.

The design work has been categorized into three different parts. The first one deals with the equilibrium modelling of the fluidized bed to determine the output gas composition. The equilibrium model is analyzed with the help of a matlab code giving the volumetric/ molar composition of the product gas. The higher heating value (HHV) found is 2.69 MJ/kg with the moisture content of 15%. A thermal efficiency of 50.78% was obtained which would have reached about 80% if the sensible heat of the product gas was put under consideration. The second part of this design work aims at determining the appropriate fluidization parameter of the reactor since efficient fluidization is required for effective reaction and maximum output efficiency. Parameters like the minimum fluidization velocity, the terminal fall velocity, the operational velocities and the bed and freeboard geometries have been determined. The third part of this design work investigates the dimension of the reactor, its insulation and the openings of the shell and other components of the reactor. The reactor has a 4.2 m outside diameter by 11.3 m height.

Finally an economic analysis was done on the cost of the gasifier which compares natural gas use as an energy source. The configurations of the reactor and the distributor of the reactor are also the core focus of the design work.

Key words: Biomass, gasification, producer gas, Thermal efficiency, fluidization, higher heating value.

ACKNOWLEDGEMENTS

Firstly I thank the almighty ALLAH for the strength and the calm He gave me through the difficult times during my study.

I would like to express my deepest gratitude to **Dr. Tesfaye Dama**, for his invaluable comments and excellent supervision. I would also like to thank my co-advisors Desta Lemma (MSc) and Abera Mellese (MSc) for their cordial relations showed to me, which was very helpful and very much cherished. I would also like to extend my thanks to the entire members of the Mechanical Engineering Department for their support for the success of this thesis.

I would also like to thank working Staffs of the Fincha sugar Industry for providing the necessary data in the time of need. My gratitude also goes to Dr. Venkata Ramayya (Jimma University) for his contribution in giving ideas of the thesis and his excellent supervision.

Finally, I would like to thank close friends and family of mine for their priceless contribution with moral and material support throughout my academic career.

Acronyms

BFBG Bubbling Fluidized Bed Gasifier

Btu British thermal unit(s)

CO Carbon monoxide

CO_2 Carbon dioxide

CFBG Circulating Fluidised Bed Gasifier

HHV Higher heating Value

LHV Lower heating Value

HC Hydrocarbons

kWh kilowatt hour

MWh Megawatt hour

MJ Mega Joules (10^6 Joules)

R&D Research and development

GCV Gross calorific value

Contents

List of Tables

page

List of Figures

Page

1. INTRODUCTION

The world today is in a rapid development and change demanding an adequate energy supply besides fuels like coal and petroleum. Hence, Biomass is being used widely as an energy source. In developing countries like Ethiopia where most of the population live in rural communities, Biomass is a major source of energy for cooking and lighting purposes but its industrial use is limited [1]. Recently, Biomass besides being used in solid form is being converted into gaseous form through gasification process. Gasification is the process of converting Biomass in to gaseous fuels. The chemistry behind the process is to thermally convert the biomass into combustible gas, where produced gas might be of low, medium or high calorific value depending on the process used in gasification [2].

Table 1.1: World commercial Energy consumption 1950-2009
(Millions of barrels a day of oil equivalent) [3]

					Average annual growth [%]		
Year	1980	1985	1990	2009	1975-80	1980-1990	2009
World	137.8	166.0	201.5	82,769,370.4	2.5	3.9	10
Developing countries	16.7	22.3	30.6	5,834,745	3.7	6.2	42
Oil importing dev. Countries	12.4	16.8	22.8	2,456,876	3.6	6.3	28

Energy consumption in developing countries accounts for a small part of the world total, but has been growing much faster than in the developed countries. During the 1960s commercial energy consumption in these countries is projected to grow at 6.2 % a year [2]. It is obviously a matter of great urgency that all countries take effective measures to reduce their energy consumption, but no country can afford to wait for a unified global effort. It is crucial both to continue to expand efforts to use energy efficiently and to increase domestic production. Under this realistic scenario energy containing wastes can be considered as a low grade fuel.

In Ethiopia currently it has been observed that many new sugar industries are being implanted requiring adequate amount of electrification and energy. The energy demand of these industries can be partially met through gasification of biomass residue for the production of premium. We know that the sugar industries have a considerable amount of residue biomass in the form of a bagasse which can be used as an input for gasification process producing a syn (producer gas) which can be used for running engines, boilers and turbines.

A proper design of an efficient bagasse gasifier is in prime position for producing the required producer gas which later can be used for any process of energy generation. The proper design of this gasifier should meet criteria's like selecting the right type of gasifier from the lists. Setting important parameters that are used in the construction of the gasifier that maximizes its efficiency is also another important aspect of the design work.

The process of gasification to produce combustible from organic feeds was used in blast furnaces over 180 years ago. The possibility of using this gas for heating and power generation was soon realized and there emerged in Europe producer gas systems, which used charcoal and peat as feed material. At the turn of the century petroleum gained wider use as a fuel, but during both world wars and particularly World War II, shortage in petroleum supplies led to widespread re-introduction of gasification. By 1945 the gas was being used to power trucks, buses and agricultural and industrial machines. It is estimated that there were close to 900,000 Vehicles running on producer gas all over the world [2].

After World War II the lack of strategic impetus and the availability of cheap fossil fuels led to general decline in the producer gas industry. However Sweden continued to work on producer gas technology and the work was accelerated after 1956 Suez Canal crisis. A decision was then made to include gasifiers in Swedish strategic emergency plans. Research into suitable designs of wood gasifiers, essentially for transport use, was carried out at the National Swedish Institute for Agricultural Machinery Testing and is still in progress. The contemporary interest in small scale gasifier R&D, for most part dates from 1973 oil crisis. The manufacturing also took off with increased interest shown in gasification technology. At present there are about 64 gasification equipment manufacturers all over the world [2].

The production of generator gas (producer gas) called gasification, is partial combustion of solid fuel (biomass) and takes place at temperatures of about 1000^0C. The reactor is called a gasifier.

The combustion products from complete combustion of biomass generally contain nitrogen, water vapour, carbon dioxide and surplus of oxygen. However in gasification where there is a surplus of solid fuel (incomplete combustion) the products of combustion are (Figure 1.1) combustible gases like Carbon monoxide (CO), Hydrogen (H_2) and traces of Methane and non useful products like tar and dust. The production of these gases is by reaction of water vapour and carbon dioxide through a glowing layer of charcoal. Thus the key to gasifier design is to create conditions such that a) biomass is reduced to charcoal and, b) charcoal is converted at suitable temperature to produce CO and H_2.

Currently, most of the electrical or thermal energy consumed in the world is generated through the use of non-renewable energy sources that, in the future, their price will increase strongly due to their potential shortage in the market. On the other hand, there are renewable energetic sources that can in the long term be used permanently without any exhaustion threat. This is the case of the vegetal-type biomass, which is currently being considered a promising energy source. The world's existing preoccupation about the contamination of the atmosphere with harmful gases for the stability of the planet's weather is combined with the necessity to valorise agricultural wastes like cane bagasse, among others. In Fincha sugar industry about 1450 tonnes of bagasse per day is being produced; where part of it is being used for boiler propose [4].

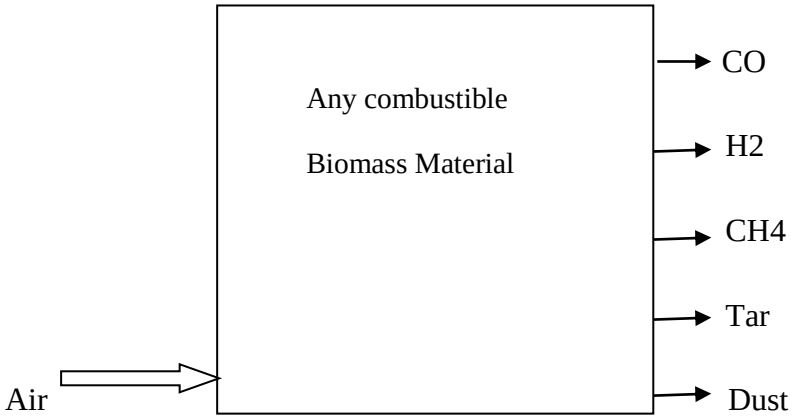

Figure 1.1 products of gasification

In recent years, there has been a lot of work in bagasse combustion technologies; however, the controlled production of energetic gas obtained through gasification processes has attracted a greater interest. In this process, the biomass is thermally decomposed in an atmosphere with oxygen deficiency. The fuel gas obtained can be used in many applications such as feeding furnaces or boilers and fuelling internal combustion engines for electrical power generation [5].

1.1 Properties of Biomass relevant to gasification

1.1.1 Chemical composition

Cellulose comprises approximately 50 % of all biomass while lignin comprises about 25 %. The third major cell wall component is hemicelluloses which is closely associated with the skeletal polysaccharide cellulose, comprising approximately the remaining 25 % of the cell wall material. The different chemical compositions are responsible for varying heat contents among different biomass fuels [5].

A more traditional approach to combustible fuels evaluation employs the ultimate analysis of the material. Table 1.2 presents the ultimate analysis of numerous biomass and coal fuels on a dry weight basis.

Table 1.2**:** Ultimate analysis of selected fuels [6]

ULTIMATE ANALYSIS							
FUEL	C	H	0	N	S	ASH	HHV MJ/kg
Utah coal	77.9	6.0	9.9	1.5	0.6	4.1	31.6
Pittsburgh coal (a)	75.5	5.0	4.9	1.2	3.1	10.3	31.6
Pittsburgh coal (b)	73.3	5.3	10.2	0.7	2.8	7.6	30.3
Wyoming coal	70.0	4.3	20.2	0.7	1.0	13.8	33.4
Bagasse	47.3	6.1	35.3	0.0	0.0	11.3	21.2
Rice husks	38.5	5.7	39.8	0.5	0.0	15.5	15.3
Rice straw	39.2	5.1	35.8	0.6	0.1	14.2	15.1
Municipal solid waste	33.9	4.6	22.4	0.7	0.4	38.0	13.1
Sewage sludge	14.2	2.1	10.5	1.1	0.7	71.4	4.7

These data demonstrate generally that bagasse is much oxygenated fuel with about two-thirds the energy content of coal. The ultimate analysis shown in Table 1.2 strongly indicates a relationship between carbon content and higher heating value. These data also suggest that bagasse is the transition fuel between the waste materials (4.7 - 13.1 MJ/kg) and coal (31.6 - 33.4 MJ/kg).

1.1.2 Moisture content

Bagasse has the disadvantage of the presence of moisture in significant quantities compared to coal. Fresh bagasse may contain upward of 15 to 50 wt % moisture and at times may contain as much as 55 wt% moisture on as received basis. The moisture successfully denotes the many variations in bagasse fuel because the moisture content significantly influences the net heating value of bagasse fuels, the ignition properties and the overall efficiency of fuel utilization. The moisture content found in the bagasse from Fincha sugar factory is as high as 50% which indicates a lower heating value than indicted in table 1.2. Major preheating process is required to decrease the moisture content to the desired value.

The influence of moisture on higher heating value can be calculated by the following conceptual formula:

$$NHV = HHV - (Lw + LHV) \quad \ldots\ldots 1.1$$

Where NHV is the net heating value, HHV the higher heating value, Lw the heat loss for weight of combustible products as water replaces bagasse and LHV the loss due to heat of vaporization required to remove the water. The above conceptual formula leads to a more precise formula which is:

$$HHV^{*} = HHV - (0.0114\,(HHV) \times M) \quad \ldots\ldots 1.2$$

Where M is the moisture content expressed as a percent of total as received fuel material [6].

1.1.3 Potential pollutants analysis

Traditionally, sulphur and ash are considered the principal impurities in combustible fuels. The sulphur on combustion forms sulphur dioxide which is a pollutant. It also can combine with rain to form dilute sulphurous acid. The ash results in the release of particulates up the smokestack. These pollutants can be controlled by devices such as gas scrubbers, cyclones and baghouse installation. All such installations, however, reduce the energy efficiency of a given operation.

The ultimate analysis presented in Table 1.2 shows bagasse to be very low in sulphur and ash. These values demonstrate that bagasse is essentially pollution free in relation to the other fuels, although bagasse thermochemical processing plants require some particulate control. From the point of view of controlling formation of sulphur dioxide and prohibiting the release of particulate matter, bagasse is a more desirable fuel than any of the other fuels of Table 1.6.

In an era of environmental consciousness, this advantage is a compelling attraction for the biomass energy source.

1.2 NATURE OF GASIFICATION

Gasification of biomass is a combination of several individual processes which take place in series and or in parallel in a gasifier. Five different stages can be broadly distinguished in the gasification of biomass [2].

1. Drying of the biomass: moisture is evaporated.
2. Pyrolysis or thermal degradation: volatile components are distilled off to produce char, condensable (tar) and non condensable gases.
3. Gasification of the char: reactions of steam and carbon dioxide with the char that yield hydrogen and carbon monoxide
4. Combustion of the remaining char to produce carbon dioxide and water and to supply the energy required for sustaining a certain operating temperature.
5. Gas phase pyrolysis/gasification of tars.

However, there is usually no clear distinction between the various stages especially with reactors which under normal operating conditions exhibit high local heating rates (above 100° C/s, see section 3.3.3).

1.3 DEFINITIONS

In the literature on waste disposal the terms" pyrolysis" and "gasification" are regularly used. Their significance is however often blurred and not well understood. This is also the case for the term "biomass" which is used among others for wood and municipal solid waste. The following definitions will apply for this thesis:

Biomass is the wide range of products which have been derived from the process of photosynthesis. These include standing forests and crops; products, wastes and residues from forestry and agricultural processes; aquatic plants and weeds; as well as the lignocellulosic fraction of urban waste. Thus everything which has been derived from the process of photosynthesis is a potential source of energy.

Pyrolysis is the thermal degradation of organic matter in the absence of an oxidizing reactant (Anaerobic atmosphere). In pyrolysis the volatiles are driven-due to thermal effects - out of the substrate, resulting in char condensable liquids or tars and gaseous products.

Gasification or partial oxidation is the combination of thermal decomposition of organic matter followed by reactions of the char, tar and primary gases with oxidizing reactants, yielding mainly low molecular weight gaseous products (aerobic atmosphere).

In this thesis the term Pyrolysis will refer to strict thermal decomposition processes in anaerobic conditions and will be considered as a precursor to gasification; while gasification is the entire process of thermochemically converting biomass into a predominantly gaseous fuel with an oxidant.

1.4 Background and description of the study Area

Fincha Sugar Factory, founded in 1991 G.C., is one of the largest state owned sugar factories in Ethiopia. The Fincha Valley is located in Wollega Province in west-central Ethiopia, at N9°47.25 E 37°25, some 350 km north west of Addis Ababa. The factory has a capacity of 5000tones of cane per day (TCD) and an annual production capacity of 8 million litters of Ethanol. The factory is currently undertaking the expansion project to increase its crushing capacity to 12,000TCD [4].

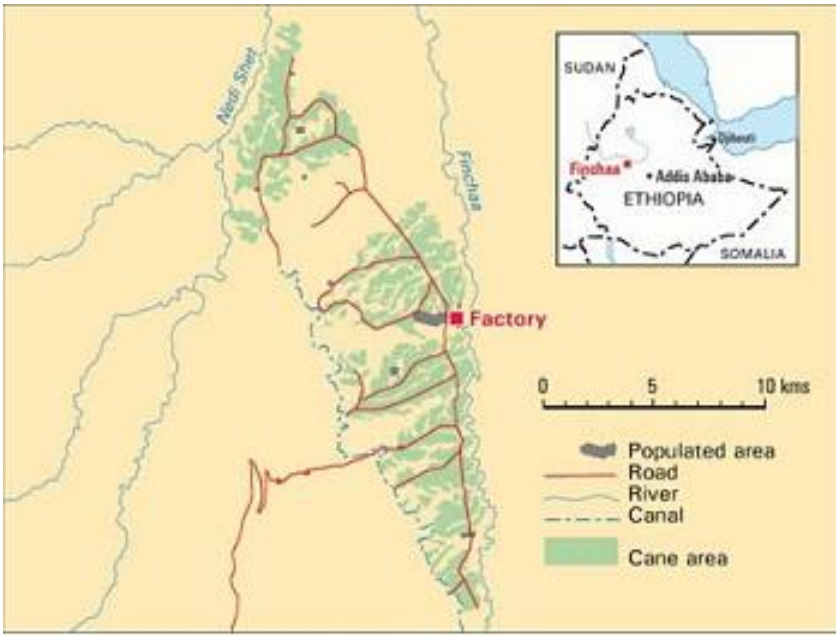

Figure 1.2:- The Geographic Location of Fincha Valley

Fincha sugar industry is one of Ethiopia's famous and a major sugar contributor to the market. This sugar industry has a bulk amount of bagasse output which is readily available to be converted to a producer gas. One third of daily bagasse production is simply being deposited as a waste where the rest two third is being used by the boilers in the industry for producing steam which is another mechanism of energy production. So by gasification of

one third bagasse available per day in to a useful gas one can maximize the industry's energy input whenever necessary.

With respect to global issues of sustainable energy and reduction in greenhouse gases, biomass energy as one of the key sources of renewable energy is getting increased attention as a potential source of energy in the future.

The paper has focused on designing a fluidized bed bagasse gasifier which meets the requirement in combusting the surplus bagasse left from the boiler in to a useful syngas. The fluidized bed gasifier type is chosen because it is been observed that for a higher amount of biomass feed and energy needs this type of gasifier is best for its efficiency [28].

1.5 Statement of the problem

Fincha sugar industry has the following data available in order to have a basic need analysis for designing a gasifier for production of a producer gas.

Table 1.3 Fincha sugar industry operation data [4].

Cane Crushed	5000 TCD /208 TCH
Fiber % cane	14%
Pol % bagasse	2.35
Moisture % bag	48.5
HGCV (kCal/kg)	2340.8
LGCV (KCal/kg)	1869.6
Bagasse percent on cane	29%

Having bagasse percentage of 29%, the core objective of this study is to estimate the amount of calorification value that can be obtained by designing an efficient bagasse gasifier using the surplus bagasse from the boiler. A research done in Mauritius shows that for an estimate of 300,000 tons bagasse surplus about 291 Gwh electricity (0.97 kWh/kg of bagasse) can be produced. The intention here is at least to approach this figure within good margin.

The basic design criteria arise from the available bagasse amount to be gasified. As indicated in the earlier table in the Fincha sugar industry there are 2 boilers of high pressure (31 bars absolute) each working at a temperature of 400^{o}C. Each boiler consumes 29 tonnes

of bagasse per hour. Under 22 average working hours of the factory the total consumption of bagasse on daily basis would be 638tonnes of bagasse per day.

The data from the factory (table 1.3) states that the amount of sugar cane available per day is 5000 tons of cane per day having 29% of bagasse content. With simple analysis we can estimate the quantity of bagasse produced which is 29% of the total cane usage which is around 1450 tons of bagasse per day and this would be the capacity of the factory's bagasse production. From the total available bagasse about 638 tones of bagasse have been consumed by one boiler; and 1276 tones of bagasse by the two boilers. The remaining about 174 tone of bagasse per day will be the design parameter we have at hand. Generally the project is focused in designing a reactor gasifier that can handle this amount of bagasse on daily basis for gasification.

1.6 Objectives

1.6.1 General objectives

Directly heated circulating fluidized bed (CFB) and bubbling (BFB) [Figure.1.3] gasification of biomass has not been demonstrated to the same extent as the fixed bed gasifier types. Very few demonstrations have been carried out at elevated pressures, and all results reported are for temperatures less than 1000^{o}C. Because of their tendency to produce large quantities of tar or unconverted char, fixed bed bagasse gasifier have not been prime candidates for this paper. The majority of past biomass gasifier designs have been for the generation of process heat, steam and electricity.

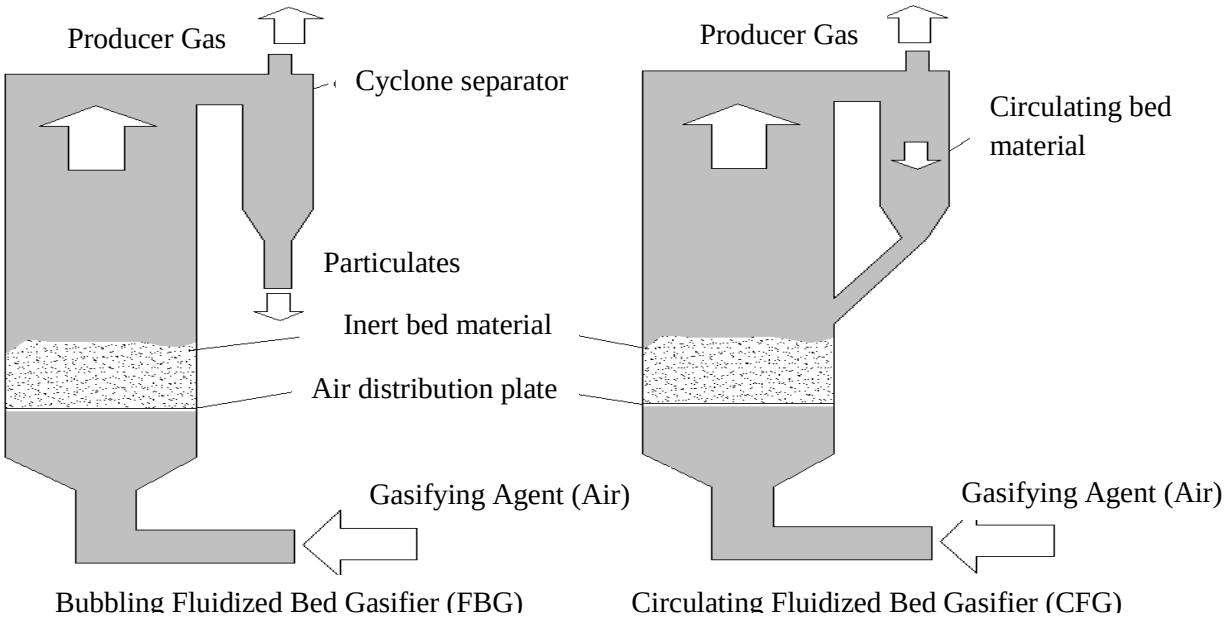

Figure 1.3 Fluidized bed gasifier

1.6.2 Specific objectives

The specific objective of this study is to develop a new method of producing an energy source for Fincha sugar industry in the form of producer gas from gasified bagasse. By designing a highly efficient gasifier i.e. (Fluidized bed gasifier) the design work will be done to address the required parameters which the gasifier should be operating with. It also includes the biomass feed requirements like:-

- The moisture content of the bagasse
- The air and fuel ratios to be used
- The geometry of the gasifier.
- The fluidization velocities with the available particle size of the biomass and the bed particles etc.

1.7 Significance and application of the study

The cane sugar industry has long recognised the enormous potential in the use of bagasse for the production of energy. Many sugar factories are presently producing considerable amounts of electricity for export to the utility grid while at the same time meeting on-site energy needs by installing modern condensing-extraction steam turbines for cogeneration. However, biomass gasification technology applied to bagasse gasification in conjunction with gas fired turbines, which could become commercially available in the near future, offer higher thermodynamic efficiencies.

Designing of bagasse gasifier for Fincha Sugar Industry has great benefits towards its potential energy supply for different equipments and processes in the system. By effectively designing a gasifier which takes every amount of surplus bagasse and later integrating it to a gas turbine cycles the industry will have another even clean energy resource. This paper will also provide adequate information and basic ideas for future researchers to do experimental and manufacturing jobs on gasifiers by any sugar industry in Ethiopia.

As far as fluidized bed gasifiers are concerned many designs have been made on a pilot or micro level. But most of them use rice husks or wood as a feed biomass; the intention here is to use bagasse as an input biomass and design the gasifier as well as establish the best working parameters of the gasifier specifically for Fincha sugar industry. This also can be tested later with experiments so that this design work will be used as a bench mark by other interested researchers.

2. LITRATURE REVIEW

2.1 Energy situation in Ethiopia

Excluding human and animal energy, the sources of energy supply in Ethiopia can be classified into traditional and modern energy. Traditional sources include wood fuel, agricultural residue, and charcoal and cattle dung collectively known as biomass. It accounts to about 95.8% of the total energy supply of the country. Modern energy consists of electricity and petroleum products, and accounts to the remaining 4.2% of the national energy supply sources. From the total modern energy supply, on average, petroleum constitutes 86% and the remaining 14% is derived from electricity, of which 96.7% is from hydro and 3.3% from diesel generators. From the national energy consumption the share of the household sector, is more than 88%, service is 3%, industrial is 5%, transport is 3% and agriculture is 1%. Out of this share, rural households account for about 92% of the total household consumption [7].

Sugar industries are one of the providers of biomass in the form of bagasse. With rapid expansion of sugar industries in the country there would be a surplus of bagasse ready to be converted into energy to the factories themselves or as the public's energy source.

2.2 APPLICATIONS OF FLUIDIZED BED GASIFIERS

The interest in using fluidized bed systems for thermochemical processing of solid feedstocks has steadily increased over the last decade due to their attractive features. A comprehensive review and assessment of the large variety of ideas, proposals and plants is beyond the scope of this thesis, since the intention here is to develop a method of gasifier reactor design which uses bagasse as the feedstock. Hence, a review of fluidized bed reactors that are previously designed and their efficiencies will be discussed in this section no matter what the feed stock material is.

It is necessary to obtain a clear understanding of the process, the problems encountered by other research groups and to identify the limitations of fluidized bed gasifiers, in order to interpret the results obtained from the process development unit, and develop empirical correlations and conceptual design for fluidized bed gasifiers. Only Air gasification will be reviewed since this work is only entitled to air gasification (for example oxygen gasification, use of catalysts, pyrolysis and dual bed systems) are not going to be reviewed.

2.2.1 Early work with fluidized bed systems (pre 1970)

Early work on the thermochemical processing of biomass in fluidized bed reactors was aimed at producing useful chemicals such as aldehydes, phenols and waxes. Little information was given concerning the reaction conditions, gas composition and higher heating value of the product gas.

The first work found in the field of biomass gasification in fluidized bed systems, aiming at producing a fuel product, was carried Out by Vroom [8]. He studied the pyrolysis and gasification of bark and examined the possible use of the product gas as fuel in internal combustion engines. He also concluded that burning the charcoal produced by the pyrolysis in pulverized coal boilers might produce as much steam as that obtained from the combustion of wet Bark in industrial ovens. Several efforts [8] were also made to identify the components of tar and gas produced by the gasification of paper and leaves. Several analytical techniques were employed including wet chemical methods, gas chromatography, infrared and mass spectroscopy. However, the most important contribution of this work was the identification of defluidization in case of biomass beds with no inert material and the improvement in fluidization by the addition of an inert bed such as silica sand.

2.2.2 Gasification with no inert bed

The unique features of fluidized bed reactors are mainly due to the bed material and its efficient fluidization (see section 3.2). The bed may either be an inert material such as sand, or it can be a reactant (such as char) or a catalyst (such as alkali metals). Since the fluidization properties of a reactor are strongly influenced by the physical and/or chemical properties of the bed [8], the selection of a suitable material is of considerable importance, otherwise defluidization or elutriation of the bed may occur.

When biomass is gasified, the char residue can form a bed material of its own. Hence char fluidization can reduce the complexity of the gasification process by eliminating the inert bed. This idea was "borrowed" by the research community of coal gasification in fluidized bed systems, where beds of ash and char are often used. However, one condition for formation of a fluidized bed is a certain degree of homogeneity of the bed. Biomass char fluidization is very difficult due to the relatively low bulk weight and the variation in its specific gravity. Thus, most of the processes under development use a system with an inert bed, usually silica sand. It is, however, possible to fluidize a bed of coal ash/char which has specific gravity about 2 to 3 times higher than biomass char/ash beds. The available literature on fluidized bed gasification of biomass with a char bed is summarized in Table 2.1.

Table 2.1: Gasification of biomass in fluidized bed with char as bed material [8]

Institutes/ Author(s)	Internal bed diameter(m)	Feed stock	Oxidizing medium	Temperature Range in ^oC	HHV MJ/m^3
Texas Tech. university	0.05	Manure	Air+ steam	680-800	2.6-5*
	0.15	Manure	Air+ steam	517-670	10.1-15.8*
	0.15	Oak saw dust	Air+ steam	600-800	11.2*
	0.15	Various Agri. Wastes +biomass	Air+ steam	600-800	9.0-14.1*
Saskatchevan Power Corp	1.2	spruce, poplar chips	Air	400-1000	3.4-5.7
Technical research centre of Finland	0.15	peat	Air+ steam	650-900	3.0-6.6
Livet. al	0.60	Hemlock saw dust	Air+ steam	550-1100	5.8*

*) indicates units in MJ/Nm^3

It is of interest to note that of the research projects shown on Table 2.1; all but two were abandoned when it became evident that it was not possible to fluidize efficiently the bed of char. In all publications, severe temperature gradients were reported between the distributor and surface of the bed (from 50 to 200 °C), a proof that the bed of char was not well fluidized. Some authors concluded that since loss of fluidization occurred, the reactors were effectively operated as an updraft gasifier. They also noted that excessive amounts of tars were produced, which supported their conclusions. Another complication of char beds is the necessary continuous mechanical removal of part of the bed in order to maintain a constant bed height. This can be achieved by means of screws or overflows; which is an added complexity to the design of a system and also increases the capital cost.

It can be concluded that under normal operating conditions, it is not possible to fluidize efficiently a bed consisting of biomass char only. This problem can be overcome by using complicated mechanical char removal systems. However, for a gasification process - which main objective is to produce fuel gas - this loss of char would represent a significant reduction of the overall efficiency. Because this work aimed at studying the gasification process of biomass in a fluidized bed reactor, and since from the literature review it was deduced that good and stable fluidization of the bed is a prerequisite for achieving the advantageous properties (Isothermal bed, high mass and heat transfer rate coefficients) of this type of reactor (see section 3.2), it was decided to use an inert bed (silica sand) in the process development unit see chapter 5.

2.2.3 Research work on Air gasification

Most processes under development use air as the fluidizing and oxidizing medium. Steam is sometimes added either to control the temperature of the reactor or to increase the fluidization velocity at low air flow rates. In this section those processes which use an inert bed (mostly silica sand) are discussed. Most of the references that have been found use air as a fluidizing agent. So it is apparent that this is the most widely used configuration.

2.2.3.1 Early research activities

With the purpose of contributing to the energetic valuation of the solid wastes generated by the Colombian Agricultural Industry, a practical methodology for the design of a fluidized bed gasifier for rice husk on pilot scale was developed. The gasifier equipment, made up of a reaction chamber of 0.3 m of internal diameter and 3 m of overall height, was designed from theoretical and experimental information available in the literature and from the past experiences of the research group. It was intended to produce an energetic gas with approximately 70 kW of useful energetic power. Experimental tests performed with a gasifier fabricated according to the designs showed that the developed procedure was adequate, with a maximum deviation close to 50% for the operational performance variables [5]. Therefore, the basic model developed in this work shows that it is helpful for preliminary prediction of the equivalence ratio, low heating value, volumetric yield, gas power and cold efficiency obtained in experimental atmospheric bubbling fluidized bed biomass gasification tests.

As referred by [9] from (Nieminen and Kivela, 1998) Commercial scale fluidized bed biomass gasifiers have been built in Finland by Foster Wheeler. The Lahti power plant built in Finland is an integration of a biomass gasifier to a coal boiler. It has been in operation since March 1998 and has maintained stable operation for the main boiler, gas burner and also the gasifier itself. The maximum power capacity is 167MWe and 240MWh for district heat production. The heating value of gas produced is very low especially when the moisture content of biomass is high. When the moisture content was 50% the heating value was only 2.2MJ/kg. The energy that the plant has produced up to the year 2002 is 1700GWh. The average operating temperatures were between 800°C-1000°C. In this system the gas is used back to preheat the fluidization air to 270°C. The design issues faced by the plant include the fuel feeding method into the gasifier and also the bed material used. Bed materials and additives used were sand and limestone.

A study on fluidized bed gasifiers referring [9] (Cao et al, 2006)] showed that the maximum cold gas efficiency was obtained at an air-to-wood ratio of 2.557Nm^3/kg. The heating value

of gas was 4.911MJ/Nm^3 giving a cold gas efficiency of 58%, and produced 3.266Nm^3 of gas per kg of wood. When the air-to-wood ratio was increased to 3.155 Nm^3/kg the LCV decreased to 3.072MJ/m^3 with a cold gas efficiency of only 39.1%. The fluidized bed used sand as bed material with an average size of 0.11mm and a density of approximately 1470kg/m^3. Gas compositions and light hydrocarbons were determined through a gas chromatograph with thermocouple detectors (TCD) and flame ionization detectors (FID), using Porapak Q, Porapak R and a 5A molecular sieve column. The maximum concentration of fuel gas was reported to be 9.27%, 9.25%, and 4.21% for H2, CO and CH4 respectively, which gave a heating value of 3.67MJ/m^3. The maximum carbon efficiency was 87.1%.

2.2.3.2 Temperature

The operating temperature of a fluidized bed gasifier at steady state has attracted the greatest attention and has been studied by many of the research groups presented above as an independent variable.

There is agreement in general that the gas yield, the heating value of the gas produced and the energy recovery increase as the operating temperature is increased in the range of 650-900°C[8]. This is shown in Figures 2.1 to 2.3 for the gas yield, thermal efficiency and higher heating value of the product gas respectively. None of these groups has extended the temperature range to higher temperatures due to limitations of ash-sand bed sintering.

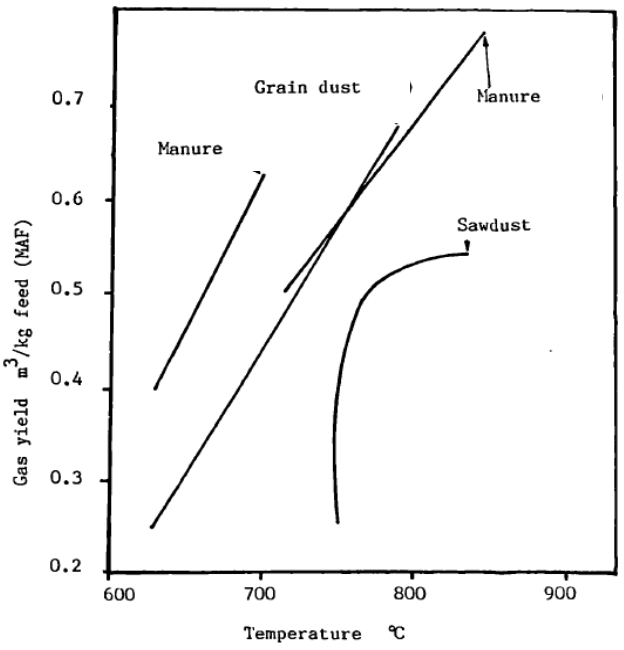

Figure 2.1 Effect of temp. on gas yield

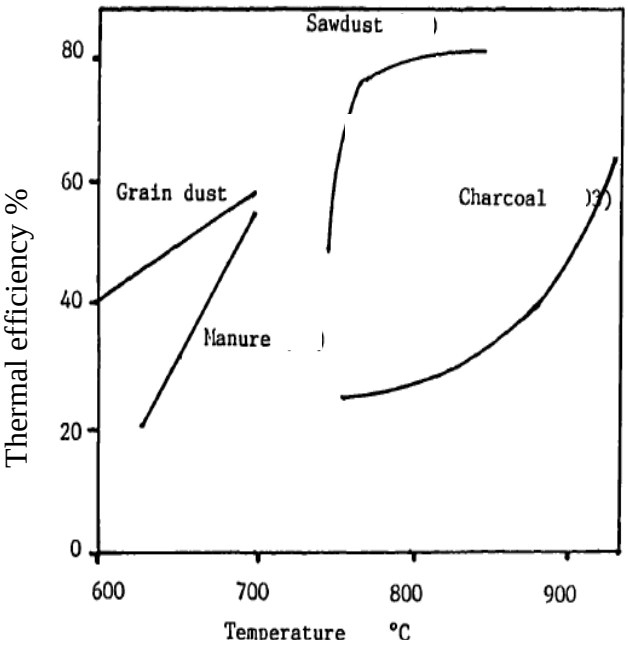

Figure 2.2 Effect of temp. on thermal efficiency

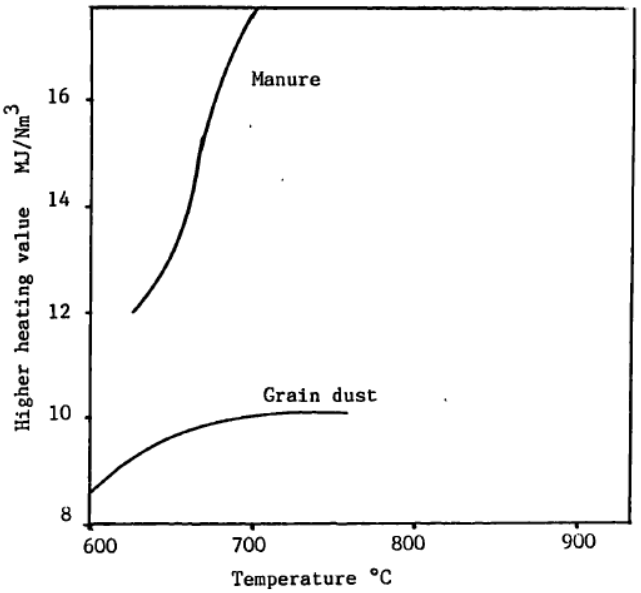

Figure 2.3 Effect of temp. on higher heating value

Since these results were obtained under different experimental conditions and with different feedstocks, it can be concluded with certainty that an optimum operating temperature should be around 800 + 50 °C. Operation below this temperature range will result in low gas yields, low thermal efficiency and low calorific value of the gas. Operation close to 900 °C will cause the biomass ash to melt and consequently the bed will sinter. In contrast to systems operating without inert bed all publications presented in section 2.2.3.1 reported isothermal conditions in the sand bed.

2.2.3.3 Air to fuel ratio

The amount of air in relation to the amount of biomass fed to a gasifier (sometimes termed equivalence ratio or air factor is a parameter which strongly influences the performance of a system. It is defined as the amount of oxidant fed to the reactor divided by the amount required for stoichiometric combustion. This ratio must be equal to 1 for complete combustion of the feedstock to carbon dioxide and water [8], though in practical application values greater than 1 are used. When this ratio is equal to 0, it corresponds to pyrolysis of biomass in the absence of oxygen [8]. Commonly, fluidized bed gasifiers operate in the range of 0.2 to 0.5. Figure 2.4 shows the influence of the equivalence ratio to the adiabatic flame temperature. These results were computed with a thermodynamic model and show the operational range of the different processes [8]. It has been shown that as the air to fuel ratio increases, the temperature of reaction will also increase. Similarly, with higher values of air to fuel ratio, the gas yield and the heat of reaction will increase as well [8].

In the same figure the char formation in relation to air factor is also shown. At 0 air factor, the maximum char production is predicted at about 0.34 kg char per kg of dry biomass. However at an air factor of 0.23, the char formation drops to 0. This is an important conclusion, since operation at air factors above 0.23 would theoretically beyond the carbon boundary in the gas phase region, see Figure 2.4. Thus thermodynamics predict no char above an air factor of 0.23 and the only possible products can be in the gaseous state. However, this is not always the case in practice, as gasifiers often operate in the gas phase region and yet solid carbon is removed from the gasifier.

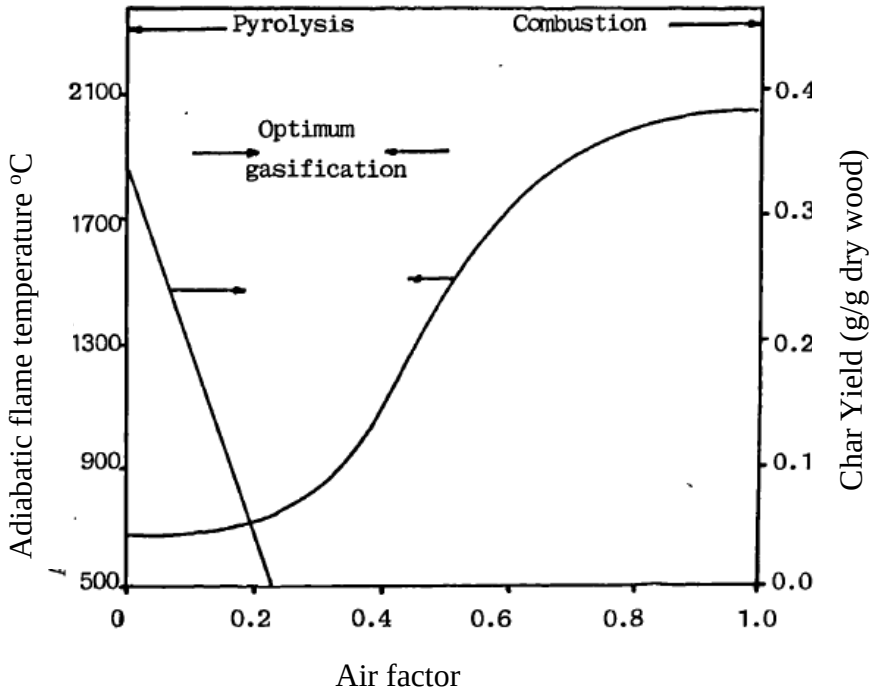

Figure 2.4: Effect of air factor on the adiabatic flame temperature and char yield

A common conclusion of the above articles is that the quality of the gas produced and the thermal efficiency (defined as the chemical energy (higher heating value) of the cool gas over the chemical energy of the feedstock) drop significantly above an air factor of 0.5, while below a value of 0.2 the yields of pyrolysis products (tars and pyroligneous acids) increase considerably. Figure 2.5 shows that the chemical energy of the gas decreases with air factors above 0.3.

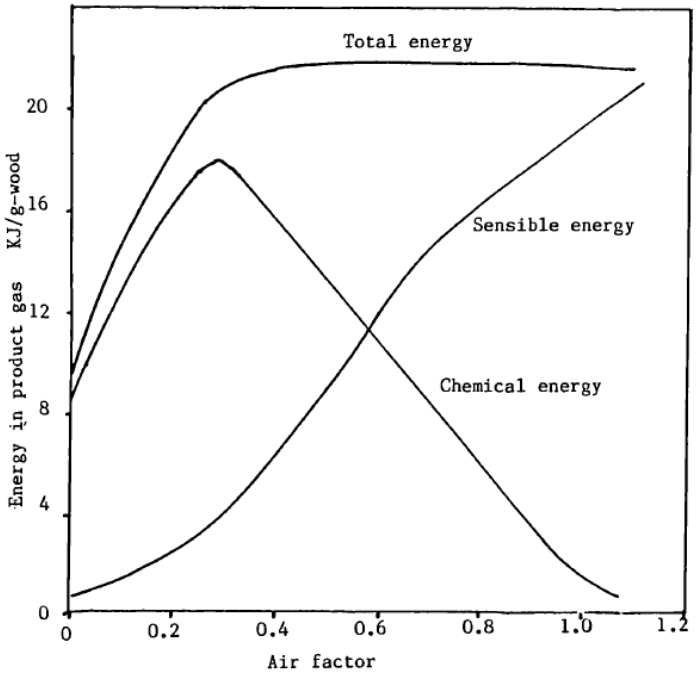

Figure 2.5: Effect of air factor on energy of the product gas [8]

2.2.3.4 Gas composition

There is good agreement (variations less than 10 % under similar operating conditions) amongst the various publications of Table 2.1 concerning the gas composition of the product gas. Typical operating data for fluidized bed gasifiers are given in Table 2.2, (A common characteristic is that ethylene and ethane are typical components of the product gas. These gas components are not found in the product gas of dense phase reactors; although their concentrations are low they significantly improve the higher heating value of the gas. Several groups have also reported low concentrations of C_3 and C_4 hydrocarbons [8]. However, they are often ignored, as their detection is much difficult.

Table 2.2: Typical gas composition and operational data of fluidized bed reactor [8]

Parameter	Units	Value
Grate energy release	GJ/hm^2	6-9
Operating temperature	^oC	700-850
Off gas temperature	^oC	500-800
Moisture cont. max	Wt%	40
Fuel size max.	mm	60x60x30
Gas composition	Vol. %	
N_2		50
CO_2		20
CO		14
H_2		9
CH_4		5
C_2 hydrocarbons		2

Evidence was recently produced by the group of the Free University of Brussels that the gas composition is greatly affected by the approach to equilibrium of the homogeneous water gas shift reaction by which the equilibrium conversion for hydrogen, water, carbon monoxide and carbon dioxide is set [8]. It was found that at about 800°C the gas composition approaches the equilibrium position. The same group also identified the temperature of the freeboard zone as a significant influence on the gas composition [8]. The freeboard region of a fluidized bed gasifier assumes a great importance as a disengagement zone for entrained particles; as a cracking zone for tars and pyroligneous acids; and as a zone for continued gas phase reactions. The fact, that higher operating temperatures improve the gas quality, is in accordance with the conclusion of several works.

2.2.3.5 Thermal efficiency

Thermal efficiencies as low as 15% have been reported when operating a fluidized bed gasifier at high air to fuel ratios of above 0.5 [8]. However under normal operating conditions with introduction of cogeneration system thermal efficiencies in the range of 60-70% have been attained by several researches [8] (see section 2.2.3.1.). A common conclusion is that the overall efficiency can be improved further if the sensible heat of the product gas could be recuperated in a heat exchanger.

The thermal efficiency is favoured by higher operating temperatures, dry feedstock and an air to fuel ratio in the range of 0.25 - 0.35 [8].

2.2.3.6 Bed sintering

Sintering and loss of fluidization have been reported by several groups as a major problem with beds of silica sand [8]. Bed agglomeration typically occurs at temperatures above 850 °C. The ash content and composition of the feedstock also play an important role in bed sintering, as well as the particle size and method of feeding. It has been reported [8] that slagging was experienced when feeding wood shavings in a fluidized bed above the surface of the bed. This was attributed to the "floating behaviour" of the wood shavings (the material was segregated at the top of the bed) which caused very high local temperatures.

In order to avoid bed sintering, several other materials such as limestone, quartz sand, alumina sand and even chromite sand have been tested by various groups as alternative bed materials [8]. In general alumina sand is considered a better bed material than silica sand, since the reactions between ash components and alumina proceed at a lower rate than those between ash and silica, to form low temperature melting eutectics. However, [8] the author

has reported that even with a bed of alumina sand, it was not possible to operate a fluidized bed gasifier fed with Euphorbia Tirrucalli at a temperature above 650 °C, due to ash-sand agglomeration. Instead, chromite sand had to be used.

2.2.3.7 Feedstock properties and feeding

Feedstock characteristics and properties influence the performance of a gasifier significantly. However, few studies have investigated these parameters. It has been shown [8] that the calorific value of the product gas decreases more than 50 % as the moisture content of the feedstock increases from 20 to 50 wt %. Recently, equilibrium and non equilibrium thermodynamic models have been developed, which studied the influence of the moisture content on the volume concentration of the gas components [8]. The volume percentage concentration of hydrogen, carbon monoxide, carbon dioxide and methane were all decreased by 2/3 for the moisture content range of 0-40 wt%. It has also been reported [8] that the feed size fraction of manure had a definite influence on the composition, heating value and gas yield of the product gas. Feedstock characteristics also influence the selection of an appropriate feeding system. Several problems such as bridging in the feed hopper have been encountered with biomass feeding systems and this led to the design and creation of special feeding units. A centre-bottom feed arrangement [8] had to be developed to feed cotton ginning wastes in a fluidized bed gasifier in order to eliminate freeboard combustion. In general there is no standard feeding system and the feeding arrangement is dictated by the properties of the feedstock: However, for easy to handle feedstocks (such as wood chips and bagasse with dimensions 4x4x1 cm) above bed feeding with a screw conveyor is the preferred system, since they are reliable and relatively of low capital cost.

Problems of reduced efficiency due to high carbon losses (6-10 wt %) in the fly ash have also been reported [8] when feeding fine biomass (sawdust) above the surface of the bed. It was recommended to modify the feeding system for in-bed feeding to minimize the carbon losses with such feedstocks.

The content of inerts and/or ash in the feedstock also has to be considered. If this is significant (above 3-5 wt %) and it has the tendency to accumulate in the bed, then special provisions have to be made to ensure the continuous or semi-continuous removal of part of the bed material.

2.2.3.8 Scale of operation

The majority of studies have been carried out in relatively small laboratory units with inside bed diameters smaller than 0.40 m. Only few works have been found using reactors with internal bed diameter larger than 1 m [8]. However, since the groups represented private concerns few results were published thus limiting evaluation of these systems.

The most comprehensive study concerning the scale of operation has been carried out at the University of Missouri Rolla [8], where units with internal bed diameters of 0.10, 0.15, 0.56 and 0.70 m have been tested and the results compared. Their results indicated that the quality of the dry gas produced was only slightly affected by the size of reactor and the location of the feed addition point. This conclusion gives credence to the results obtained by the other groups which used only small units. Nevertheless, it is apparent that much more research is needed with larger scale units in order to obtain reliable results over a wide range of values of all significant parameters.

2.5 Conclusions of the literature review

Biomass gasification has been studied extensively during the last decade and commercial units have already appeared. From the different types of gasifiers, fluidized bed units offer several advantages over the other types; the most important of which are versatility, easy to scale up to very high capacities and good turn down ratios.

The best opportunities are identified for fluidized beds, which operate with an inert bed in the reactor with air as the gasifying medium. Oxygen, steam and pressurized gasification for synthesis gas production are left out because they are not in the scope of this thesis. However market indications of the last two gears show that a methanol synthesis plant would not be economically viable at current prices. Similarly interest in pyrolysis of biomass in fluidized bed units for producing liquid fuels or chemicals has increased recently, due to the increment in the price of oil.

The underlying nature of pyrolysis, a precursor to gasification, is still poorly understood although important findings have been reported. The complexity is such, that practically all available models either do not include pyrolysis at all or use rude empirical relationships to account for the process.

Thermodynamic models have been successfully employed in predicting the performance of gasifiers and new techniques such as non-equilibrium models and by-passing of pyrolysis

products can improve their accuracy. However, at the present stage of sophistication they must be used alongside some empirical models for design purposes.

It is evident that a complete design procedure incorporating:

a) Model to predict the performance of a fluidized bed gasifier,
b) Method to determine the fluidization parameters and characteristics for designing the fluidized bed gasifier and
c) Conceptual design of a fluidized gasification reactor is missing from the literature.

It was therefore decided:

I. To design fluidized bed gasifier for the gasification of biomass at atmospheric pressure employing an inert bed of sand on the basis of previous laboratory results and experience;
II. To develop an empirical model and design procedure for a fluidized bed reactor including analytical determination of the product gas composition using the thermodynamic equilibrium model.
III. To show the best working condition of the reactor to be designed including an analysis of effective fluidization parameters.

The general method in designing a fluidized bed reactor is presented as a summary in Appendix III.

3. THEORY OF GASIFICATGION AND FLUIDIZED BED GASIFIERS

3.1 THE THERMOCHEMICAL CONVERSION OF BIOMASS

There are three thermochemical processes by which biomass can be converted into useful products: gasification, pyrolysis and liquefaction. The general principles of these processes are presented in Figure 3.1. Of these three processes, the liquefaction process is beyond the scope of this thesis, since it produces predominantly liquid products under particular processing conditions in an essentially liquid phase process. The gasification route has been shown to be the more versatile one in view of possible products and applications. This characteristic of gasification offers the advantage that in principle a single reactor concept could be used in more than one gasification route (for example fluidized beds can be operated either with air, oxygen, steam or mixture of these oxidants to produce low or intermediate higher heating value gas under different operating conditions).

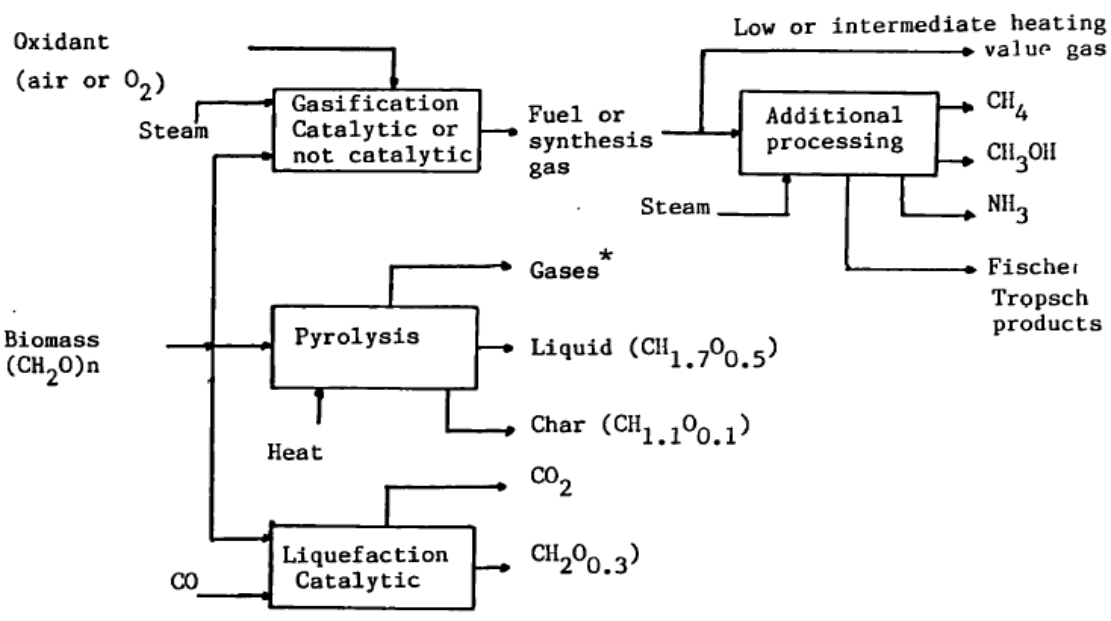

Figure 3.1 Generalized block diagram for the thermochemical conversion of Biomass [10]

3.1.1 Pyrolysis and gasification- general principle

Pyrolysis and gasification are two thermochemical processes by which solid organic materials can be converted into useful products. Pyrolysis is the thermal degradation of

organic material in the absence of oxygen. It is a relatively low temperature process (300 ^{o}C to 700 ^{o}C) with pyrolysis oil and solid char residue as the main products, while some gas produced which can be used as fuel. Pyrolysis is also a precursor to gasification.

Gasification on the other hand, is the thermochemical conversion of organic materials in the presence of oxidizing gases. This process takes place at relatively high temperatures (650 ^{o}C to 1300 ^{o}C) and can be used to convert biomass virtually completely in to combustible gas or synthesis gas. This is why the entire thesis would be concerned in the gasification of the biomass (Bagasse) rather than pyrolysis process. The combustible gas can be utilized as fuel, while synthesis gas can be used as feedstock for chemical synthesis or fuel synthesis (ammonia, methanol) as well as in the petrochemical industry.

The relative yields of the products of both processes depend upon many factors, the most important of which are the physical properties of the feedstock, the rate of heating, the initial and final temperatures, the type of contacting device used, and in the case of gasification the gasifying medium as well. Furthermore in the case of gasification, these changes are accompanied by chemical reactions amongst the volatiles, the char residue and the gasifying medium, which influence the characteristics of the product gas (composition, yields). Thermodynamics also have a significant influence on the final composition of the product gas, since under most high temperature operating conditions thermodynamic equilibrium is closely approached [10].

3.1.2 Types of reactors used in thermochemical conversion of biomass

Many different kinds of contacting devices such as moving bed, entrained bed, fluidized bed and rotary kilns have been proposed and used for the pyrolysis and/or gasification of carbonaceous feedstocks. A variety of methods have been used to classify the different types of reactors [11]. In this work gasifiers are classified in terms of the amount of biomass present in the reactor under normal operating conditions relative to the total reactor volume. This density factor is an important characteristic of gasifiers. Hence gasifiers can be classified as lean and dense phase reactors. The ratio of the volume of biomass over the volume of reactor can be used as an illustrative parameter. Typical values are in the range of 0.05-0.2 and 0.5-0.8 respectively for lean and dense phase gasifiers [8]. In general lean phase reactors have a low solid to reactor volume ratio, with relatively small amounts of feedstock occupying only a small fraction of the total reactor volume. In dense phase reactors the feedstock occupies most of the reactor volume.

3.1.2.1 Dense phase reactors

The most common reactors of this type are the co-current downdraft and the counter-current updraft. The names co-current and counter current indicate the relative motion of the gases and the biomass bed with respect to each other, while the names updraft and downdraft indicate the relative motion of the gases with respect to the gasifier. The biomass bed is generally supported on a grate and always moves downwards by gravity [11].

Dense phase reactors have a long history and were the first types of gasifiers produced commercially. Their main advantages are simplicity in construction and operation. One important characteristic of dense phase reactors is that distinct reaction zones of drying, pyrolysis, oxidation and reduction exist within the reactor [11].

The co-current downdraft gasifier features a co-current flow of gases and solids through a descending packed bed for a major part of its volume. The pyrolysis gases pass through the hot char bed which is supported on the grate, and this cracks the larger, more complex compounds into non condensable gases and water [11].

In the counter-current updraft configuration, the flow of gases and solids is in opposite direction. The pyrolysis gases which ascend do not pass through the hot bed of char or through a high temperature gasification zone and consequently the product gas contains a high level of tar and organic condensables [12].

The operating principles, together with typical temperature and conversion profiles, are given in Figure 3.2 for both types of gasifiers. From this figure it can be seen that typical operating temperatures are about 1000 °C and 1200 °C for the counter-current updraft and the co-current downdraft respectively. Conversion of feedstock into gas for both types generally approaches 100%. Figure 3.2 also depicts a common feature of co-current downdraft gasifiers, being a "throat" or restriction. This is normally at or below the inlet of the oxidizing medium and its main purpose is to avoid channelling and bypassing of pyrolysis products through the oxidation zone. These pyrolysis products are cracked to lower molecular weight hydrocarbons as they pass through the high temperature zone at the throat [13].

Co-current downdraft gasification is simple, reliable and proven for certain fuels, such as relatively dry (about 15 wt % moisture) with low ash content (below 1 wt %) and neither fine nor coarse particles (chips not smaller than about 2 cm and not bigger than about 10 cm longest dimension) [13]. Due to the low content of tars in the gas, it is generally favoured for electricity generation via an internal combustion engine and is usually promoted for Third World applications, since gasifiers of this type can easily be fabricated and operated and relatively small scale units are feasible for low shaft power generation (e.g. irrigation pumps)

[8]. There is however difficulties in scaling up, but this can be overcome with multiple units if economics permit.

Producer gas from counter-current updraft gasifiers requires substantial clean up if further processing is to be performed. This configuration is therefore more suitable for close coupled combustion applications and retrofitting boilers as no clean up is then required, since tars are fully burned out [8].

Figure 3.2

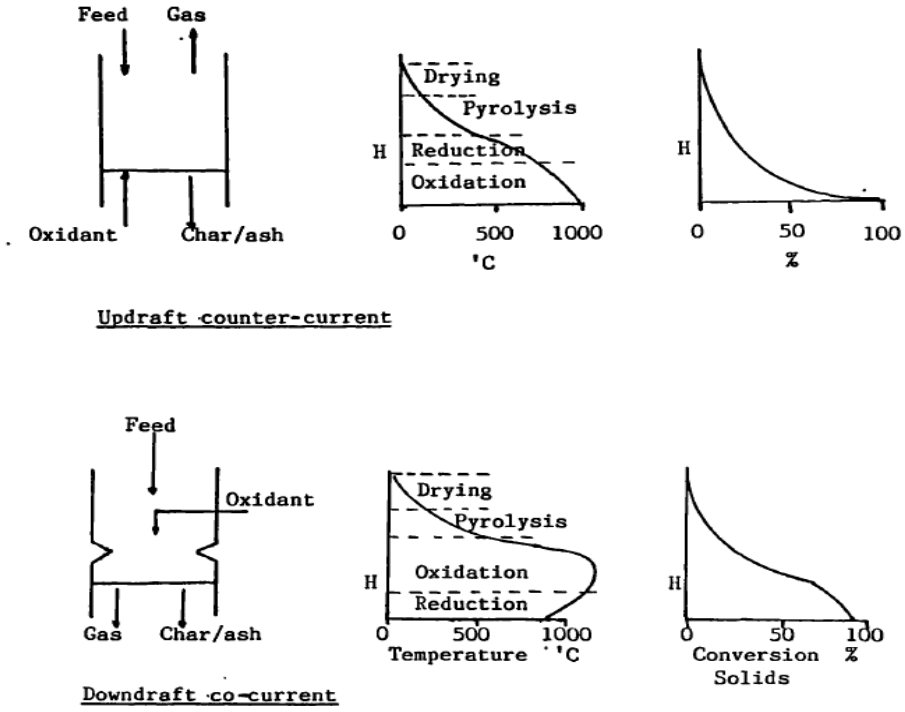

Principles of dense phase gasifiers [10].

3.1.2.2 Lean phase reactors

Lean phase gasifiers were originally developed for coal gasification and have only recently been adapted for biomass conversion. Contrary to dense phase reactors, no distinct reaction zones exist within the gasifier and drying, oxidation, pyrolysis and reduction take place effectively in the same region. Fluidized bed and entrained bed are the most commonly used lean gasifiers [8].

Fluidized beds are attractive as gasifiers as they provide many features that are not present in the dense phase types, including high rates of heat and mass transfer and well mixing of the solid phase, which means that reaction rates are high and the temperature is more or less constant in the bed. A relatively smaller particle size than for dense phase gasifiers is necessary and this may require additional size reduction. Due to the small particle size many types of feeding devices can be used; solids are thus easily introduced and ash generally is

removed as fine particulates entrained in the off gas [15]. Fluidized beds generally have the attraction of being easy to scale up and operate at lower maximum temperatures (in the range of 700-850 °C) than dense phase gasifiers. It is also possible to separate the pyrolysis and the char gasification processes by using a dual bed system. One fluidized bed is commonly used as a combustor (e.g. char) and the other as pyrolyser. The heat for the pyrolysis reaction is most commonly provided by circulation of hot sand from the combustor to the pyrolyser [12]. A more detailed review and problems associated with fluidized bed gasifiers are presented in later sections.

In entrained bed gasifiers no inert material is present but a finely reduced feedstock is required. This type of lean phase reactor is still under development and problems such as scaling up and feeding have still to be overcome.

The principles of lean phase gasification with temperature and conversion profiles are shown in Figure 3.3. From this figure it can be seen that fluidized beds are the only gasifiers with isothermal bed operation. Typical operating temperatures for biomass gasification are about 800 °C. Most of the conversion of the feedstock to product gas takes place within the bed. However conversion to product gas continues in the freeboard section and in most cases approaches 100%, unless excessive carryover of fines takes place. Entrained bed gasifiers however operate at much higher temperatures of about 1500 °C and hence the product gas has low concentrations of tars and condensable gas. However, this high temperature operation creates problems of materials and ash melting. Conversion in entrained beds can also approach 100%.

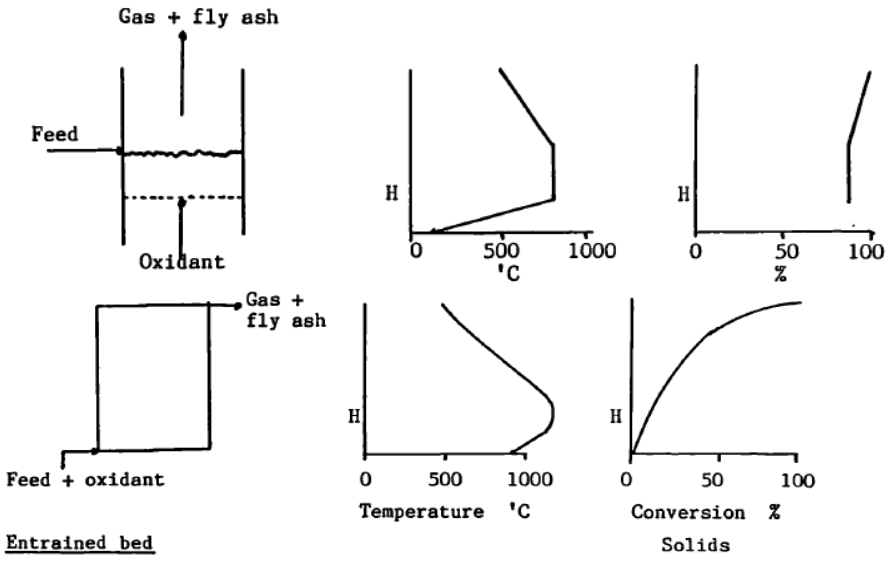

Figure 3.3 Principles of lean phase gasifier with temperature and conversion profiles [12, 13].

Table 3.1 summarizes the general advantages and disadvantages of dense and lean phase gasifiers reviewed in this section, while fluidized bed reactors in particular will be described in more detail because they are the focal point of the thesis.

Table 3.1: Comparison of various gasifiers [8]

<table>
<tr><td colspan="2">Dense phase gasifiers</td><td colspan="2">Lean phase gasifiers</td></tr>
<tr><td>Updraft</td><td>Downdraft</td><td>Fluidized bed</td><td>Entrained bed</td></tr>
<tr><td>Low gas outlet temperature</td><td>Low tar yield
High thermal efficiency</td><td>Good temperature Control, Low tar yield
Can tolerate variation in quality of fuel.
Can operate at part load, started and stopped easily.</td><td>Produces tar free gas and little methane
High feedstock utilization due to high reaction rates.</td></tr>
<tr><td colspan="2">High carbon conversion, Low ash carryover. Large residence time of solids.
Relatively simple construction.</td><td colspan="2">Very good gas-solid contact and mixing,
High throughputs.</td></tr>
<tr><td colspan="2">High tar yield</td><td>Carbon loss with ash.
Low operating temperature.</td><td>Refractories and materials of construction. High outlet gas temperature, Slugging.</td></tr>
<tr><td colspan="2">Low specific capacity, Poor turn down capability, Uniformly sized feedstock with required, minimum of fines
Ash fusion and clinker formation on grate.</td><td colspan="2">Low feedstock inventory.
Extensive particulates clean up is required.</td></tr>
</table>

3.2 FLUIDIZED BED GASIFIERS

The contacting pattern between biomass and gasifing medium is a very important aspect of any gasifier. Fluidized bed reactors are considered to be two phase systems in both the contacting pattern and flow of reactants and products, since two distinct phases (solid and gas) exist [8].

Most biomass gasifiers under development employ one of two types of fluidized bed configurations: bubbling fluidized bed and circulating fluidized bed. A bubbling fluidized bed consists of fine, inert particles of sand or alumina, which have been selected for size, density, and thermal characteristics. As gas (oxygen, air or steam) is forced through the inert particles, a point is reached when the frictional force between the particles and the gas counterbalances the weight of the solids. At this gas velocity (minimum fluidization), bubbling and channelling of gas through the media occur, such that the particles remain in the reactor and

appear to be in a “boiling state”. The fluidized particles tend to break up the biomass fed to the bed and ensure good heat transfer throughout the reactor.

The ***advantages*** of bubbling fluidized-bed gasification are

- Yields a uniform product gas
- Exhibits a nearly uniform temperature distribution throughout the reactor
- Able to accept a wide range of fuel particle sizes, including fines
- Provides high rates of heat transfer between inert material, fuel and gas
- High conversion possible with low tar and unconverted carbon

The ***disadvantages*** of bubbling fluidized-bed gasification are:

- Large bubble size may result in gas bypass through the tubes By far,

Bubbling fluidized bed biomass gasification has been operated over a wide range of conditions, such as temperature, pressure and throughput, using a variety of biomass feed stocks. For fuels, chemicals and hydrogen applications, it is beneficial to operate at high temperatures as is done for coal gasification. At temperatures greater than 1200-1300^{o}C, little or no methane, higher hydrocarbons or tar is formed, and H_2 and CO production is maximized without requiring a further conversion step. In this section the phenomenon of fluidization and the various models describing the hydrodynamic behaviour of fluidized bed reactors are discussed.

3.2.1 The phenomenon of fluidization

If a fluid passes upwards through a bed of solids, the fluid first percolates through the voids of the particles and a pressure drop builds up across the bed [16]. As the fluid flow is increased, the pressure drop increases roughly proportionally, but when the frictional drag on the particles becomes equal to their apparent weight (actual weight less buoyancy), the particles become rearranged, to offer less resistance to the flow of the fluid and the bed starts to expand. Eventually, as the fluid flow rate is increased, the bed begins further to expand until a point is reached when the particles are all just suspended by the upward flowing fluid. At this point the bed is said to be at the point of "incipient" fluidization. If the fluid flow is further increased, the particles separate still further and the pressure drop remains approximately equal to the bed weight per unit area of the bed. Up to this point the system behaves in a similar way whether the fluid is liquid or gas. With a liquid the bed continues to expand with increasing flow rate and the fluidization is known as "particulate" fluidization [16].

With a gas, however, at high velocities two separate phases are formed; the continuous phase, which is known as the dense or emulsion phase and the discontinuous phase known as the lean or bubble phase. The fluidization is then said to be "aggregative". Bubbles are formed at the distributor and rise up the bed. As they rise, they coalesce with other bubbles and become larger. If the bed is sufficiently deep and narrow, the bubble may become large enough to spread across the entire bed section. Then as it rises, it moves the solids upwards until it collapses. Then the bed is known to be "slugging". These various kinds of contact regimes are shown in Figure 3.4.

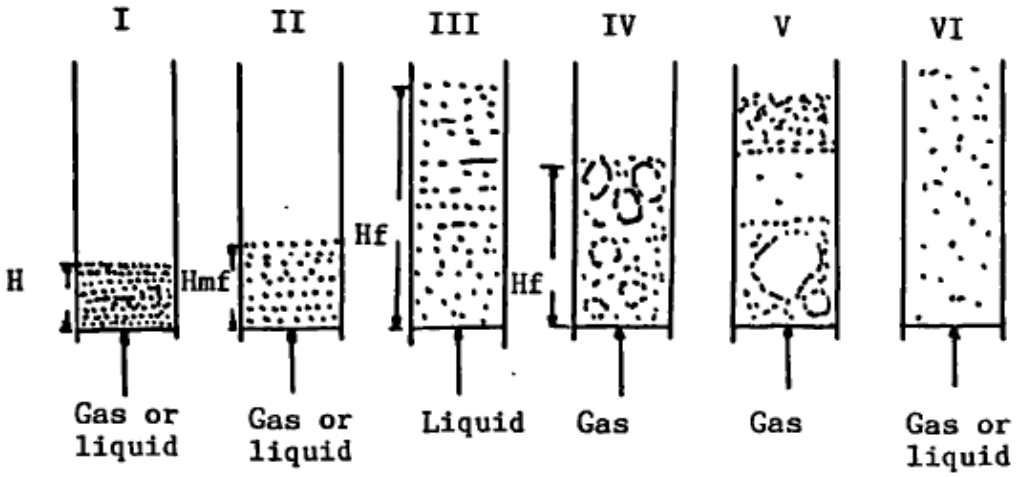

I. Fixed bed
II. Incipient or minimum fluidization
III. Particulate or smooth fluidization
IV. Aggregative or bubbling fluidization
V. Slugging
VI. Lean phase fluidization with pneumatic transport

Figure 3.4: Various kinds of contacting of a batch of solids by fluid [17]

3.2.2 Definition of the minimum fluidization velocity and types of fluidizations

The minimum fluidization velocity, U_{mf}, is the theoretical fluid flow velocity, at which the pressure drop through a bed is just enough to support the weight (including the drag and the buoyancy forces) of the bed. The ideal fluidization characteristics can be shown on a graph of pressure drop against air flow for a bed consisting of one mono sized component, see Figure 3.5 [18]. The broken line parallel to the abscissa represents the weight of solids per unit cross sectional area of the bed and in this idealized case, according to the definition; it is exactly equal to the pressure drop required for U_{mf}. Line ABDE represents increasing gas flow rates

and EDC represents decreasing rates. After fluidization, the particles are more loosely packed and therefore the pressure drop for each particular flow rate is lowered, giving the hysteresis loop ABDC. Any further increase in air flow however would produce a pressure drop on the path CDE [17].

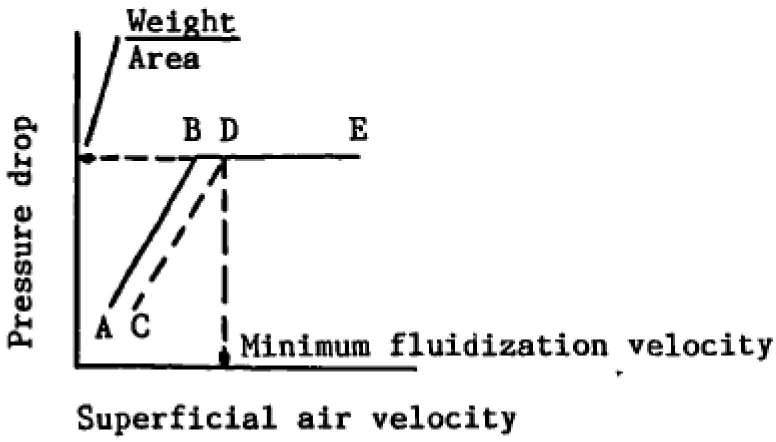

Figure 3.5 Idealized pressure drop-flow characteristics for a fluidized bed

In this ideal case, U_{mf} would be defined uniquely as the point D, which in fact is the intersection of the two straight lines CD and DE representing respectively the fixed bed and the fluidized bed. But such an idealized pressure drop versus air flow rate is never obtained in practice. A typical real system could be obtained from experiment where the U_{mf} of the fluidized bed pilot plant reactor would be determined**.**

There are several regions under which fluidized beds can operate. These regions are roughly separated in terms of the slip velocity (U_t), which characterizes the motion of particles in a fluidized bed, and are defined by equation 2.1, [18].

$$U_t = \frac{U_g}{e} - U_p \quad \ldots\ldots 3.1$$

Where U_g = the superficial gas velocity

e = bed voidage

And U_p = the particle velocity

Under gas velocities slightly higher than the minimum fluidization velocity a "bubbling fluidized bed" is established and the voidage in the bed is close to 1- e_{mf}. Higher gas velocities will result in a "turbulent fluidized bed", where many solid particles are entrained with the gas. Nevertheless the bed maintains a certain height and the entrained particles are either discharged or fall back in the fluidized bed. However, when the gas velocities increase

even further, then the slip velocity increases significantly and a "fast" or circulating fluidized bed is established. This is characterized by a high degree of particle turbulence with slip velocities, an order of magnitude greater than the terminal fall velocity of the individual particles (above this velocity, the particles are entrained from the bed) [17]. The solids are almost uniformly distributed over the reactor height. The quantity of solids entrained by the gas is separated in the recycle cyclone and recycled to the reactor. This leads to the recycle cyclone being a permanent constituent of the reactor system.

3.2.3 Models describing the behaviour of fluidized bed reactors

In order to describe the behaviour of a fluidized bed, a model to represent the flow of gas through the bed and its contacting of solids is required. This is especially necessary for gasification reactions, which are heterogeneous in nature (more than one phase are present: solid and gas). Therefore the contact and interactions between the phases strongly influence the rates of the chemical reactions. Considerations of bubble flow are therefore central to the design of any gas-solid fluid-bed process and some aspects of bubble behaviour will be discussed. The earliest theory to be proposed for the division of gas between the bubble phase and the emulsion phase of a bubbling bed was the "Two Phase theory".

3.2.3.1 Two phase theory

This theory was proposed originally by Twoomy and Johnston [8] and states that all gas in excess of that necessary to just fluidize the bed, passes through in the form of bubbles. Thus if Q_t is the total volumetric flow rate into the bed, Q_{mf} the minimum fluidization flow rate and Q_b the bubble flow rate:

$$Q_t = Q_b + Q_{mf} \quad \ldots\ldots 3.2$$

Dividing equation 3.2 by the bed area, A, gives the bubble flow in terms of the superficial velocities U and Umf.

$$\frac{Q_b}{A} = U - U_{mf} \quad \ldots\ldots 3.3$$

In recent years, however, a large number of experimental studies have been reported, in which the flow of bubble gas has been measured and the general conclusion drawn has been that in the majority of systems the two phase theory overestimates the actual bubble flow. In

other words, in these systems a larger quantity of gas flows through the emulsion phase than is predicted by equation 3.2. It has been suggested therefore that equation 3.3 be rewritten in the following form [8]:

$$\frac{Q_b}{A} = U - U_{mf}(1 + nf_b) \quad \ldots \quad 3.4$$

Where $\boldsymbol{n}$ is a positive number and $\boldsymbol{f_b}$ is the volume fraction of bed occupied by bubbles.

3.2.3.2 General approach to fluidized bed modelling

Most models are based on the two-phase theory of fluidization, but differ considerably in the assumptions they make regarding the exact nature of the phases, the mode of inter-phase gas exchange and the degree of gas mixing in the phases among others.

The Davidson-Harrison [16] and the Kunii-Levenspie [17] models have received most attention, since they can predict the hydrodynamics of fluidized beds better than other models [18].

In both these two phase theory models the bed is depicted as two regions, a bubble and an emulsion phase with gas interchange between phases, while the Kunii-Levenspiel model also considers a third phase - the cloud phase. This third phase is made of a "cloud" of gas which surrounds the bubble and moves with it. Both postulate plug flow for the bubble phase, while for the emulsion phase the D-H model postulates it as well mixed and the K-L model as stationery. Numerous extensions and alternative analyses for both models have been published in recent years [19]. A detailed description and comparison of the various models is beyond the scope of this study.

The two phase theory is a very useful concept in understanding the behaviour of fluidized bed reactors. . This is essential, besides the chemical and/or physical processes taking place in the reactor, since unless efficient fluidization is established, the other processes cannot proceed according to the desired specifications and rates. Later in this work, principles of the two phase theory are used in evaluating the operation of the process plant fluidized bed reactor.

3.2.3.3 Multiple region models

During a model comparative study, Chavarie and Grave [8] concluded that fluidized bed reactor models take insufficient account of reaction in the entry and exit regions of the bubbling bed, i.e. in the region close to the distributor and in the freeboard space above the bed surface. There is widespread agreement with this conclusion [18], since a number of authors have commented on the abnormally high rate of reaction near the distributor, where interphase mass transfer appears to be very fast and gas solid contact most pronounced. Similarly, observations have been made concerning freeboard space temperature increases in the case of exothermic gas - solid reactions, indicating an extra degree of reactant conversion in this region [8].

It would thus seem more realistic to model fluidized bed reactors on the basis of, three consecutive regions: the grid region, the bubbling bed itself and the freeboard [20]. On the other hand the consideration of three different regions would increase the complexity of an overall model and design.

3.3 MODELLING OF FLUIDIZED BED GASIFIERS

3.3.1 Introduction

Modelling implies the representation of a chemical or physical system by a set of equations which in a limited way can represent the system under study. Relevant in reactor design, is a mathematical description that can predict reactor outlet concentrations and temperature from inlet concentrations, flows and reactor dimensions [8].

In general there are two approaches by which fluidized bed gasifiers can be modelled:

A) Modelling a fluidized bed reactor which contains biomass and

B) Modelling biomass gasification which happens to be in a fluidized bed.

In the former approach emphasis is given on the hydrodynamics of the reactor, while biomass is considered as nonreacting (such as modelling of the fluidization characteristics of a char bed). In the latter approach, the fluidization characteristics of the bed are set constant while the gasification of biomass is modelled. It is this second approach that is of particular interest for this work, since fluidized bed reactors have been extensively covered in the literature and gasification of biomass taking place in a fluidized bed reactor is the main subject of this thesis.

There are two aspects to any theoretical investigation of gasifier behaviour [8]. The first is a thermodynamic approach which gives information on gas composition and its dependence on feed and oxidant compositions. The second is a kinetic approach which considers the effects of rate laws of chemical reaction and heat and mass transfer. Finally the behaviour of a gasifier can also be studied on the basis of empirical models.

In this section only the thermodynamic modelling and the empirical approach will be reviewed since these two models have been found sufficient to design the reactor. The advantage and disadvantage of both models will be discussed later. From that the design procedure of the fluidized bed reactor is developed.

Figure 3.6 is a state of the art depiction of the stages through which each biomass particle and intermediates must pass during a typical thermochemical process. In principle all stages could be separated in different reactors; however, in practice, they are taking place in a single reactor (e.g. moving bed reactors, single fluidized bed), or in two reactors (dual fluidized bed systems) where the pyrolysis and gasification stages are separated.

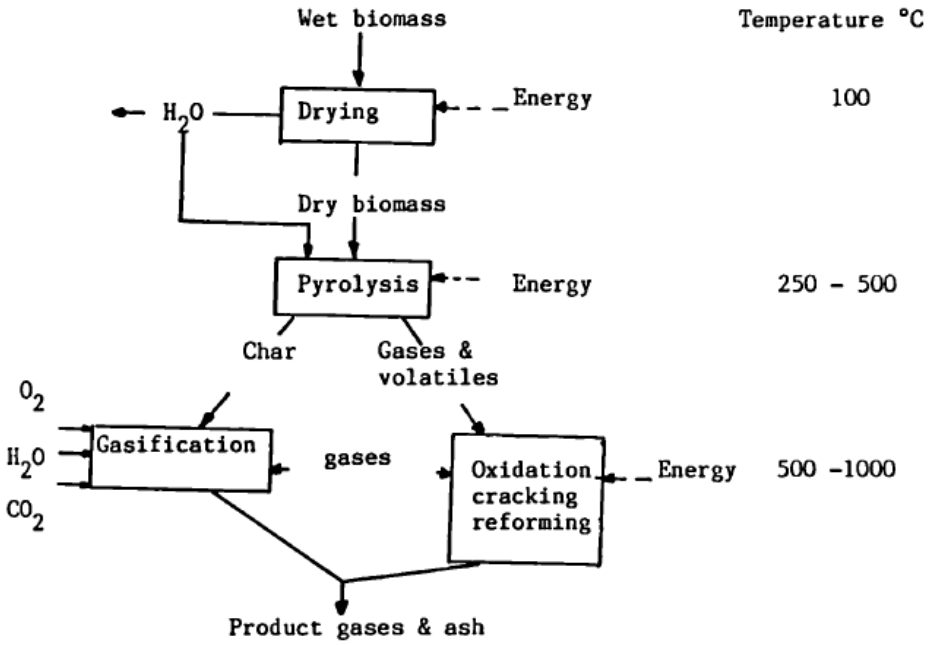

Figure 3.6: Stages in thermochemical processing of biomass [21]

3.3.2 Drying of biomass

3.3.2.1 Introduction

Removal of water reduces the weight of material that must be transported or handled in a processing plant, thereby lowering operating costs and it generally improves the quality of biomass for thermochemical processing. On the other hand, the disadvantages of drying-equipment and operating costs must be carefully evaluated in any process.

3.3.2.2 Periods of drying

When a material is dried, a drying curve can be plotted as moisture content (dry basis) versus time, as shown in Figure 3.7a [22]. This curve represents the general case, when wet biomass loses moisture first by evaporation from a saturated surface on the solid, followed in turn by a period of evaporation from a saturated surface of decreasing area and finally by a period when the water evaporates in the interior of biomass.

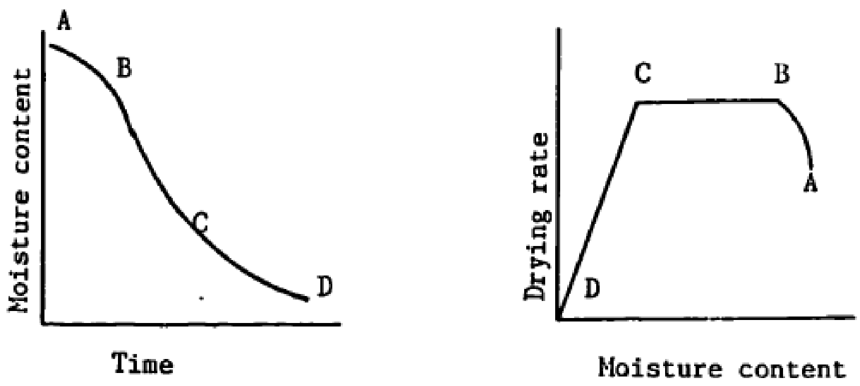

a)

b)

Figure 3.7 The periods of drying

The variation in drying rate can be better illustrated by plotting the drying rate versus moisture content (Figure 3.7b). The rate curve shows that drying is not a smooth, continuous process in which a single mechanism controls throughput. Section BC represents a constant rate period, the portion CD is termed "the falling rate period" and section AB is the heating up period [22].

During the constant rate period, drying proceeds by diffusion of vapour from the saturated surface of the material across a stagnant-air film into the environment. Moisture movement within the solid is rapid enough to maintain a saturated condition at the surface and the rate of drying is controlled by the rate of heat transfer to the evaporating surface. The rate of mass transfer balances the rate of heat transfer and the temperature of the saturated surface remains constant. Point C, where the constant rate ends and the drying rate begin to fall, is termed "the critical moisture content".

Specifically for biomass, the moisture movement during the falling rate period is controlled by diffusion. Since the rate of drying during the constant rate period is proportional to the temperature difference.

$$drying\ rate = \frac{h_t A\Delta t}{l} = K_g A\Delta P \ldots\ldots\ldots\ldots\ldots\ldots\ldots\ldots\ldots\ldots\ldots\ldots\ldots\ldots\ldots\ldots\ldots\ldots\ldots\ldots. 3.5$$

Where: - $h_t = \ heat\ transfer\ coefficient\ (KJ/hm2°C)$

$A = \ area\ of\ heat\ transfer\ (m2)$

$l = \ latent\ heat\ of\ evaporation\ (KJ/kg)$

$K_g = \ mass - transfer\ coefficient\ \left(\frac{Kg}{hm2.atm.}\right)$

$\Delta t\ = t\ - \ ts\ where\ t\ = \ gas\ temperature\ (°C)$

$ts\ = \ temperature\ of\ surface\ (°C)$

$$\Delta p = Ps - p$$

Where: $Ps = vapour\ pressure\ of\ water\ at\ surfaces\ temperature\ (atm.)$

$p = partial\ pressure\ of\ water\ vapour\ in\ the\ gas\ (atm.)$

Under normal operating conditions of gasifiers (700-1200 °C) drying of biomass attains very high rates [8]. In dense phase reactors the operating temperatures in the drying zone are relatively low (100-350 °C) [10, 11], while in lean phase reactors, since distinct zones do not exist, the temperature is relatively high (600-950 °C). Thus for lean phase gasifiers the rates of heating and drying attain very high rates and these processes are generally considered to be instantaneous in view of a model development [8]. Therefore these processes can safely be ignored in the formulation of a model. However, this assumption does not hold for dense phase reactors, since the preheating and drying zone represents a significant fraction of the total reactor volume.

3.3.3 Pyrolysis of biomass

Pyrolysis is a very important process in thermochemical processing of biomass. It is a complicated process and despite serious efforts by several groups it is still not very well understood. Low temperature pyrolysis of cellulose has been extensively studied and some success in modelling has been achieved in this area. However high temperature pyrolysis of cellulose is still not adequately covered and no reliable models exist in this field.

Pyrolysis of hemicelluloses and lignin are understood even less than pyrolysis of cellulose. More specifically, in relation to this work, pyrolysis of bagasse at high temperatures (above 500 °C) and at high heating rates (higher than 1000 °C/s) is poorly understood and its mechanisms and kinetics still have to be extensively examined, before they could be successfully used in design.

However it can be safely assumed that the rate of pyrolysis is faster than the rate of char gasification by at least an order of magnitude and especially for lean phase reactors, it does not have to be accounted for in a model [8]. The same is also true for drying of biomass. Therefore, since this thesis is concerned with the development of a design procedure for fluidized bed gasifiers, emphasis will be given in the next section to char gasification only.

3.3.4 Thermodynamic models

3.3.4.1 Introduction

Thermodynamic prediction is the most widely used technique to model the performance of gasifiers [12].

In the foregoing discussion, pyrolysis and gasification were identified as the two major stages in biomass gasification. The products of pyrolysis and char gasification reactions are not in chemical equilibrium because gas phase reactions are slow below 500 °C; there is great complexity in terms of product formations and temperatures gradients exist in and around the pyrolysing particle. However, at temperatures above 500 °C, chemical equilibrium is approached fast enough, so that thermodynamic calculations can be increasingly accurate in predicting important trends and in some cases the gas composition to be expected from biomass gasification [8].

The condition at which all the carbon in the char is theoretically gasified is called the solid carbon boundary (see Figure 3.2). To one side of this boundary some charcoal is predicted, to the other side no solid carbon leaves the gasifier [8]. Such a system represents an idealized case and operation of a thermodynamically equilibrated gasifier on the solid carbon boundary results in maximum thermal efficiency. However, in practice a range of factors including the temperature, residence times and gas-solid contacting methods employed in gasification reactors, significantly affect the degree of attainment of equilibrium. The uniformly high temperatures in a fluidized bed offer favourable conditions for equilibrium but the degree attained depends on gas residence time. However, this is also the case with downdraft gasifiers.

3.3.4.2 Heterogeneous and homogeneous reactions

The most important char gasification reactions are listed in Table 3.2. The first two reactions which are irreversible represent the oxidation of char with oxygen and the heat released by these reactions drives subsequent processes.

Table 3.2: Gasification reactions [8]

Equation	Reaction	Heat of reaction (kJ/mole) 20 ^{0}C
	Heterogeneous	
3.6	$C+1/2\ O_2 \longrightarrow CO_2$	-110.6
3.7	$C+\ O_2 \longrightarrow CO_2$	-393.8
3.8	$C+\ CO_2 \rightleftharpoons 2CO$	+172.6
3.9	$C+\ H_2O \rightleftharpoons CO + H_2$	+131.4
3.10	$C+\ 2H_2 \rightleftharpoons CH_4$	-74.9
	Homogeneous	
3.11	$CO\ +\ H_2O \rightleftharpoons CO_2 + H_2$	-41.2
3.12	$CH_4 + H_2O \rightleftharpoons CO + 3H_2$	-201.9
3.13	$2H_2 + 2CO \rightleftharpoons CO_2 + CH_4$	+321.3

High temperatures favour the Boudouard (eq. 3.8) and water gas (eq. 3.9) reactions - both kinetically and thermodynamically - which are highly endothermic. Conversely the methane reaction (eq. 3.10) is not favoured by high temperatures. In order to compute the equilibrium composition, only two methods of approach can be applied.

a) The equilibrium constant method of Gumz and
b) The rarely applied approach of minimizing the total Gibbs free energy of the reacting system

Both methods are largely discussed in many literatures [8].

The former method uses the equilibrium constants of a set of reactions, which represent -the reacting system and with material balances a set of equations is formed, the solution of which gives the equilibrium composition. The second method applies the total Gibbs function for the given system:

$$G = \sum (n_i \bar{G}_i) \quad \ldots\ldots\ldots\ldots 3.14$$

Where: $G = total\ Gibbs\ function,$

$n_i = moles\ of\ component\ i\ and$

$G_i = the\ partial\ molar\ Gibbs\ function\ of\ component\ i.$

The problem then is to find a set of n_i's which minimizes G at constant temperature and pressure subject to the restrains of the material balances. This is solved by the method of Lagrange's undetermined multipliers. It is important to note that in this procedure the question to know which chemical reactions are involved never enters directly into any consideration. However, the choice of a set of species is entirely equivalent to the choice of a set of independent reactions among the species. A disadvantage of this procedure is that the standard Gibbs heat of formation of the components must be known at the temperature of the system. .However in both cases some assumptions have to be made:

a) All gases are ideal
b) The only gaseous products are H_2, CO, CO_2, H_2O, CH_4, and N_2, while O_2 is fed in the gasifier (in the form of air or oxygen).

3.3.4.3 Illustrative example

In this section a thermodynamic model on the carbon solid boundary is developed. It is postulated that all fuel fed to the gasifier is gasified (it contains no ash), while the assumptions a) and b) of the previous section are valid. The homogeneous reactions 3.11 and 3.13 are considered to be at equilibrium. Such a set of equations is more suited for lean phase

gasifiers than heterogeneous reactions, since the excess of carbon in lean phase gasifiers is not always certain. On the other hand dense phase gasifiers operate always with excess of carbon and a set of heterogeneous equilibrium reactions is valid. When the heterogeneous equilibria are established, the homogeneous equilibria are automatically attained. However the reverse is not always true [11].

The corresponding equilibria constants of reactions 3.11 and 3.13 at atmospheric pressure are:

$$K_w = \frac{P_{CO_2} \times P_{H_2}}{P_{CO} \times P_{H_2O}} \quad \ldots \ldots \quad 3.15$$

$$K_m = \frac{P_{CO2} \times P_{CH4}}{P^2{}_{H2} \times P^2{}_{CO}} \quad \ldots \ldots \quad 3.16$$

Where K_w and K_m equilibrium constants of reactions 3.11 and 3.13 respectively and P_i is partial pressure of component *i*. These constants were evaluated from standard thermodynamic relationships.

Using a fuel of known elemental composition and a blast consisting of a mixture of air and steam, the only variable parameter is the operating temperature. The mass conservation equations for each element are:

For $C: F_{fc} = G\left(M_{CO2}\frac{12}{44} + M_{CO}\frac{12}{28} + M_{CH4}\frac{12}{16}\right) \ldots \ldots 3.17$

$H: F_{fH} + B_{bH2} = G\left(M_{H2} + M_{CH4}\frac{4}{16} + M_{H2O}\frac{2}{18}\right) \ldots \ldots 3.18$

$O: F_{fO} + B\left(b_{O2} + b_{H2O}\frac{16}{18}\right) = G\left(M_{CO2}\frac{32}{44} + M_{CO}\frac{16}{28} + M_{H2O}\frac{16}{18}\right) \ldots \ldots 3.19$

$N: F_{fN} + Bb_{N2} = GM_{N2} \ldots \ldots 3.20$

$Total: M_{N2} + M_{H2} + M_{CO2} + M_{CO} + M_{H2O} + M_{CH4} = 1 \ldots \ldots 3.21$

Where: $F = amount\ of\ feedstock\ consumed\ in\ kg/h$

$G = amount\ of\ gas\ produced\ kg/h$

$B = amount\ of\ blast\ gas\ consumed\ kg/h$

$fi = mass\ fraction\ of\ component\ i\ in\ fuel$

$bi = mass\ fraction\ of\ component\ i\ in\ blast$

$Mi = mass\ fraction\ of\ component\ i\ in\ gas\ produced$

Substituting the volume fraction of each component i in the gas (using$P\ i/Pt\ = Vi/V_t$), and assuming atmospheric pressure, equations 3.15 and 3.16 can be written as:

$$(V_{CO2}.V_{H2}) - (K_W.V_{CO}.V_{H2O}) = 0 \ldots\ldots\ldots\ldots\ldots\ldots\ldots\ldots\ldots\ldots\ldots\ldots\ldots\ldots\ldots\ldots\ldots\ldots\ldots 3.22$$

$$(V_{CO2}.V_{CH4}) - \left(K_M.P_t{}^2.V_{H2}{}^2.V_{CO}{}^2\right) = 0 \ldots\ldots\ldots\ldots\ldots\ldots\ldots\ldots\ldots\ldots\ldots\ldots\ldots\ldots\ldots\ldots\ldots\ldots\ldots 3.23$$

From: $V_i = \left(\frac{M_i}{\rho_i}\right).\bar{\rho} \ldots\ldots\ldots\ldots\ldots\ldots\ldots\ldots\ldots\ldots\ldots\ldots\ldots\ldots\ldots\ldots\ldots\ldots\ldots\ldots\ldots\ldots\ldots\ldots\ldots\ldots 3.24$

Where: $\rho_i = specific\ weight\ of\ component\ kg/m3$

$\bar{\rho} = specific\ weight\ of\ product\ gas\ kg/m3$

Substituting equation 3.24 into equations 3.22 and 3.23 we have:

$$M_{CO2}.M_{H2} - K_w\left(\frac{\rho_{CO2}.\rho_{H2}}{\rho_{CO}.\rho_{H2O}}\right)M_{CO}.M_{H2O} = 0 \ldots\ldots\ldots\ldots\ldots\ldots\ldots\ldots\ldots\ldots\ldots\ldots\ldots\ldots\ldots\ldots 3.25$$

$$M_{CO2}.M_{CH4} - K_m.P_t{}^2.\left(\frac{\rho_{CO2}.\rho_{CH4}}{\rho_{H2}{}^2.\rho_{CO2}{}^2}\right)M_{CH4}{}^2.M_{CO}{}^2.\bar{\rho}^2 = 0 \ldots\ldots\ldots\ldots\ldots\ldots\ldots\ldots\ldots\ldots 3.26$$

$\bar{\rho}$:Is calculated from the following equation:

$$\frac{1}{\bar{\rho}} = \frac{M_{N2}}{\rho_{N2}} + \frac{M_{H2}}{\rho_{H2}} + \frac{M_{CO2}}{\rho_{CO2}} + \frac{M_{CO}}{\rho_{CO}} + \frac{M_{CH4}}{\rho_{CH4}} + \frac{M_{H2O}}{\rho_{H2O}} \ldots\ldots\ldots\ldots\ldots\ldots\ldots\ldots\ldots\ldots\ldots\ldots\ldots\ldots 3.27$$

Thus a set of 8 equations (3.17 - 3.21, 3.25, 3.26 and 3.27) with 8 unknowns M_{N2}, M_{H2}, M_{CO}, M_{CO2}, M_{H20}, M_{CH4}, G and $\bar{\rho}$ is formed. By using a MATLAB code one can solve these sets of equations numerically to predict the output gas composition and the specific density of the product gas. As far as this thesis is concerned a brief description and analysis will be given in the next chapter.

3.3.4.4 Evaluation of thermodynamic models

From Figure 3.8 important conclusions can be derived concerning that particular set of conditions. However, such a model is of limited value if it is to be used in a design procedure, since

a) It contains no heat balance (the equilibrium is calculated on set temperatures),
b) It is not specific as far as gasifier configuration is concerned,
c) It cannot predict concentrations at hydrocarbons higher than CH_4 (C_2, C_3),
d) It requires other models to be used for detailed gasifier design because it ignores the effect of internal processes,

e) It ignores kinetics, rate processes and heat losses from the system,

f) It ignores ash and tars and other pyrolysis products and

g) It assumes idealistic and that equilibrium is attained.

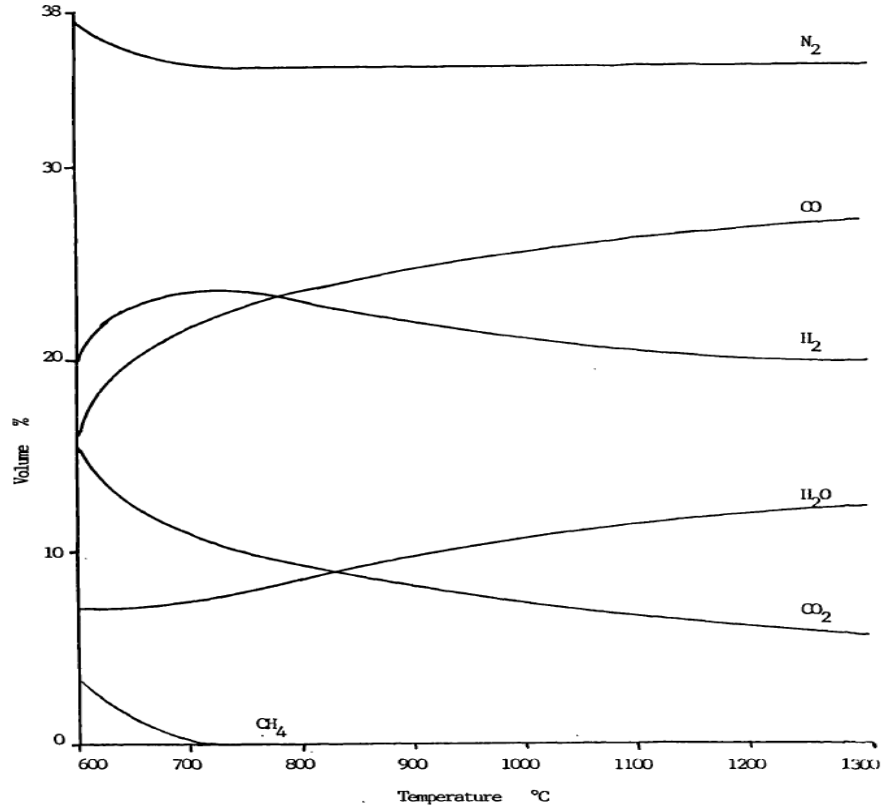

Figure 3.8 Sample equilibrium composition of a product gas from equilibrium modelling

3.3.4.5 Conclusions

Thermodynamic models are widely used for predicting the performance of gasifiers based either on heterogeneous or homogeneous equilibria. However, the higher concentrations of methane and other hydrocarbons found in actual gasifiers cannot be predicted by thermodynamic models. These discrepancies can be attributed either to the fact that gasifiers operate far from equilibrium, or to physical and operational limitations of such systems, such as by-passing or channelling of pyrolysis products, variations in the composition of the feed, heat losses which change the temperature and hence the oxygen requirement and kinetic limitations.

The development of semi-empirical models can overcome some of the disadvantages of thermodynamic models. At present, however, only thermodynamic model by itself is not enough in designing gasifiers. This is a fundamental limitation of thermodynamic models, since they can only be used for prediction of the performance of a gasifier but not for its design. For design empirical models have to be used alongside the thermodynamic model.

3.3.5 Empirical models

3.3.5.1 Introduction

Empirical models are based on mathematical correlations which have been derived from experimental results. Usually a set of independent variables is defined and from these empirical correlations are developed, from which dependent variables can be calculated. On the basis of the dependent and independent variables it is often possible to derive a design procedure.

The most suitable independent variables are:

a) The feedstock flowrate
b) The equivalence ratio (or air factor)
c) The temperature.

However, the total carbon to nitrogen ratio has also been used as an independent variable.

Usually only 1 or 2 independent variables are used in a model.

The following dependent variables are usually obtained:

a) Gas composition
b) Higher heating value of the product gas
c) Thermal efficiency
d) Gas yield
e) Condensate yield
f) Freeboard temperature.

Three such models have recently appeared in the literature and are discussed in this section.

3.3.5.2 The Beck model

The first of these models [59] was derived from experiments for the gasification of feedlot manure in a laboratory reactor with no inert material in the fluidized bed.

Empirical correlations were derived for product gas yield, hydrogen to carbon monoxide mole ratio and carbon conversion as a function of gasifier temperature, oxygen to biomass ratio, steam to biomass ratio and mean solid residence time. Apart from the fact that only a few parameters could be determined by application of the model, these did not include the calorific value or the 'composition of the gas, which are the most important in predicting the performance of the gasifier. Another limitation of the model is that the mean solid residence time has to be used as an independent variable, while there is little information in the

literature about this parameter. However, the most serious drawback of this model is that it was derived from a reactor, which did not operate as conventional fluidized bed, but as a semi updraft- semi fluidized bed unit. Its validity for fluidized bed design is doubtful and in any case, the authors made no attempt to propose a design procedure.

3.3.5.3 The Hoveland model

In this work [60] a set of seven equations were proposed by which the gas yield, calorific value and gas composition could be estimated, with operating temperature as the only independent variable. The results were obtained for the gasification of grain dust in a small laboratory fluidized bed unit (ID 0.05m). The disadvantage of this model, besides the small scale of operation, is that temperature was selected as an independent variable. This is not true in practice, since the operating temperature is determined by the air factor. Also no attempt was made to correlate the data with any other variables and no design procedure was proposed for its application. Therefore it is not considered a reliable model.

3.3.5.4 The Flanigan model

The most comprehensive empirical model was derived at the University of Missouri Rolla, based on numerous experiments made in three fluidized beds of different dimensions [8].

Several attempts were made to derive correlations by using both linear and non-linear equations, semi-empirically based on equilibrium or rate type equations. Little success was obtained with non-linear types of correlations and only slight improvements were obtained by including several variables in the linear equation. These trials also indicated that the ratio of total carbon to nitrogen in the dry gas correlated better than any other variable, with tile important variables of the product gas, including total carbon in the dry gas, higher heating value and total hydrogen in the dry gas. Their results indicated that at a given total carbon to nitrogen ratio, the gas quality was only slightly affected by wide variations in the type of reactor, the existence of a thermal state, the type of feed, the moisture content, the residence time or the bed temperature. However, these variables do affect char and tar formation and the total carbon to nitrogen ratio.

A set of ten equations were proposed by which the fraction of char and tar, the total carbon in dry gas, the higher heating value of the gas, the total hydrogen in the dry gas and the composition of the gas (H_2, CO, CO_2 and CH_4 only) could be determined. A design procedure was also developed. However for the application of the model the total carbon to nitrogen ratio on the gas must be known. This requires detailed pyrolysis studies to determine the fraction of char and tar and their elemental composition, as well as the elemental composition

of the feedstock, before this parameter can be determined. This is a serious limitation of the Flanigan model since usually these data are not available, thus its applicability is restricted. Moreover, by basing the model on the total carbon to nitrogen ratio, the possibility to extend it for oxygen gasification is excluded.

3.3.5.5 Conclusions

It is possible to develop empirical or semi-empirical models based on experimental results. Although these kinds of models are generally applicable only for similar experimental conditions under which they were developed, they can be very useful in scaling up the reactors with a good degree of performance prediction and simpler and more reliable computational procedures.

A common drawback for all the above models is that they include no information whatsoever concerning the design and determination of the hydrodynamics of the fluidized bed or how they could be predicted. Good and stable fluidization is necessary if a gasifier is to operate successfully.

4. ESTIMATION OF BIOMASS SYNTHESIS GAS COMPOSITION USING EQUILIBRIUM MODEL

4.1 Introduction

The central part of the Biomass gasification process is the gasifier reactor. The thermal chemical conversion process that takes place inside the reactor can be described well by the term ‘‘gasification’’, and the model development will be based on the chemical reactions that describe better the gasification process. During the plasma gasification process, various chemical reactions take place that are difficult to be reproduced by a simple equilibrium model. Nevertheless, models based on thermodynamic equilibrium have been used widely, and they are convenient enough for process studies on the influence of the most important waste and process parameters [23].

The following simplified chemical conversion formulae describe the basic gasification process as discussed in section 3.3.4.2: [23]

$$C(s) + H_2O = CO + H_2 \ldots . (Hetrogeneous\ water\ gas\ shift\ eqaution - endothermic\ )$$

$$C(s) + CO_2 = 2CO \ldots\ldots\ldots\ldots\ldots\ldots\ldots\ldots\ldots\ldots (boundouard\ equilibrium - endothermic)$$

$$C(s) + 2H_2 = CH_4 \ldots\ldots\ldots\ldots\ldots\ldots\ldots\ldots\ldots\ldots (hydrogenating\ gasification - exothermic)$$

$$CH_4 + H_2O = CO + 3H_2 \ldots\ldots\ldots\ldots\ldots\ldots\ldots\ldots\ldots (Methane\ decomposition - endothermic)$$

$$CO + H_2O = CO_2 + H_2 \ldots\ldots\ldots\ldots\ldots\ldots\ldots\ldots\ldots (water\ gas\ shift\ reaction - exothermic)$$

For the development of an equilibrium model approach, the number of independent reactions has to be determined by applying the phase rule [8]. In the case where no solid carbon remains in the equilibrium state, only two independent reactions need to be considered for the equilibrium equations. In the case of some remaining solid carbon, i.e. soot, in the gasification products, three independent reactions have to be considered in the equilibrium calculations.

An important point in the modelling procedure is whether equilibrium is reached in the gasification process, i.e. whether the operating conditions allow the chemical reactions to reach an equilibrium state. As far as the gasification temperature is concerned, it is stated that equilibrium is not achieved when the gasification temperature is sufficiently below 800 ^{o}C

[61] (common gasifiers), while it is reached for higher temperatures like those of Bagasse gasification at a temperature around 900°C.

Regarding the other crucial factor relevant to an equilibrium state, i.e. residence time, it has been reported that for air gasification, the residence time is sufficiently long and equilibrium is well verified, while for steam gasification, equilibrium may not reached due to the lower operating temperatures [23].

4.2 Technical and Thermodynamic Data

For evaluating the composition of the output gas there are couple of working variables that must be feed in to the system. These include the working temperature, the ultimate analysis of the fuel to be used, and the composition of the gasifaying medium (Air).

4.2.1 Fuel analysis (Fincha sugar) bagasse

The following table summarizes the ultimate analysis of bagasse found from Fincha Sugar industry including its higher heating value and lower heating value.

Table 4.1 Elemental analysis of the bagasse (Fincha sugar) [24]

Component	Percentage composition	Higher heating value (HHV)
Carbon (C)	23.62%	2340.8 kCal/kg (9.794 MJ/kg)
Hydrogen	3.27%	
Oxygen	22.11%	
Sulphur	0.00%	
Ash	1.00%	Lower heating value (LHV)
Moisture	50%	1869.6 kCal/kg (7.815 MJ/kg)
Total	100%	
Available bagasse on wet bases	174 tone/day	In 22 working hours per day

4.2.2 Set of specifications

a) Type of gasifier :

The gasifier type selected for this thesis is a bubbling fluidized bed gasifier type since extensive literature review regarding the advantage and disadvantages of this type of reactor have been dealt with in the previous chapter.

b) Feed stock:

From Table 4.1, the feed stock flow rate per hour that is available on wet basis is 174,000 kg/day. Preparation of the feed stock is required because the moisture content of the bagasse must be reduced to 15%. The drying of biomass has been discussed in

section 2.5.2. When the moisture content is reduced to 15% , there will be a weight loss of about 35% from the total feedstock flowrate.

$$Wl = available\ bagasse\ on\ wet\ bases \times 35\% \ldots\ldots\ldots\ldots\ldots\ldots\ldots\ldots\ldots\ldots\ldots\ldots\ldots\ldots 4.1$$

where: *Wl= weight lost*

$$Wl = 174{,}000\frac{kg}{day} \times 0.35 = 60{,}900\frac{kg}{day}\ \text{Or}$$

$$Fs = 174{,}000 - 60{,}900 = 113{,}100\frac{kg}{day}(113.1\ \ tone/day)$$

c) Operating condition:

Since the gasification process requires a human control, the operational period (working hour) of 23 hours/day has been selected. This will eventually affect the feedstock flow rate available.

Since all the bagasse produced in the working hours of the factory is not available during the 8 working hours of the reactor one should take only the available bagasse during the 8 hours.

As stated in Table 4.1 working hour of the factory is 22 hours. So the available bagasse within the hour is:

$$Fs = 113.1\frac{tone/day}{22hours} = 5.14\frac{tones}{hour}$$

The other parameters that must be specified here are the working (inlet) temperature and pressure which are 20^{o}C and 1 atm respectively.

d) Ultimate analysis

Table 4.2 gives the ultimate analysis of the bagasse on dry bases after pre-treatment (drying process of the bagasse) and the composition of the blast to be used as a gasifaying medium. These are the compositions or elements we use in the equilibrium modelling to predict the output gas composition.

Table 4.2 Ultimate analysis of bagasse and blast [20]

Components in bagasse	Percentage composition	Blast (Air)	Percentage composition
Carbon (C)	47.3%	Oxygen (O_2)	23.3 %
Hydrogen (H)	6.1%		
Oxygen (O)	35.3%		
Nitrogen (N)	0.00%	Nitrogen (N_2)	76.7%
Sulphur (S)	0.00%		

Ash	11.3%		
		H_2O	0.00%

e) Air factor (S)

Besides the feedstock flow rate the air factor value (equivalency ratio) is the basic parameter. For fluidized bed gasifier a value between [0.2-0.6] is usually selected [8].

The selection of the air factor is "back-end" related, that is, it depends on the application of the product gas. If the gas is to be combusted directly without cooling, then the problem of tar is eliminated (tar does not condense) and the air factor can be selected so that it would produce the highest possible higher heating value of the gas. If the gas is to be cooled and used in an application which cannot tolerate any tar, then the air factor has to be selected so that it would result in high operating temperature in the bed and freeboard in order to crack the tar [25]. The following table gives recommended air factor values for different working conditions. As far as this work is concerned the product gas is going to be used as a combustible gas for a diesel generator it is associated with direct combustion. The air factor (S) best used for better efficiency under the operating condition is 0.233.

Table 4.3 Recommended values of air factor [8]

Application of gas	Air factor	EMCM model			Gas yield
		HHV MJ/NM^3	T bed ^oC	T exit ^oC	kg gas/kg feed MAF
Direct combustion	0.2	6.85	724	651	1.78
Some tar permitted	0.3	5.55	729	737	2.32
No tar permitted	0.4	4.45	848	797	2.80

f) Determination of air flow rate.

In this step, the air flowrate required to achieve the desired air factor is determined. The air flow rate is required for the specification of the compressor, distributor etc. It is calculated on the basis of the definition of air factor. The amount of air required for stoichiometric combustion is determined on basis of the elemental analysis of the feedstock [8]. Thus:

$$S = \frac{G_{air}}{(X_i \times {q_i}^{air}).G_{feed}(MAF)} \quad \ldots\ldots 4.2$$

where: $G_{air} = Mass\ flowrate\ of\ air\ per\ unit\ time\ \left(\frac{kg}{hr}\right)$

$X_i = Fraction\ of\ component\ i\ (O,H,C)\ in\ the\ feed\ stock$

${q_i}^{air} = Amount\ of\ air\ required\ for\ stoichiometric\ combustion$

$$of\ component\ i, in\ kg/kg\ feed$$

$$G_{feed}(MAF) = Mass\ flowrate\ of\ feedstock, in\ kg/h$$

And

$$S = \frac{G_{air}}{(X_c \times {q_C}^{air} + X_H \times {q_H}^{air} - X_O \times {q_O}^{air}).G_{feed}(MAF)} \quad \ldots\ldots 4.3$$

Had the oxidant been oxygen equation 4.3 would become

$$S = \frac{G_{O_2}}{(X_c \times {q_C}^{O2} + X_H \times {q_H}^{O2} - X_O \times {q_O}^{O2}).G_{feed}(MAF)} \quad \ldots\ldots 4.4$$

Where q_i^{O2} is the amount of oxygen required for stoichiometric combustion of i, in kg.

The parameters ${q_i}^{air}$ and q_i^{O2} were determined from stoichiometry.

Thus for ${q_C}^{O2}$:

$$C + O_2 \rightarrow CO_2 \quad \ldots\ldots 4.5$$

For 1 gr. atom carbon requires 1 gr.-mole oxygen for combustion to carbon dioxide, and

$${q_C}^{O2} = \frac{32}{12.01} = 2.665 \frac{kgO_2}{kgC} \quad \ldots\ldots 4.6$$

Thus ${q_C}^{air}$ can be determined as follows:

$${q_C}^{air} = {q_C}^{O2} \times \frac{fraction\ of\ N\ in\ the\ air}{fraction\ of\ O_2\ in\ the\ air} + {q_C}^{O2} \quad \ldots\ldots 4.7$$

$${q_C}^{air} = 2.665 \times \frac{0.767}{0.233} + 2.665 = 11.480$$

The same procedure can be followed to calculate the other stoichiometric values of ${q_H}^{air} and\ {q_O}^{air}$.

The oxygen fraction of the feedstock is subtracted in equation 4.3 and 4.4, since it can also react with carbon and hydrogen. This is supported by pyrolysis studies which have shown that carbon dioxide, carbon monoxide and water are amongst the primary products of pyrolysis [8].

The values of q_i^{O2} and ${q_i}^{air}$ are given in Table 4.4. In this table only carbon, hydrogen and oxygen were considered, since these were the only elements measured in the elemental analysis of the feedstock.

Table 4.4 Stoichiometric values for the combustion of C, H and O by oxygen and air.

Element	q_i^{O2}	${q_i}^{air}$

C	2.665	11.480
H	7.936	34.194
O	0.0	4.308

Thus the air flow rate based on the above definition of air factor and from the selected value of $S = 0.233$ will be calculated as follows by rearranging equation 4.4.

$$G_{air} = S \times (Wt\%C \times 11.48 + Wt\%H \times 34.194 - wt\%O \times 4.308) \times G_{feed}(MAF) \ldots\ldots\ldots\ldots 4.8$$

$$G_{air} = 0.233 \times \left(\frac{47.33}{100} \times 11.48 + \frac{6.1}{100} \times 34.194 - \frac{35.3}{100} \times 4.308\right) \times 5140 \frac{kg}{hr} = 7180.06 \frac{kg}{hr}$$

4.3 Energy analysis

The thermodynamic equilibrium of fluidized bed gasifier model is used with the following assumptions:

(i) The chemical equilibrium between gasifier products is reached,

(ii) The ashes are not considered and

(iii) Heat losses in the gasifier are neglected

A system is said to be in thermodynamic equilibrium when it is in thermal, mechanical and chemical equilibrium. Chemical equilibrium is the state of minimum Gibbs free energy and maximum system entropy. Mechanical equilibrium occurs when the system is not performing or receiving any work. Thermodynamic equilibrium modelling provides a closer prediction when the reaction temperature is sufficiently higher. Equilibrium conditions are difficult to achieve in practical operating conditions and results obtained from thermodynamic equilibrium modelling can serve as the maximum limit on syn gas composition [26].

The global gasification reaction can be written as follows:

$$C_aH_bO_cN_dS_e + wH_2O + m(O_2 + 3.76N_2) \rightarrow n_1H_2 + n_2CO + n_3CO_2 + n_4H_2O + n_5CH_4 + n_6N_2 + n_7H_2S \ldots\ldots\ldots\ldots 4.9$$

Since in this case the compositions of $N = 0\%$ and $S = 0\%$ in the ultimate analysis of the bagasse equation 4.9 will be rewritten as follows:

$$C_aH_bO_c + wH_2O + m(O_2 + 3.76N_2) \rightarrow n_1H_2 + n_2CO + n_3CO_2 + n_4H_2O + n_5CH_4 + n_6N_2 \ldots\ldots\ldots\ldots\ldots\ldots\ldots\ldots\ldots\ldots\ldots\ldots 4.10$$

In which $C_aH_bO_c$ is the substitution fuel formula which can be calculated by the ultimate analysis of the fuel and the mass fractions of the carbon, hydrogen, oxygen. “m” and “w” are

the molar quantity of air entering the gasifier and moisture molar fraction in the fuel, respectively. The variable "m" corresponds to the molar quantity of air used during the gasifying process which is entering the BFBG and depends on the gasification relative fuel/air ratio and the stoichiometric fuel/air ratio relating to the biomass waste as a fuel. On the right-hand side, n*i* are the numbers of mole of the species i that are unknown.

From mass and energy balance

Carbon balance: $a = n_2 + n_3 + n_5$ ……4.11

Hydrogen balance: $2w + b = 2n_1 + 2n_4 + 4n_5$ ……4.12

Oxygen balance: $c + w + 2m = n_2 + 2n_3 + n_4$ ……4.13

Nitrogen balance: $7.52m = 2n_6$ ……4.14

From the independent equilibrium reactions the selected ones are:

1. $CH_4 + H_2O = CO + 3H_2$ ……$(Methane\ decomposition)$
2. $CO + H_2O = CO_2 + H_2$ ……$(water\ gas\ shift\ reaction)$

As per the literature review on section 3.3.4.3 the equilibrium constants are:

$$K_1 = \frac{[CO].[H_2]^3}{[CH_4].[H_2O]} = \frac{[n_2].[n_1]^3}{[n_5].[n_4]} \quad \text{……4.15}$$

$$K_2 = \frac{[CO_2].[H_2]}{[CO].[H_2O]} = \frac{[n_3].[n_1]}{[n_2].[n_4]} \quad \text{……4.16}$$

The values of the equilibrium constants K_1 and K_2 are calculated from the Gibbs free energy [66]:

$$K_p = exp\left(\frac{-\Delta G_T{}^0}{R_u T}\right) \quad \text{……4.17}$$

$\Delta G_T{}^0$ is the difference of the Gibbs free energy between the products and reactants of the equilibrium reactions at standard atmospheric pressure:

$$\Delta G_T{}^0 = \Delta H^0 - T\Delta S^0 \quad \text{……4.18}$$

Back substituting the Gibbs free energy to the equilibrium constants.

$$K_1 = exp\left[-\frac{\left[G_T{}^o{}_{,CO} + 3G_T{}^o{}_{,H_2} - G_T{}^o{}_{,CH_4} - G_T{}^o{}_{,H_2O}\right]}{R_u T}\right] \quad \text{……4.19}$$

$$K_2 = exp\left[-\frac{\left[G_T{}^o{}_{,CO_2} + G_T{}^o{}_{,H_2} - G_T{}^o{}_{,CO} - G_T{}^o{}_{,H_2O}\right]}{R_u T}\right] \quad \text{……4.20}$$

The reference Gibbs free energy is calculated from the following thermodynamic relation [64, 66]:

$$G_T{}^o, i = \widetilde{\Delta h}_f{}^o, 298k + \int_{298}^{Tb} \overline{Cp}(T)dT - T\Delta s^o \ldots\ldots\ldots\ldots\ldots\ldots\ldots\ldots\ldots\ldots\ldots\ldots\ldots\ldots\ldots\ldots 4.21$$

Where $\overline{Cp}(T)$the specific heat at constant pressure is in $(J/mol\,K)$ and is a function of temperature empirically [27]:

$$C_p(T) = A + BT + CT^2 + DT^3 \ldots\ldots\ldots\ldots\ldots\ldots\ldots\ldots\ldots\ldots\ldots\ldots\ldots\ldots\ldots\ldots\ldots\ldots\ldots\ldots 4.22$$

The coefficients are obtained from the following table

Table 4.5 Ideal gas specific heat coefficients of various gases$(T\ in\ K, Cp\ in\ KJ/kmol.k)$[27]

Substance	Formula	A	$BX10^{-2}$	$CX10^{-5}$	$DX10^{-9}$
Hydrogen	H_2	29.11	-0.1916	0.4003	-0.8704
Oxygen	O2	25.48	1.52	-0.7155	1.312
Carbon mono oxide	CO	28.16	0.1675	0.5372	-2.222
Carbon dioxide	CO_2	22.26	5.891	-3.501	7.469
Methane	CH_4	19.89	5.024	1.269	-11.01
Water	H_2O (g)	32.24	0.1923	1.055	-3.595

Entropy of ideal gas is also given as follows [27]:

$$S = \bar{s}^0 + \int_{T0}^{Tb} \frac{\overline{C_p}}{T} dT - Rln\frac{P}{P_o} \ldots\ldots\ldots\ldots\ldots\ldots\ldots\ldots\ldots\ldots\ldots\ldots\ldots\ldots\ldots\ldots\ldots\ldots\ldots\ldots 4.23$$

T_b=900 ^{o}C or 1173K and T_o= 25^{o}C or 298K while the working pressure is slightly above P_{atm}. The enthalpy of formation $\widetilde{\Delta h}_f{}^o$ and the entropy s^o of ideal gas at the reference state (at 298k) are listed in the table 4.5 to be substituted in equation 4.21.

Table 4.6: $\widetilde{\Delta h}_f{}^o, 298k$ for some gas compounds. [27]

Compound	$\widetilde{\Delta h}_f{}^o, (\frac{kJ}{kmol})$	$\bar{s}^0(J/mol\,K)$
H2	0.0	130.59
O2	0.0	205.03
CO	-110.530	197.91
CO2	-393.52	213.64
CH4	-74.85	186.19
H2O(l)	-285.84	69.94
H2S	-20.501	205.757
SO2	-296.833	284.094

After finding the Gibbs free energy for each of the compounds using equations 4.21-4.23 the values will be substituted in equation 4.19 and 4.20 to find the equilibrium constants K_1 and K_2. Solving these sets of equation by hand is rigorous and very tiresome so a MATLAB code

listed in Appendix I is used to evaluate the equilibrium constants analytically as a function of the bed temperature selected for equilibrium. These equilibrium constants are going to be used as an input for solving equations 4.15 and 4.16 in the process of solving for product gas composition evaluation which will be discussed in the following section.

From the Mat lab code we were able to predict the values of equilibrium constants.

$K_1 = 0.866 \text{ and}$

$K_2 = 0.5773$

These values strongly agree with the values that can be found in literatures like the chemical properties hand book [23].

Substituting the equilibrium constants K_1 and K_2 in equations 4.15 and 4.16 respectively:

$$0.866 \times [n_5].[n_4] = [n_2].[n_1]^3 \quad \ldots\ldots 4.24$$

$$0.5773 \times [n_2].[n_4] = [n_3].[n_1] \quad \ldots\ldots 4.25$$

Generally there are 6 unknowns to be determined n_1-n_6 wt% composition of each product gas. And we also have 6 equations 4.11-14 and 4.24 and 4.25 which makes it mathematically defined to be solved. A mat lab numerical analysis is also used in solving these equations as presented in the Appendix II.

4.4 Algorithm and General Formula Derivation

Equations 4.11-14 and 4.24 and 4.25 will be converted in to a more suitable form of the following which makes it easy to be computed numerically.

$$F_1 = n_2 + n_3 + n_5 - a = 0$$

$$F_2 = 2n_1 + 2n_4 + 4n_5 - 2w - b = 0$$

$$F_3 = n_2 + 2n_3 + n_4 - c - w - 2m = 0$$

$$F_4 = 2n_6 - 7.52m = 0$$

$$F_5 = [n_2].[n_1]^3 - 0.866 \times [n_5].[n_4] = 0$$

$$F_6 = [n_3].[n_1] - 0.5773 \times [n_2].[n_4] = 0$$

For solving the system of equations, Newton-Jacobi method is used. After an input of the bed temperature which gives the equilibrium model constants and the ultimate analysis composition of the biomass (bagasse) it requires an initial guess for each of the syn gas composition. The method has a general mathematical model approach of the following form.

$$F_{x1} = F_{x0} + J(x_1 - x_0) \quad \ldots\ldots 4.26$$

Where $F_{x0} = \text{values of the functions at the initial guess point}$

$$F_{x1} = values\ of\ the\ functions\ at\ the\ new\ points$$

$$J = the\ jacobian\ matrix$$

$$J = \begin{bmatrix} \frac{\partial F_1}{\partial x_1} & \cdots & \frac{\partial F_1}{\partial x_n} \\ \vdots & \ddots & \vdots \\ \frac{\partial F_m}{\partial x_1} & \cdots & \frac{\partial F_m}{\partial x_n} \end{bmatrix} \quad \text{.....4.27}$$

The new values of the unknowns $X1 - X6$ are found from the following relation of Newton Jacobi method.

$$X_{new} = X + J^{-1}F \quad \text{.....4.28}$$

After finding the inverse of the jacobian matrix by multiplying it with the functional value of the previous $X1 - X6$ first from the initial guesses and adding it to the previous values of X's we will find the new value for X's to be inserted in equation 4.26. The iteration continues until equation 4.26 is satisfied or the difference between the consecutive values of X's is less than the desired error margin.

The mat lab code presented in Appendix II works on the above principle of Newton Jacobi method. Another variable on the model besides the working temperature and the ultimate analysis is the moisture content of the biomass. The output gives the value of the output gas compositions at different moisture contents. As far as this thesis is concerned the moisture content at hand is 15% in dry biomass level or 50% in wet bases. The following algorithm flow chart shows the general approach used in the Mat-lab code.

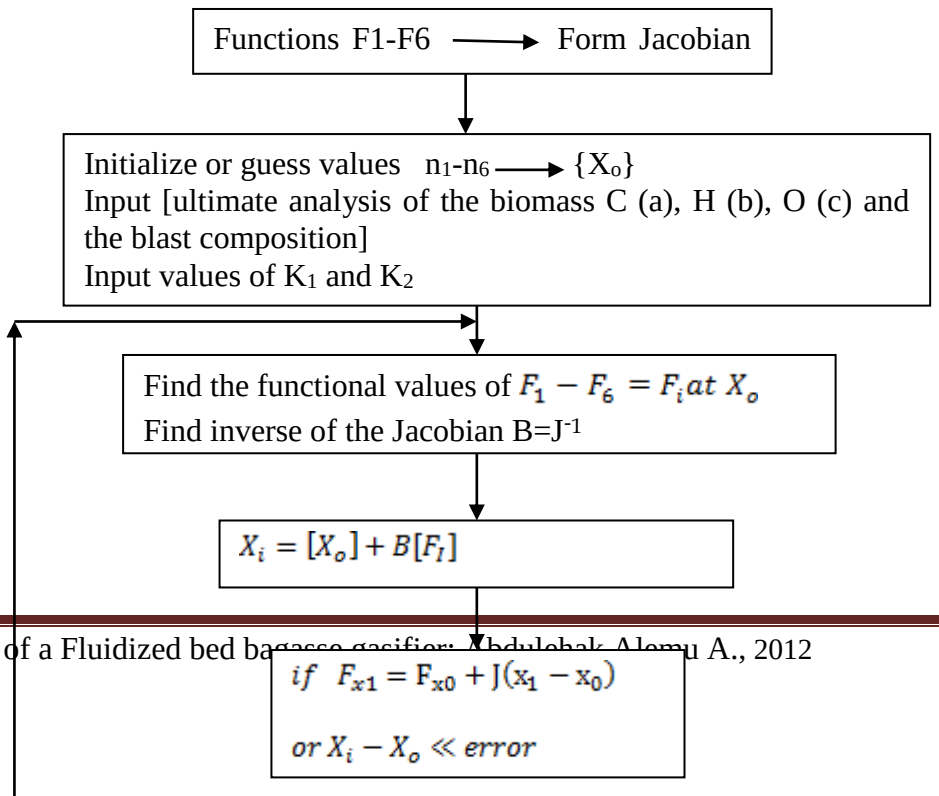

Figure 4.1 Algorithm flow chart for product gas composition

4.5 Result and Discussion

From the ultimate analysis of Table 4.2 the output from the Mat lab code is presented in table 4.7. Although the result obtained is at different moisture contents of the bagasse; but we only had to focus on the moisture content percentage of 15% since the bagasse at hand has the same amount of moisture content after preliminary drying. The result is also categorized on two bases either in dry biomass (ultimate analysis) or on wet bases with moisture content of 15%. The results are in Molar fraction or volumetric fraction then a percentage of each syn gas composition is calculated.

Table 4.7 Output from Mat lab Code (percentage composition of the product gas)

			Dry basis		On wet basis at moisture content of 14.6324≈15 %		
Variable	Gas	Molar mass M	Molar/ volumetric fraction	Vol.%	Molar/ volumetric fraction	Vol. %	Wt%
n_1	H_2	2.016	0.0915	9.15%	0.3810	9.24%	0.7210%
n_2	CO	28.011	0.0776	7.76%	0.5332	12.93%	14.017%
n_3	CO_2	44.01	0.1630	16.3%	0.4363	10.58%	18.025%
n_4	H_2O	18.015	0.00	0%	0.5399	13.09%	9.1256%
n_5	CH_4	16.043	0.0054	0.54%	0.0305	0.739%	0.460%
n_6	N_2	28.013	0.6625	66.15%	2.2028	53.418%	57.933%

The composition presented in table 4.7 has agreed significantly to those presented in table 2.2 and most literatures available are closely related to this output. As it can be seen in the above table the composition of methane gas is very small since the operating temperature is around 900^0C which validates the theories presented on literatures.

4.5.1 Higher heating value "HHV"

This is the higher heating value of all cool and clear gas product components added together (the higher heating value is numerically equal to the standard heat of combustion of a component but of opposite sign), with all the water initially present as liquid in the fuel and

that present in the combustion products, condensed to the liquid state, at constant pressure and at temperature of 25 ^{0}C: [8]

$$HHV = \sum_{1}^{n} wt\%\, i \times HCi \ldots\ldots\ldots\ldots\ldots\ldots\ldots\ldots\ldots\ldots\ldots\ldots\ldots\ldots 4.29$$

Where HCi is the standard heat of combustion of component inMJ/kg. The standard heat of combustion of the components found in the cool and clean gas is given in the Table 4.8.

Table 4.8.Standard heat of Combustion of product gas [27]

Component	Standard heat of combustion MJ/kg
H_2	141.80
CH_4	55.50
CO	10.11
C_2H_4	50.30
C_2H_6	51.87

Thus the higher heating value of a gas consisting of the above five (amongst others) components is given by equation 4.28

$$HHV = H_2Wt\% \times 141.8 + CH_4Wt\% \times 55.5 + COWt\% \times 10.11 + C_2H_4Wt\% \times 50.3 + C_2H_6Wt\% \times 51.87 \ldots\ldots\ldots\ldots\ldots\ldots\ldots\ldots 4.30$$

The weight of the higher hydrocarbons (C_2H_4 *and* C_2H_6)has never been determined by the Equilibrium model since there composition is negligible.

$$HHV = 0.00721 \times 141.8 + 0.00436 \times 55.5 + 0.1407 \times 10.11 = 2.687 \frac{MJ}{kg}$$

4.5.2 Specific Weight of the product Gas

Density of the product gas is calculated based on the density of each components of the product gas using the following relation.

$$\rho_{gas} = \sum_{1}^{n} vol\%\, i \times \rho_i \ldots\ldots\ldots\ldots\ldots\ldots\ldots\ldots\ldots\ldots\ldots\ldots\ldots\ldots 4.31$$

The following table gives densities of some important gasses that are found in the product gas.

Table 4.9: Densities of different gasses [27]

Gas	Formula	Density Kg/m^3 (STP)
Hydrogen	H_2	0.0899
Oxygen	O_2	1.429
Nitrogen	N_2	1.2506

Carbon monoxide	CO	1.250
Carbon dioxide	CO_2	1.977
Methane	CH_4	0.717
Ethylene	C_2H_4	1.260
Ethane	C_2H_6	1.264
Propane	C_3H_6	1.748

Excluding the higher hydrocarbons due to their insignificance in the composition of the product gas equation 4.30 can be re written as follows:

$$\rho_{gas} = H_2Vol\% \times 0.0899 + O_2Vol\% \times 1.429 + N_2Vol\% \times 1.2506 + CO\ Vol\% \times 1.250 + CO_2Vol\% \times 1.977 + CH_4Vol\% \times 0.717 \ldots\ldots\ldots\ldots\ldots\ldots\ldots\ldots\ldots\ldots\ldots\ldots 4.32$$

$$\rho_{gas} = (0.0924 \times 0.0899) + (0.53418 \times 1.251) + (0.1293 \times 1.25) + (0.1058 \times 1.977) + (0.00739 \times 0.718) = 1.052 \frac{kg}{m^3}$$

$$HHV = 2.687 \frac{MJ}{kg} \times 1.052 \frac{kg}{m^3} = 2.827 \frac{MJ}{m^3}$$

Both the density and the higher heating values of the product gas are in agreement with the various literatures presented in chapter one of this thesis.

4.5.3 MASS BALANCE

4.5.3.1 Introduction

The total quantity of gas produced was calculated from a nitrogen balance over the air input and the nitrogen content of the product gas analysis. [8]

$$Total\ product\ gas\ flowrate \frac{kg}{h} = \frac{Total\ amount\ of\ N2fed\ to\ reactor\ (from\ air\ flow\ rate) kg/h}{Weight\ \%\ of\ nitrogen\ in\ product\ gas\ analysis} \ldots\ldots\ldots\ldots\ldots\ldots 4.33$$

It was assumed that nitrogen did not react with oxygen at these temperatures (below 950 °C) to any significant extent.

4.5.3.2 Input flow rate

Note: Q- represents volumetric flow and G- represents mass flow rates.

I. $Mass\ air\ flow\ rate\ (G) = Q_{air} \times \rho_{air} = 7180.06 \frac{Kg}{hr}$

$$Q_{air} = \frac{G_{air}}{\rho_{air}} = \frac{7180.06}{1.293} = 5553.02\frac{m^3}{hr}$$

II. $Bagasse\ feed\ flow\ rate\ (G_{feed}) = 5140\frac{kg}{hr}$

$$Total\ input\ flow\ rate\ = G_{air} + G_{feed} = 7180.06 + 5140 = 12{,}320.06\frac{kg}{hr}$$

III. Ash, moisture and elemental input flow rate

a) Ash flow rate:

$$G_{ash} = G_{feed} \times \frac{A.C}{100} = 5140 \times \frac{11.3}{100} = 580.82\frac{kg}{hr}$$

b) Moisture flow rate:

$$G_M = G_{feed} \times \frac{M.C}{100} = 5140 \times \frac{15}{100} = 771\frac{kg}{hr}$$

c) Feed (MAF) flow rate:

$$G_{MAF} = G_{feed} - G_M - G_{ash} = 5140 - 771 - 580.82 = 3788.2\frac{kg}{hr}$$

d) Oxygen input:

$$O_{input} = G_{air} \times \frac{23.3}{100} + G_{MAF} \times \frac{Owt\%}{100} + G_M \times \frac{16}{18}$$

$$O_{input} = 7180.06 \times 0.233 + 3788.2 \times 0.353 + 771 \times \frac{16}{18} = 3695.52\frac{kg}{hr}$$

e) Nitrogen input:

$$N_{input} = G_{air} \times \frac{76.7}{100} + G_{MAF} \times \frac{wt\%}{100}$$

$$N_{input} = 7180.06 \times 0.767 + 3788.2 \times 0\% = 5507.1\frac{\text{kg}}{\text{hr}}$$

f) Carbon input:

$$C_{input} = G_{MAF} \times \frac{\text{Cwt\%}}{100} = 3788.2 \times 0.437 = 1791.818\frac{\text{kg}}{\text{hr}}$$

g) Hydrogen input:

$$H_{input} = G_{MAF} \times \frac{\text{H Wt\%}}{100} + \text{G}_\text{M} \times \frac{2}{18} = 3788.2 \times \frac{6.1}{100} + 771 \times \frac{2}{18} = 316.746\frac{\text{kg}}{\text{hr}}$$

4.5.3.3 Output flow rate

From equation 4.32 the output gas flow rate is calculated as follows:

$$Total\ product\ gas\ flowrate\frac{Kg}{h}$$
$$= \frac{Total\ amount\ of\ N2fed\ to\ reactor\ (from\ air\ flow\ rate)kg/h}{Weight\ \%\ of\ nitrogen\ in\ product\ gas\ analysis} \ldots\ldots\ldots\ldots\ldots\ldots 4.34$$

$$G_{gas} = \frac{\text{Total N input}}{\text{N}_2\text{Wt\%in gas}} \times 100 = \frac{5507.1}{57.933} \times 100 = 9{,}505.98\frac{\text{kg}}{\text{hr}}$$

$$Q_{gas} = \frac{G_{gas}}{\rho_{gas}} = \frac{9{,}505.98}{1.052} = 9036.10\frac{\text{m}^3}{\text{hr}}$$

4.5.3.4 Output product gas flow rates

Similarly the flow rate of each syn gas constitutes can be calculated for example Hydrogen gas flow rate in the syn gas has been demonstrated and the rest of the gasses flow rate are summarised as follows:

H_2 flow rate:

$$\left(G_{H_2}\right) = G_{gas} \times \frac{H_2 Wt\%}{100} = 9{,}505.98 \times \frac{0.7210}{100} = 68.54 \frac{kg}{hr}$$

$$N_2 \text{ flow rate} = 5507.1 \frac{kg}{hr}$$

$$CH_4 \text{ flow rate} = 43.727 \frac{kg}{hr}$$

$$CO_{flowrate} = 1332.45 \frac{kg}{hr}$$

$$CO_{2\ flow\ rate} = 1713.453 \frac{kg}{hr}$$

$$G_{steam} = 9505.98 \times \frac{9.1256}{100} = 867.50 \frac{kg}{hr}$$

Calculation for the fly ash output flowrate:

Since the equilibrium model doesn't predict the output ash it's common to consider the rest of the flow rate as a fly ash from the total input flow rate. And of course since from the air ratio we used and from the assumption of the equilibrium model that all carbon is burned out at equilibrium point the rest of the flow rate is a condensate having a content of Oxygen and hydrogen gas in it. One can multiply the Input ash flow rate value by $\frac{100}{30} = 3.33$ since it was found in literatures that the fly ash has a carbon content of 70wt% what was left 30 % is the condensate which consists hydrogen and oxygen [8].

$$G_{flyash} = G_{ash} \times 3.33 = 580.82 \times 3.33 = 1934.13 \frac{kg}{hr}.$$

$$Total\ output\ flow\ rate = G_{gas} + G_{flyash} = 9{,}505.98 + 1934.13 = 11{,}440.11 \frac{kg}{hr}$$

4.5.3.5 Elemental output flow rates

I. Oxygen output:

$$O_{output} = G_{CO_2} \times \frac{32}{44} + G_{CO} \times \frac{16}{28} + (G_{flyash} \times 30\% + G_{steam}) \times \frac{16}{18}$$

$$O_{output} = 1713.453 \times \frac{32}{44} + 1332.45 \times \frac{16}{28} + ((1934.13 \times 0.3) + 867.5) \times \frac{16}{18}$$
$$= 3294.42 \frac{\text{kg}}{\text{hr}}$$

II. Nitrogen output:

$$N_{output} = 5{,}507.1 \frac{\text{kg}}{\text{hr}}$$

III. Carbon output:

$$C_{output} = G_{CH_4} \times \frac{12}{16} + G_{CO} \times \frac{12}{28} + G_{CO_2} \times \frac{12}{44} + (G_{flyash} - \text{G}_{\text{cond}}) \times 0.7$$

$$C_{output} = 43.727 \times \frac{12}{16} + 1332.45 \times \frac{12}{28} + 1713.453 \times \frac{12}{44} + (1934.13 - 580.24) \times 0.7$$
$$= 2018.87 \frac{\text{kg}}{\text{hr}}$$

IV. Hydrogen output:

$$H_{output} = G_{H_2} + G_{CH_4} \times \frac{4}{16} + (G_{flyash} \times 30\% + \text{G}_{\text{cond}} + \text{G}_{\text{steam}}) \times \frac{2}{18}$$

$$H_{output} = 68.84 + 43.727 \times \frac{4}{16} + \left((1934.13 \times 0.3) + 580.24 + 867.5\right) \times \frac{2}{18}$$
$$= 305.1 \frac{\text{kg}}{\text{hr}}$$

4.5.3.6 Balance

$$Total = \frac{total\ output\ flow\ rate}{total\ input\ flow\ rate} \times 100 = \frac{11440.11}{12320.06} = 92.85\%$$

$$O_{balance} = \frac{3294.42}{3695.52} \times 100 = 89.14\%$$

$$N_{balance} = \frac{5507.1}{5507.1} \times 100 = 100\%$$

$$C_{balance} = \frac{2018.87}{1791.818} \times 100 = 112.97\%$$

$$H_{balance} = \frac{305.1}{316.76} \times 100 = 96.3\%$$

The total mass balance closure was in the range of 89-112%. The errors associated are of various parameters, but also the fact that two of the parameters (condensate and fly ash) were considered only on facts of previous works not on the values found by the material balance. The unsteady feedstock flowrate was another source of error which was revealed in the mass balance calculations. In addition, higher hydrocarbons than C_4 were sometimes detected (but

not in sufficient concentrations to allow for accurate qualitative and quantitative determination), but could not be used in the calculations.

It was generally accepted that on different literatures [8], if the mass balance closures are in the range of 110-90%, the results can be considered acceptable. Considering the various uncertainties explained above, the results of the mass balance were fairly good. The results of the mass balance are fairly good when compared to other published works but care should be taken in improving the efficiency by varying different parameters.

4.5.4 Gas yield "Y''

This is ratio of weight (kg) of gas produced over that of feedstock (kg) (moisture and ash free basis) fed to the reactor per unit time. When specifying the optimum air factor for a specific reactor and feedstock, the gas yield must be taken into consideration, since it is increasing with higher values of air factor while the higher heating value of the gas is decreasing. Thus:

$$Y = \frac{\text{weight of gas produced per unit time}}{\text{weight of feedstock (MAF) fed per unit time}} \quad \ldots\ldots\ldots\ldots\ldots\ldots\ldots\ldots\ldots\ldots\ldots\ldots\ldots\ldots\ldots\ldots 4.35$$

$$Y = \frac{9{,}505.98}{3788.2} = 2.509$$

The gas yield is an important parameter, since it can predict the total flow of gas from the feedstock flow. In general a gas yield between 2 and 3.5 kg gas/kg MAF feedstock was achieved [8] in the air factor range of interest (0.2-0.4) in most of the literatures found indicating that the value of gas yield calculated above is fairly acceptable value.

4.5.5 Thermal efficiency ''y''

This is defined as the ratio of the chemical energy in the cool, clean gas produced to that of the chemical energy in the feedstock per unit time, expressed in percentage [8].

$$y = \frac{G_{gas} \times HHV_{gas}}{G_{feedstock} \times HHV_{feedstock}} \times 100 \quad \ldots\ldots\ldots\ldots\ldots\ldots\ldots\ldots\ldots\ldots\ldots\ldots\ldots\ldots\ldots\ldots\ldots\ldots\ldots\ldots\ldots\ldots 4.36$$

$$y = \frac{9{,}505.98 \times 2.687}{5140 \times 9.794} \times 100 = 50.74\%$$

This value of thermal efficiency is fairly acceptable value. Had the sensible heat of the product gas have also been recuperated, and then the overall efficiency of the gasification

process in the fluidized bed could increase to about 80% [8]. Most of the literatures presented in chapter one have a thermal efficiency range of 40-55% that agrees with the work that has been done here despite the working biomass differs since we are using bagasse only while those works are entitled to wood and barks.

4.5.6 Heat of reaction "HR"

This is defined as the change in enthalpy resulting from the reaction taking place under a pressure of 1 atm., starting and ending with all materials at a constant temperature of 25°C [8].

For a reaction between organic compounds the basic thermochemical data are generally available in the form of standard heats of combustion. The standard heat of reaction where organic compounds are involved can be calculated by using directly the standard heats of combustion instead of standard heats of formation [8]. An energy balance is employed (see equation 4.36) where the standard reference state is not the elements, but the products of combustion at 25 ^{0}C and 1 atm. in the state of aggregation specified by the heat of combustion data. For example, the enthalpy of methane relative to its products of combustion, gaseous carbon monoxide and liquid water, is equal to the negative value of its standard heat of combustion or 55.5 MJ/kg. Therefore in any equation involving combustible materials the formula of a compound may be replaced by its enthalpy relative to its products of combustion. The enthalpy of the products minus the enthalpy of the reactants, or the standard heat of combustion of the reactants minus the standard heat of combustion of the products, is equal to the standard heat of reaction, ΔH_r [8]. Thus:

$$\Delta H_r = \sum \Delta H_c(reactants) - \sum \Delta H_c(products) \ \ at\ 25°C \ldots\ldots\ldots\ldots\ldots\ldots\ldots\ldots\ldots\ldots\ldots 4.37$$

Where ΔH_c is the standard heat of combustion of the reactants and products in $\frac{MJ}{kg}$.

The heat of reaction H_R is then calculated by dividing the standard heat of reaction ΔH_r by the amount of feedstock (MAF) fed in the reactor per unit time. Thus:

$$H_R = \frac{\Delta H_r}{G_{feedstock\ (MAF)}} \ldots\ldots\ldots\ldots\ldots\ldots\ldots\ldots\ldots\ldots\ldots\ldots\ldots\ldots\ldots\ldots\ldots\ldots\ldots\ldots\ldots\ldots\ldots\ldots\ldots\ldots 4.38$$

The overall gasification reaction can be written as:

$$Feedstock + air \rightarrow aH_2 + bCH_4 + cCO + dCO_2 + eH_2O \ldots\ldots\ldots\ldots\ldots\ldots\ldots\ldots\ldots\ldots\ldots 4.39$$

In terms of mass, equation 3.38 becomes:

$$X_{1kg}feedstock(MAF) + X_{2kg}air$$

$$\rightarrow X_{3kg}H_2 + X_{4kg}CH_4 + X_{5kg}CO + X_{6kg}CO_2 + X_{7kg}H_2 \ldots\ldots\ldots\ldots\ldots\ldots\ldots 4.40$$

Where $X_1 - X_7$represent the amount for each component, in kg.

Substituting equation 3.40 in to equation 3.37 gives:

$$\Delta H_r = (X_1\Delta H_c feedstock(MAF) + X_2\Delta H_c air) - (X_3\Delta H_c H_2 + X_4\Delta H_c CH_4 + X_5\Delta H_c CO + X_6\Delta H_c CO_2 + X_7\Delta H_c H_2O) \ldots\ldots\ldots\ldots\ldots\ldots\ldots\ldots\ldots\ldots\ldots\ldots\ldots\ldots\ldots\ldots\ldots\ldots\ldots\ldots\ldots\ldots 4.41$$

But $\Delta H_c air = \Delta H_c CO_2 = \Delta H_c H_2O = 0$

$$\Delta H_r = \left(X_1\Delta H_c feedstock(MAF)\right) - (X_3\Delta H_c H_2 + X_4\Delta H_c CH_4 + X_5\Delta H_c CO)$$

$$\Delta H_c feedstock(MAF)\ from\ HHV\ of\ feed\ stock = 9.794\frac{mJ}{kg}\ table(3.1)$$

$\Delta H_c H_2, \Delta H_c CH_4 and\ \Delta H_c CO\ can\ be\ obtained\ from\ table$ 4.8, thus the standard heat of reaction is:

$$\Delta H_r = [(3788.2 \times 9.794) - (68.54 \times 141.80) - (43.727 \times 55.50) - (1332.45 \times 10.11)]$$
$$\Delta H_r = 11484.741MJ$$

Then the heat of reaction will be:

$$H_r = \frac{\Delta H_r}{G_{feedstock\,(MAF)}} = \frac{11484.741}{3788.2} = 3.03\frac{MJ}{kg}$$

These results indicate that the overall pyrolysis reaction with this feedstock is mildly exothermic, with a heat of reaction of about 3 MJ/kg. For a feedstock with high moisture content the heat of pyrolysis would become endothermic, while for a dry feedstock the exothermicity of the heat of pyrolysis would increase. These results are consistent with published results. There is a clear trend that the heat of reaction increases with increasing air factors. This is readily explained by the occurrence of more complete combustion as the oxygen content increases in relation to the feedstock flowrate. Under such conditions the concentrations of hydrogen, methane, carbon monoxide, ethylene, ethane and tars decrease, while the concentration of the products of combustion (carbon dioxide and water) increase so that one can increase the heat of reaction in doing so [8].

5. GASIFIER SIZING AND FLUIDIZATION PROPERTIES

5.1 Introduction

The reactor subsystem is made up of the reaction chamber (three cylindrical modules arranged vertically), external heat insulation and an air distribution plate. For the design calculations, the physical properties of the bagasse and the inert material (common sand) composing the bed were determined. The values of these properties for both materials appear in later sections [5].

The sizing of the fluidized bed is established via several sets of assumption and equations. These assumptions are important to enable a practical design of the gasifier. The air flow (and the gas flow) through the bed is assumed to be well distributed and homogeneous mixture of product gas obtained at averaged bed temperature of 800^0C. The minimum fluidization voidage (ε_{mf}) of the bed is assumed 0.5 (ranging between 0.5 and 0.85) [28]. The fluidized bed is assumed to be operated with silica sand which has a particle density (ρ_p) of 2600 kg/m^3 [28] and average particle diameter (D_P) of 0.414 mm. The bed operates at slightly above atmospheric pressure because the air delivered by the compressor is above atmospheric pressure. Two of the first steps in sizing activity are the determination of the fluidized bed reactor volume and the bed diameter [28] which will be discussed step by step in the following sections.

5.2 Determination of reactor Volume and Retention Time

The overall reactor dimensions are necessary for construction. In chemical reactor engineering science, the volume of the reactor and the flow rates of the reactants and products are related by the retention time of the reactants and/or products [8].

$$R_T = \frac{V_r}{Q_{gas}} \quad \text{.....5.1}$$

where: R_T = the retention time

V_r = The reactor volume

Q_{gas} = Volumetric flow rate of gas

The retention time of gases in a fluidized bed gasifier is a parameter of significance for two reasons [8]. Firstly at higher retention times more time is provided for the gases to remain in the reactor and thus for the different reactions to proceed further. Also, the tars remain longer

in a high temperature environment and therefore the yields of their cracking products should increase. Moreover for the elutriated char particles, their degree of gasification will increase with longer retention time and this would improve the carbon conversion efficiency as well as the overall quality of the gas.

Secondly, the retention time is a useful tool for scaling up purposes, since it is used to determine the volume of the reactor under similar operating conditions [8].

The retention time of the gases in the reactor is a function of the gas flowrate, since retention time is equal to the volume of the reactor divided by the volumetric flowrate [8]. When reactions which result in a change of volume as with gasification are dealt with, the increase or decrease of the volumetric flowrate should be accounted for.

It is very difficult - and there is lack of data - to predict the volumetric flowrate with accuracy in each region of a fluidized bed gasifier. Consider a reactor where air is introduced at the bottom of the bed and feedstock above the bed: initially the volumetric flowrate will increase considerably across the bed due to the combustion and gasification of char. Above the bed, the volumetric flowrate should also increase up to a certain height, due to the degradation of the biomass and formation of organic gases and vapours. However, above this region cracking reactions take place which further increase the volume of the gas, but the temperature is lower than the bed and thus the volumetric flowrate decreases due to lower temperatures. It is, therefore, evident that the prediction of the actual flowrate of the gases in a fluidized bed gasifier is rather complex and difficult for an accurate determination of the retention time [8].

In order to calculate the retention time of the gases, an average gas volumetric flowrate was used. It was simply assumed as the average of the air flowrate at bed temperature and the product gas flowrate at freeboard temperature.

By increasing the air flow rate, the retention time decreases significantly. The retention times deduced in this work thus ranged from about 10 to 50 seconds. The higher the retention time of gases in the reactor, the higher is the possibility that the gasification reactions will attain equilibrium, since the gases remain at high temperatures longer and since more time will be provided for fines and tars to be gasified or cracked. In principle this should affect the higher heating value of the gas, since at longer retention time the yields of the gasification products are supposed to increase [8].

The average flowrate of the gas at reactor conditions is:

$$Q_{gas,avr} = \frac{1}{2} \times \left[Q_{air} \times \left(\frac{T_B + 273}{273} \right) + Q_{gas} \times \left(\frac{T_o + 273}{273} \right) \right] \ldots\ldots\ldots\ldots\ldots\ldots\ldots\ldots\ldots\ldots 5.2$$

Where: $Q_{gas,avr} = Average\ gas\ flowrate$

$Q_{air} = Air\ flowrate$

$Q_{gas} = Product\ gas\ flowrate$

$T_B = Temperature\ at\ the\ bed\ surface$

$T_o = Temperature\ at\ the\ outlet\ of\ the\ reactor$

$$Q_{gas,avr} = \frac{1}{2} \times \left[\frac{5553.02}{3600} \times \left(\frac{800 + 273}{273} \right) + \frac{9036.1}{3600} \times \left(\frac{750 + 273}{273} \right) \right] = \frac{6.0626 + 9.4057}{2}$$

$$Q_{gas,avr} = 7.734 \frac{m^3}{s}$$

The volume of the reactor can be calculated by first applying equation 5.1 and then assuming a retention time.

The retention time can be selected on the basis of the application of the product gas. Thus, if the gas is to be combusted directly, then the importance of retention time is significantly reduced and low values 10-15 are acceptable. However, if high concentration of tar is undesirable, then higher retention times must be selected to minimize tar by providing longer residence time in the reactor. The same is true when high carbon conversion efficiency is required. The recommended retention times according to the application of the product gas are given in Table 5.1.

Table 5.1 Recommended retention time of Gas [8]

Application of Gas	Retention time of gas(s)
Direct Combustion	10-15
Some Tar Permitted	15-20
No Tar Permitted	20-25

Since the gas is intended to be used for direct combustion in a gas turbine we can use a retention time of 10-15. Taking a retention time R_T of 12.5; the volume of the reactor can be estimated using equation 5.1

$$V_r = R_T \times Q_{gas,avr.} = 12.5 \times 7.734 = 96.675\ m^3$$

5.3 Determination of Bed (Gasifier Internal) Diameter and Fluidization Parameters

5.3.1 Introduction

The first step in sizing activity is the determination of the fluidized bed diameter, which uses the following correlation:

The air flow rate (m_{air}) through the bed is given as a function of bed diameter (D_g) and the gas superficial velocity (U_s). [28]

$$m_{air} = \rho_{air} \times \left(\frac{\left(\pi \times {D_g}^2\right)}{4} \right) \times U_s \quad \ldots\ldots 5.3$$

The following sets of equations are required to determine the superficial velocity (U_s), which necessitates the information on the bed minimum fluidization velocity (U_{mf}). The relation between superficial velocity (U_s) and minimum fluidization velocity (U_{mf}) is given as follows [69].

$$U_s = 2 \times U_{mf} \quad \ldots\ldots 5.4$$

The minimum fluidization velocity is determined by using the following equation [20].

$$U_{mf} = \left[\frac{{d_p}^2}{\left(150 \times \mu_g\right)} \right] \times \left[g \times \left(\rho_p - \rho_g\right) \times \frac{\left(emf^3\right)}{(1 - emf)} \right] \quad \ldots\ldots 5.5$$

where:

$\mu_g = gas\ viscosity$

$\rho_p = bed\ fluidization\ particle\ density$

$\rho_g = gas\ density$

$emf = bed\ voidage\ at\ minimum\ fluidization$

Using the superficial value calculated from the above equations, the bed diameter is determined, whereby the air flow rate had already been established in previous section. The next step will require the determination of bed dynamic height (H_B), which is the section of the bed where the fluidized particles (including bagasse) will rise when air is injected for reaction. This is determined using the relationship between bed residence time (t) and U_{mf}.

The overall reaction bed height (H) is the sum of the height of bagasse feeding point (H_f) and dynamic bed height.

$$H_B = t \times U_{mf} \quad \ldots\ldots 5.6$$

$$H = H_B + H_f \quad \ldots\ldots 5.7$$

The freeboard zone is where the bed particles with terminal velocity higher than the gas superficial velocity will leave the upper reaction bed surface. To make sure the elutriation situation doesn't happen and the particles not to leave the freeboard height there is a criteria called the maximum fluidization velocity (U_{max}) given by the following relation [8, 20].

$$U_{max} = \left(\frac{8}{6}\right) \times \left(\left[d_p \times (\rho_p - \rho_g) \times \frac{g}{(Cd \times \rho_g)}\right]^{0.5}\right) \quad \ldots\ldots 5.8$$

Where: $g = garvitational\ accelaretaion\ (9.81\frac{m}{s^2})$

$Cd = drag\ coefficient$

The drag coefficient is determined using the following correlation which has a direct link with the Reynolds number at minimum fluidization velocity [8].

$$R_{emf} = \frac{(\rho_g \times U_{mf} \times d_p)}{\mu_g} \quad \ldots\ldots 5.9$$

$$C_d = \frac{24}{R_e}\ for\ low\ R_e \quad \ldots\ldots 5.10$$

Or

$$C_d = 0.44\ for\ R_e \geq 10^3 \quad \ldots\ldots 5.11$$

Finally the bed pressure drop is also an important parameter that must be determined since it has a relation with the bed height in sizing a reactor [8].

$$\Delta P_{bed} = (\rho_p - \rho_g) \times g \times H \times (1 - emf) \quad \ldots\ldots 5.12$$

5.3.2 Fluidization properties and bed diameter calculation

5.3.2.1 Gas viscosity (μ_g)

For the predicted composition of product gas from table 4.7 is estimated using online soft ware at WWW.firecad.net . After inserting the syn gas composition the software gives out different properties of the gas having the indicated composition [28].

$$\mu_g = 41.23e^{-06}\frac{kg}{ms}$$

5.3.2.2 Fluidizing particle (silica sand) properties

In order to operate a fluidized bed under optimum conditions, a bed material of a narrow size distribution is required, since the particle diameter would be well defined and representative of the complete bed. The particle diameter strongly influences the calculated value of the minimum fluidization velocity, see equation 5.5. Since at the design phase we couldn't find a way of determining sand sizes at hand and it is not of much interest at this stage; a sample of sand that was obtained from one of the literatures is used [8]. Its size distribution was determined by sieving at the University of Brussels in one of the projects they were doing.

After having different sizes of the silica sand and their weight fraction a mean diameter was calculated as follows to obtain the mean particle diameter.

Table 5.2 size distribution of sand

Particle diameter range (d_p range in mm)	d_{pi} (mm)	Weight fraction in interval x_i	$\frac{x}{d_{pi}}$	
0.075 - 0.150	0.1125	1.7	0.153	$\overline{dp} = \frac{1}{\sum\frac{(x)}{dp_i}} = \frac{1}{2.413} = 0.414mm$
0.150 - 0.250	0.2	11.3	0.565	
0.250 - 0.300	0.275	6.3	0.231	
0.300 - 0.425	0.3625	26.2	0.724	
0.425 - 0.710	0.5675	33.1	0.583	
0.710 - 1.0	0.855	7.5	0.088	
1.0 - 2.0	1.5	7.3	0.049	
2.0 - 3.5	2.75	3.5	0.013	
3.5 - 5.0	4.25	3.0	0.007	
	Total	99.9	$\sum\frac{(x)}{dp_i} = 2.413$	

i. The mean particle size is found to be d_p= 0.414mm

ii. $\rho_p(particle\ fluidizedbed)$density is assumed for sand $= 2600\frac{kg}{m^3}$

iii. The minimum fluidization voidage (εmf) of the bed is assumed 0.5 which is accepted value for sand beds. (Ranging between 0.5 and 0.85)

5.3.2.3 Minimum fluidization velocity

$$U_{mf} = \left[\frac{{d_p}^2}{(150 \times \mu_g)}\right] \times \left[g \times (\rho_p - \rho_g) \times \frac{(emf^3)}{(1 - emf)}\right]$$

$$U_{mf} = \left[\frac{(0.414 \times 10^{-3})^2}{(150 \times 41.23 \times 10^{-6})}\right] \times \left[9.81 \times (2600 - 1.052) \times \frac{(0.5)^3}{(1 - 0.5)}\right]$$

$$= 2.7714 \times 10^{-5} \times 6373.92$$

$$U_{mf} = 0.1766 \frac{m}{s}.$$

5.3.2.4 Superficial velocity

$$U_s = 2 \times U_{mf} = 2 \times 0.1766 = 0.3533 \frac{m}{s}$$

5.3.2.5 Gasifier internal diameter (bed diameter)

$$m_{air} = \rho_{air} \times \left(\frac{(\pi \times {D_g}^2)}{4}\right) \times U_s$$

$$\rho_{air} = 1.293 \frac{kg}{m^3} \text{ at intial working temprture.}$$

$$m_{air} = \frac{7180.06}{3600} = 1.9945 \frac{kg}{s}$$

$$1.9945 = 1.293 \left(\pi \times \frac{{D_g}^2}{4}\right) \times 0.3533$$

$$D_g = 2.3577m \text{ (bed diameter)}$$

5.3.2.6 Maximum fluidization velocity

a. *Drag coefficient (C_d) determination*

$$R_{emf} = \frac{(\rho_g \times U_{mf} \times d_p)}{\mu_g} \ldots\ldots \text{Reynolds number at minimum fluidization}$$

$$R_{emf} = \frac{(1.052 \times 0.1766 \times 0.414 \times 10^{-3})}{41.23 \times 10^{-6}} = 1.753$$

According to equation 5.10 for a low Re $\ll 1000$

$$C_d = \frac{24}{R_e} = \frac{24}{1.753} = 13.7$$

b. Maximum fluidization velocity (U_{max})

$$U_{max} = \left(\frac{8}{6}\right) \times \left(\left[d_p \times (\rho_p - \rho_g) \times \frac{g}{(Cd \times \rho_g)}\right]^{0.5}\right)$$

$$U_{max} = \frac{8}{6} \times \left(\left[0.414 \times 10^{-3} \times (2600 - 1.052) \times \frac{9.81}{(13.7 \times 1.052)}\right]^{0.5}\right)$$

$$U_{max} = 1.14 \frac{m}{s}$$

5.3.2.7 Minimum air flowrate

The volumetric flowrate at the temperature of the reactor $Q_{air,T}$ can be estimated by assuming ideality of gases and using equation 4.13 which is going to be used in the design of the bed:

$$Q_{air,T} = Q_{air} \times \frac{273 + T_r}{273} \quad \ldots\ldots 5.13$$

$$Q_{air,T} = \frac{5553.02}{3600} \times \frac{273 + 900}{273} = 6.63 \frac{m^3}{s}$$

$$Q_{air,min} = 6.63 \ \frac{m^3}{s}$$

5.3.2.8 Particles terminal falling velocity

The particles terminal falling velocity specifies the velocity, which if exceeded; the particles of the bed will be entrained and elutriated see section 3.2.

When R_{emf} is in the laminar region, the terminal falling velocity, Ut, is given by equation 5.14 [8]

$$U_t = 70 \times U_{mf} \quad \ldots\ldots 5.14$$

$$U_t = 70 \times 0.1766 = 12.362 \frac{m}{s}$$

5.3.2.9 Operational velocity (U_{op})

To avoid the possibility of slowly moving particles forming clusters and to ensure good heat transfer from the walls, it was considered that gas velocity at the bottom of the bed (where it is lowest) must not be less than $2.5 \times Umf$. To minimize particle carry over and to reduce the necessary freeboard, it was specified that gas velocity at the bed surface should not exceed $0.5 \times Ut$. Hence for efficient fluidization at the bottom of the bed [8]:

$$U_{op} \geq 2.5 \ U_{mf} \ (bottom \ of \ the \ bed) \quad \ldots\ldots 5.15$$

$$U_{op} \geq 2.5 \times 0.1766 = 0.4415 \frac{m}{s}$$

$$U_{op} < 0.5 \times U_t \ (surface\ of\ the\ bed) \ldots\ldots\ldots\ldots\ldots\ldots\ldots\ldots\ldots\ldots\ldots\ldots\ldots\ldots\ldots\ldots\ldots\ldots\ldots\ldots 5.16$$

$$U_{op} < 0.5 \times 12.362 = 6.181 \frac{m}{s}$$

$the\ range\ of\ operational\ velocity\ is\ then$

$$0.4415 < U_{op} < 6.181\ m/s$$

For verifying the design values the maximum output volumetric flowrate (which takes into account the increase in the volumetric flowrate due to the gasification process) is $Q_{gas,max} = 7.734 \frac{m^3}{s}$. by dividing it with the cross-sectional area of the bed then the actual operational velocity is calculated as follows:

$$A_b = \frac{\pi \times D_g{}^2}{4} = \frac{\pi \times (2.3577)^2}{4} = 4.365\ m^2$$

$$U_{op} = \frac{Q_{gas,max}}{A_b} = \frac{7.734}{4.365} = 1.772 \frac{m}{s}.$$

The above value of the operational velocity satisfies equation 5.15 and 5.16 thus the design is acceptable.

5.4 Determination of freeboard diameter and Bed Height

In section 5.2, the total volume of the reactor based on the retention time was calculated. From the total volume of the reactor, the volume of the bed must be subtracted in order to determine the volume of the freeboard. It is recommended to select an expanded freeboard configuration in order to minimize elutriation of char and sand particles. In general the freeboard diameter can be increased as follows [28].

a. Diameter of the free board:

   To allow for good disengagement of entrained bed particles and to minimize the particulate load of the product gas, the diameter of the freeboard will be expanded, according to equation 5.17. Thus:

   $$d_f = d_b \times 1.5 \ldots\ldots\ldots\ldots\ldots\ldots\ldots\ldots\ldots\ldots\ldots\ldots\ldots\ldots\ldots\ldots\ldots\ldots\ldots\ldots\ldots\ldots\ldots\ldots\ldots\ldots\ldots\ldots 5.17$$

where:

d_f = freeboard diameter

d_b = bed diameter

$$d_f = 2.3577 \times 1.5 = 3.536\ m$$

b. Bed height:

The bed height can be calculated from the empirical relationship of equation 5.18 with a maximum value of 1 m. This limitation is necessary to ensure that the compression costs of the air would not be excessive [20].

$$\frac{bed\ diameter}{Bed\ height} = 1.33 \ldots\ldots\ldots 5.18$$

$$H_b = \frac{d_b}{1.33} = \frac{2.3577}{1.33} = 1.773m$$

This value is above the allowable maximum of l m and hence it is not acceptable. The height of the bed is then set at 1 m.

c. Bed pressure drop calculation

$$\Delta P = (\rho_p - \rho_g) \times g \times H_B \times (1 - emf) \ldots\ldots\ldots 5.19$$

$$\Delta P = (2600 - 1.057) \times 9.81 \times 1 \times (1 - 0.5) = 12747.8\frac{kg}{ms^2} = 12.74\ kPa$$

5.5 Size of bubbles

Bubbles grow in size by coalescence, as they rise through the bed and correspondingly, diminish in number to maintain a roughly constant flowrate of gas in the bubble phase. The type of distributor determines the initial size of bubbles, but thereafter has no influence. Provided the vessel is big enough, bubbles grow according to equation 5.19 [8].

$$d_B = g^{-0.25} \times (U - U_{mf})^{0.5} \times (h + h_o)^{0.75} \ldots\ldots\ldots 5.20$$

where:

- d_B: is the average diameter of bubbles at any height (h) above the distributor
- U: the gas velocity, and
- ho: corresponds to the initial bubble size and is an imaginary distance beneath the distributor; where the bubbles would be of zero diameters.

Ho can only be determined empirically on the basis of the initial bubble size. When the latter is known, then a value for ho is set on basis of experimental results [8].

Assuming an initial bubble diameter of 0.005 m (which is a generally accepted value for orifices), then ho corresponds to 0.10 m [8]. Under normal operating conditions (which should satisfy equations 5.15 and 5.16), there is an appreciable expansion of the bed. For beds consisting of sand particles, this expansion is usually 30% [8]. Thus:

$$h = h_{mf} + 0.3 \times h_{mf} \ldots\ldots\ldots\ldots\ldots\ldots\ldots\ldots\ldots\ldots\ldots\ldots\ldots\ldots\ldots\ldots\ldots\ldots\ldots\ldots 5.21$$

Where: h_{mf} = the bed height at conditions of minimum fluidization,

Or $h = 1 + 0.3 \times 1 = 1.3m$

The operational velocity at reaction conditions was determined in the previous section;

$$U_{op} = 1.772\frac{m}{s}$$

Substitution of the appropriate values in equation 5.20 gives:

$$d_{B,max} = 9.81^{-0.25} \times (1.772 - 0.1766)^{0.5} \times (1.3 + 0.1)^{0.75}$$

$$d_{B,max} = 0.92m$$

When the bubble diameter is equal to or higher than the reactor diameter at the top of the bed, the bubbles will become slugs some way down the bed. This will cause large amplitude heaving of the bed surface, excessive carryover of particles and probably swamping of the cyclones. An empirical rule to avoid this problem is to ensure that the mean bubble size at the top of the bed is no more than half the vessel diameter, especially if the freeboard is not of the expanded variety [8]. Thus:

$$\frac{d_b}{d_B} \geq 2 \ldots\ldots\ldots\ldots\ldots\ldots\ldots\ldots\ldots\ldots\ldots\ldots\ldots\ldots\ldots\ldots\ldots\ldots\ldots\ldots 5.22$$

Where: d_b = diameter of bed

d_B = average diameter of bubbles

In our case: $\frac{d_b}{d_B} = \frac{2.3577}{0.92} = 2.56 \geq 2$

The restriction of equation 5.22 is satisfied indicating there won't be any slugging of the bubbles or there won't be excessive carryover of particles.

5.6 DISIGN VERIFICATION

5.6.1 Introduction

Since several assumptions were made in the design calculations and some parameters were arbitrarily chosen, it was necessary to evaluate the results obtained. A simple but reliable model was used to verify the design. The two most important parameters, which must be determined according to this model, are the residence time of gas flowing interstitially and the fraction of bubble gas in contact with particles. The former indicates whether there is enough time for the reactions to proceed, to a certain degree, while the latter represents the contact efficiency and whether the gas enclosed by the bubbles will react with the particles of the bed and up to which degree. Both must be within certain generally accepted values to ensure satisfactory operation. Application of this model also completes the design of the fluidized bed as a reactor [8].

5.6.2 Residence time of gas flowing interstitially

To a first approximation the amount of gas flowing interstitially at all levels of the bed (Q_{ig}) is given by equation 5.23, according to the two phase theory.

$$Q_{ig} = U_{mf} \times A_r \quad \ldots\ldots 5.23$$

where: $A_r = Coss - sectional\ area\ of\ the\ bed\ (A_b = 4.365\ m^2)$

Thus $Q_{ig} = 0.1766 \times 4.365 = 0.768 \frac{m^3}{s}\ or\ 2765.66\ \frac{m^3}{hr}$

This value is compared to the total gas flowrate:

$$Q_{gas}\ (flowrate\ bottom\ of\ the\ distributor) = 5553.02\ \frac{m^3}{hr}$$

$$Q_{gas}\ (flowrate\ above\ the\ distributor) = 7.734\ \frac{m^3}{s}\ or\ 27842.4\ \frac{m^3}{hr}$$

Thus at gas flow rates presented above, 49.8 % of the total gas flows interstitially at the bottom and 9.933 % at the top of the bed. An average of 29.86% can be taken of all flow occurring interstitially.

The residence time of this gas in the bed is given by equation 5.24:

$$(t_{ri}) = \frac{h_b}{u_{mf}} \quad \ldots\ldots 5.24$$

$$(t_{ri}) = \frac{1}{0.1766} = 5.66\ \text{seconds}$$

This means that the contact time between the gas and bed particles in the emulsion phase, will be about 6 seconds. Although this is not very high, however, if the rate of reaction of oxygen with char is considered at 900 ^{0}C then it is clear that this residence time is sufficient to ensure complete consumption of oxygen in the bed [28].

5.6.3 Contact efficiency

The bubble diameter at the bottom of the bed is 0.05 m and at the top 0.92 m. Hence, it can be assumed that the mean size of bubbles over the bed is 0.485 m. Similarly, the mean velocity of the gas in the bed is 1.106 m/s. The bubble velocity is given by equation 5.25 [28].

$$U_B = \sqrt{g\frac{d_b}{2}} + (U - U_{mf}) \quad \ldots\ldots 5.25$$

$$U_B = \sqrt{9.81\frac{0.485}{2}} + (1.106 - 0.1766) = 2.47\frac{m}{s}$$

Thus the residence time of bubbles in the bed is:

$$(t_r)_B = \frac{h_b}{U_B} \quad \ldots\ldots 5.26$$

$$(t_r)_B = \frac{1}{2.47} = 0.405\ sec.$$

The ratio at bubble velocity to interstitial gas velocity is [8]:

$$a = e \times \frac{U_B}{U_{mf}} \quad \ldots\ldots 5.27$$

Assuming a voidage value (e) of 0.5 (acceptable value for sand particles) the above ratio will be:

$$a = 0.5 \times \frac{2.47}{0.1766} = 6.993$$

The fraction of bubble gas in contact with particles is given by equation 5.28

$$\frac{V_{Cp}}{V_B} = \frac{1.17}{a - 1} \quad \ldots\ldots 5.28$$

Where: V_{Cp} = volume of particles in the cloud

V_B =volume of the bubble

Thus, $\frac{V_{Cp}}{V_B} = \frac{1.17}{6.993-1} = 0.195$

The above value is roughly equivalent to a contact efficiency of 19.5%. The result is satisfactory, since in general a contact efficiency of 10 % is considered acceptable [8].

5.6.4 Discussion

The above verification method is mainly based on empirical equations. Nevertheless it is valuable since it allows for a reliable check up of the design of a fluidized bed reactor. The residence time of the gas flowing interstitially was estimated to 5.66 seconds; which in principle allow sufficient time for oxygen to be completely consumed by the combustion of char. Similarly the fraction of bubbles in contact with particles was above the minimum acceptable value of 10 % which is 19.5 %. These data indicate that the fluidized bed could achieve stable fluidization under these design parameters and that the oxygen would be consumed within the bed.

5.7 Reactor dimensions

In the previous sections the reactor total volume and the bed geometry has been calculated including the bed diameter and bed height. In this section we are going to make use of these values to determine the reactor detail dimensions.

5.7.1 Calculation of the freeboard geometry

The volume of the freeboard is given by equation:

$$V_f = V_r - V_b \quad \ldots\ldots 5.29$$

where: V = volume

f = freeboard

r = reactor total

b = bed

Volume of the bed is calculated by the following relation:

$$V_b = \frac{\pi \times {d_b}^2 \times H_b}{4} \quad \ldots\ldots 5.30$$

$$V_b = \frac{\pi \times 2.357^2 \times 1}{4} = 4.36\ m^3$$

From this the volume of the freeboard is calculated using equation 5.29:

$$V_f = 96.675 - 4.36 = 92.315\ m^3$$

I. The frustum part.

The height of the frustum of the right conical part is not of any significant importance and can be selected so that the angle of the frustum satisfies equation 5.31 [8]:

$$20° < a_f < 70° \quad \ldots\ldots 5.31$$

The height of the frustum of the right cone is set at 3 m to allow for a gradual reduction. From Figure 5.1 the angle of the frustum (a_f) is:

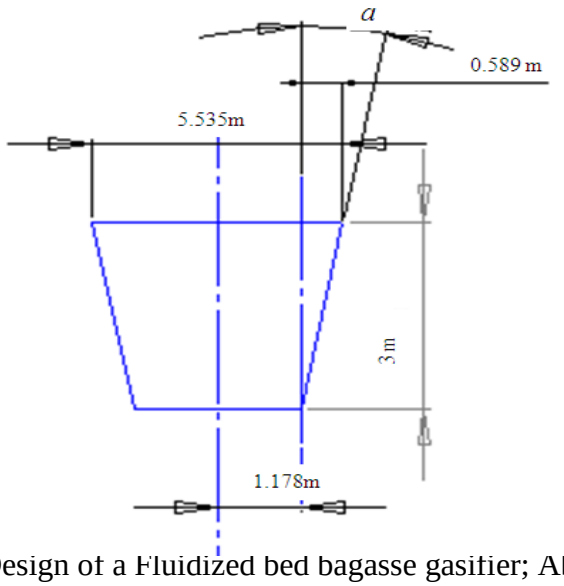

$$\sin a = \frac{0.589}{3.057}$$

$$a = \sin^{-1} 0.1926 = 11.1°$$

Angle frustum:

$$a_f = 2 \times a = 22.2°$$

Figure 5.1 Dimensions of frustum of the freeboard

This angle satisfies equation 5.31 and is considered acceptable. This inclination allows for the return to the bed of all particles falling on the frustum.

The volume of the frustum V_{fr} is:

$$V_{fr} = \frac{\pi h}{3}(R^2 + (R \times r) + r^2) \dots\dots\dots 5.32$$

$$V_{fr} = \frac{\pi \times 3}{3}(1.768^2 + (1.768 \times 1.1785) + 1.1785^2)$$

$$V_{fr} = 20.73\ m^3$$

II. The cylindrical part

The total volume of the freeboard part of the reactor is the sum of the volume of the frustum part and the volume of the cylindrical part as stated in the following equation.

$$V_f = V_{fr} + V_c \dots\dots\dots 5.33$$

Where: $V_c = volume\ of\ the\ cylinderical\ part\ of\ the\ freeboard$

Hence;

$$V_c = V_f - V_{fr} = 92.315 - 20.73 = 71.585\ m^3$$

Height of the cylindrical is then calculated by the use of equation 5.34.

$$V_c = \frac{\pi \times {d_f}^2}{4} \times (H_c) \dots\dots\dots 5.34$$

$$H_c = \frac{4 \times V_c}{\pi \times {d_f}^2} = \frac{4 \times 71.585}{\pi \times 3.536^2} = 7.3\ m$$

The overall dimensions of the reactor are given in Figure 5.2.

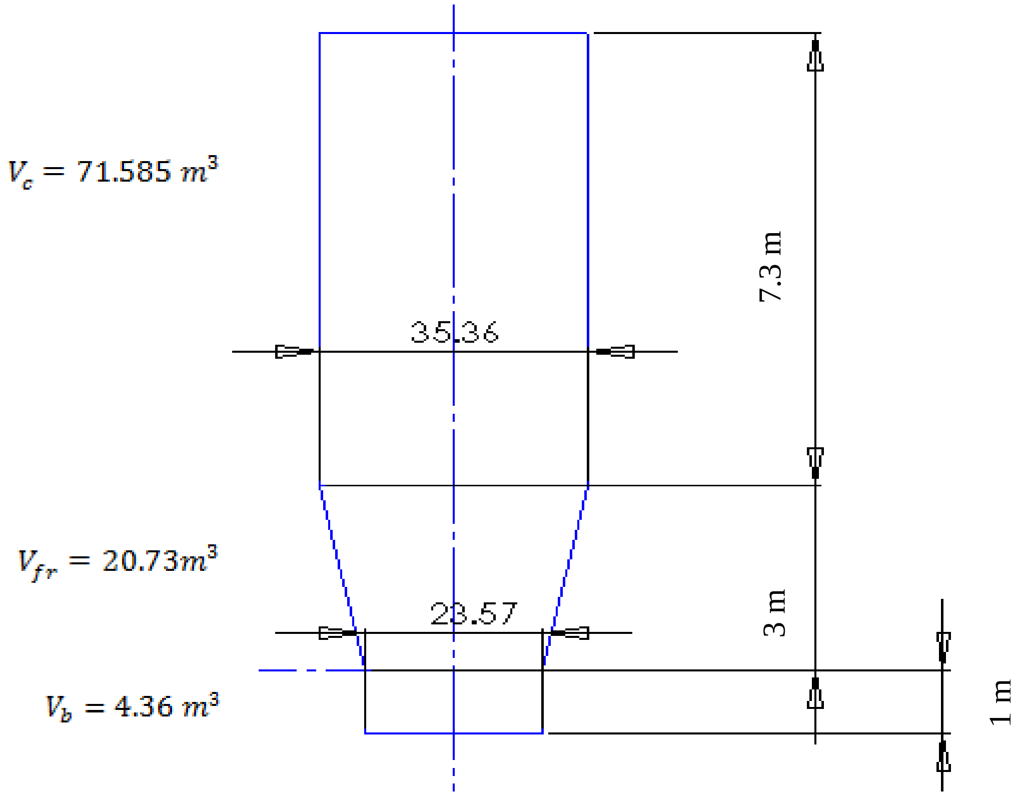

$Total = 96.675\ m^3$

$Total = 11.3\ m$

Figure 5.2 Dimensions of fluidized bed reactor

5.8 Design of Distributer

5.8.1 Introduction

It has been shown [8] that the quality of bubbling fluidization is strongly influenced by the type of gas distributor used. This is illustrated in Figure 5.3 as follows [8]. For little gas inlet openings the bed density fluctuates appreciably at all flow rates, although more severely at high flow rates. The bed density varies with height and gas channelling may be severe. For many gas inlet openings the fluctuation in bed density is negligible at low air flow rates, but again increases significantly at high flow rates. However, the bed density is more uniform throughout the bed, the bubbles are smaller and the gas-solid contacting is more intimate with less channelling of gas.

Although contacting is better when sintered plates or plates with several orifices are used as distributors, such distributors have the disadvantage of relatively high pressure drop from the standpoint of industrial or large scale operations. This may significantly increase the power requirements for the blowers, often a major cost factor.

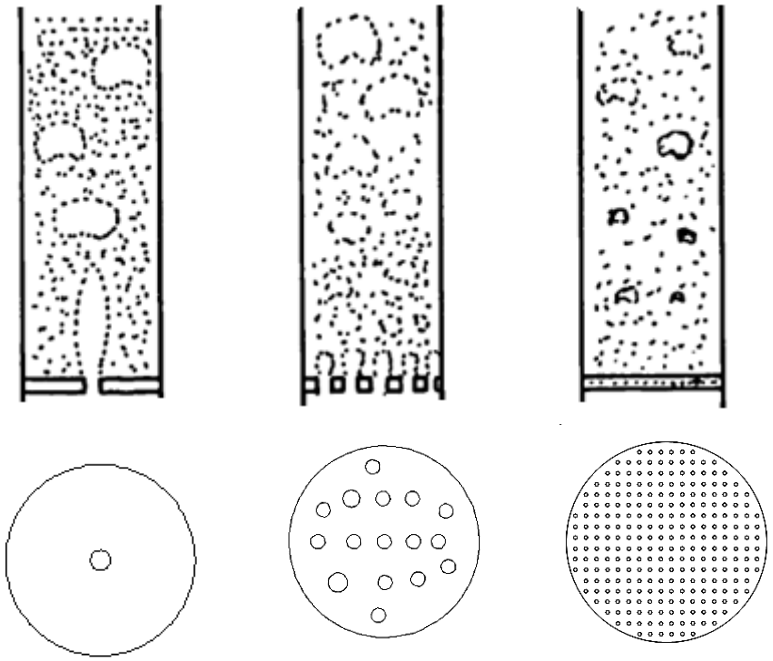

Single orifice plate Multiorifice plate sintered plate

Poor quality, Better quality

Fluctuation in density	Less fluctuation in density
Channelling, slugging	Less channelling, slugging

Figure 5.3 Schematic diagrams of distributors and their effect on the fluidization quality [28]

In general distributors have two functions:

a) To support the bed and
b) To distribute the gas equally all over the cross sectional area of the bed.

In addition, as stated above, they also have the requirement of low pressure drop. It is evident that distributors should be selected and designed with care, for this is the first step to the successful application of a fluidized bed process.

5.8.2 Design Procedure

It is rather surprising that although the distributor is one of the two most important components of a fluidized bed along with the bed material, its design is still largely empirical. Experience shows that distributors should have a sufficient pressure drop to achieve equal flow through the openings. Therefore the pressure drop across the distributor should be considerably larger than the inherent resistance to distribution of the incoming gas. As a generous estimate, the rearrangement resistance can be taken as the expansion loss when flow passes from the inlet connection into the vessel [8].

It has been suggested that the ratio of distributor to expansion loss be taken as 100 [8]. It has also been recommended that the pressure drop across the distributor plate be about 10 % of the pressure drop across the bed, with a minimum in all cases of about 350 mmH_20 [8]. The above conditions can be summarized by:

$$\Delta P_{dmin} = \max(0.1\Delta P_b; 350mm\ H_2O; 100\Delta P\ expansion\ into\ vessel) \dots\dots\dots\dots\dots\dots\ 5.35$$

where: $\Delta P = pressure\ drop$
$d = denotes\ distributor$
$b = denotes\ bed$

According to equation 5.35 the minimum pressure drop over the distributor should be the highest value of the three parameters given in this equation. However, in practice, the pressure drop over the distributor is dictated by the power requirements of the blower and industrial units have been reported with pressure drop over the distributor as low as 25 cm H_2O [8].

Distributors can be designed directly from orifice theory and since the orifice pressure drop is only a small fraction of the total pressure drop, the following procedure has been suggested.

1. Determine the necessary pressure drop across the distributor from equation 5.35;
2. Calculate the Reynolds number for the total flow approaching the distributor and select the corresponding value for the orifice coefficient C_d from standard figures;
3. Determine the velocity of fluid through the orifices, measured at the approach density and temperature.
4. Decide on the number of orifices per unit area of distributor and find the corresponding orifice diameter.

Other design procedures more or less rigorous have also been suggested; however, they are all empirical and even the most rigorous design procedure gives results that differ not more than a few per cent from the above procedure [22]. It was therefore decided that for the purpose of the design, the procedure outlined above was sufficiently accurate and it was applied for the design of the distributor of the process development unit.

5.8.3 Calculation of the minimum pressure drop over the distributor

In fluidized bed reactors envisaged to operate under a certain turn down ratio. It must be ensured that even at the minimum operational gas flowrate the distribution of the gas will be equal across the cross sectional area of the bed. Therefore in the determination of the minimum pressure drop over the distributor, the minimum gas flowrate must be considered.

Assuming no preheating of the fluidizing gas, the pressure drop over the bed is given by equation 5.36 [8]:

$$\Delta P_b = \rho_b \times H_b \quad \ldots\ldots 5.36$$

Where: $\rho_b = Bulk\ density\ of\ the\ bed$

$H_b = Height\ of\ the\ bed$

Assuming a bulk density of 2600 kg/m^3 for sand, which is a typical value, substitution in equation 5.36 gives:

$$\Delta P_b = 2600 \times 1 = 2600 \frac{kg}{m^2} = 260\ cm\ H_2O$$

Applying the first term of equation 5.35 as the limiting condition gives:

$$\Delta P_{dmin} = 0.1 \times \Delta P_b = 0.1 \times 260 = 26\ cm\ H_2O$$

However, this value is below the minimum acceptable recommended by equation 5.35, 350 mm H_20. Thus it was decided to apply the second term of equation 5.35 as the limiting condition;

$$\Delta P_{dmin} = 350\ mm\ H_2O$$

The third term of equation 5.35, (100ΔP, expansion into vessel), is rarely applied for two reasons [8]:

a. The expansion loss of circular and even conical inlets is very small and hence the rearrangement resistance of the gas is negligible; and
b. in order to determine the pressure drop due to expansion into the vessel, the velocity of the gas in the orifice must be known which is yet to be determined.

5.8.4 Calculation of the Reynolds number for the total flow approaching the distributor

The Reynolds number is given by equation 5.37 and it is a dimensionless group which characterizes the type of flow between laminar and turbulent [8].

$$R_e = \frac{d_r \times \rho_g \times U_g}{\mu_g} \quad \ldots\ldots 5.37$$

where: $\rho_g = density\ of\ gas$

$\mu_g = viscosity\ of\ gas$

$d_r = diameter\ of\ reactor$

$U_g = velocity\ of\ gas\ approaching\ the\ distributor$

The Reynolds number is of vital importance in the study of fluid flow. Thus numerous relationships are based on this dimensionless group. This is also the case with the coefficient of discharge C_d for an orifice which is a function of the Reynolds number, see Figure 5.4. [8]

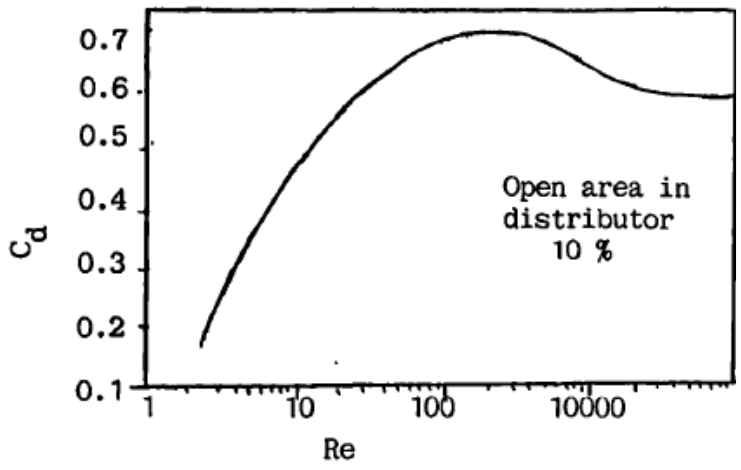

Figure 5.4 Orifice coefficients versus Reynolds number based on diameter of approach chamber

The orifice coefficient of discharge allows for the friction losses and besides the Reynolds number, it also depends on the roughness of the pipe walls, the exact shape of the orifice, the thickness of the orifice plate and the proximity of bends and valves. Thus, in order to determine the coefficient of discharge of the distributor orifices, the Reynolds number must be determined first.

Since efficient fluidization must be ensured at both maximum and minimum air flow rates, the limiting condition is the one at minimum air flowrate. Hence this value will be used in this calculation. By substitution of the following data at normal conditions [22]:

$$\rho_g = \rho_{air} = 1.293 \frac{kg}{m^3}$$

$$\mu_g = \mu_{air} = 1.8 \times 10^{-5} \frac{kg}{ms}$$

$$d_r = 2.357m$$

And $U_g = \frac{Q_{air\ min}}{A_r} = \frac{6.63}{4.365} = 1.52 \frac{m}{s}$

Where: $Q_{air\ min} = minimum\ volumetric\ flowrate\ of\ air$

$A_r = Cross - sectional\ area\ of\ the\ reactor$

Hence;

$$R_e = \frac{d_r \times \rho_g \times U_g}{\mu_g} = \frac{2.35 \times 1.293 \times 1.52}{1.8 \times 10^{-5}} = 256.3 \times 10^3$$

The value of the Reynolds number R_e is way greater than the boundary of transitional and turbulent flow boundary (usually 4000) [8]. And this value corresponds to a value of drag coefficient $C_d = 0.6$ form fig 5.4.

5.8.5 Calculation of the velocity of the gas through the orifices

The velocity of the gas through the orifices of the distributor U_{or} can be calculated at the approach density and temperature [28] by applying equation 5.38.

$$U_{or} = C_d \times \left(\frac{2 \times g_c \times \Delta P_d}{\rho_g} \right)^{1/2} \quad \ldots\ldots 5.38$$

Where: $\rho_g = density\ of\ gas = 1.293 \frac{g}{cm^3} \times 10^{-3}$

$g_c = conversion\ factor = 980\ g.\frac{cm}{g.(s^2)}$

$\Delta P_d = pressure\ drop\ over\ ditribuor = 35 \frac{g}{cm^2}$

Thus, $U_{or} = 0.6 \times \left(\frac{2\times980\times35}{1.293\times10^{3}}\right)^{1/2} = 4370.33\frac{cm}{s} = 43.7\frac{m}{s}$

The ratio of gas velocity upstream the distributor over gas velocity through the orifices gives the (U_g/U_{or}) fraction of open area in the distributor plate. This open area, an empirical parameter, signifies the total surface area of the orifices in relation to the surface area of the distributor and in normal applications it is less than 10% in order to ensure sufficient pressure drop over the distributor [8]. Thus:

$$\frac{U_g}{U_{or}} = \frac{1.52}{43.7} = 0.0345 \; or \; 3.48\%$$

Since the ratio is less than 10% the limitation has been meet.

Orifices which are too small (<1 mm) are liable to become clogged, whereas those which are too large (> 5 mm) may cause an uneven distribution of gas. Taking in account these considerations and with previous experience where different distributors were tested at the laboratory pilot plant [8], the orifice diameter was chosen as 3 mm.

5.8.6 Calculation of the number of Orifices

The number of orifices per unit distributor area, N_{or}, can be calculated using equation 5.39 [28]

$$U_o = A_{or} \times U_{or} \times N_{or} \quad \ldots\ldots 5.39$$

Where: $U_{or} = velocity\ of\ gas\ through\ orifice$

$U_o = velocity\ of\ gas\ approaching\ distributor$

$A_{or} = cross\ sectional\ area\ of\ orifice = \frac{\pi\times d_{or}^{2}}{4} = \frac{\pi\times0.003^{2}}{4} = 7.067\times10^{-6}\ m^2$

$N_{or} = number\ of\ orifices\ per\ unit\ area$

Rearranging equation 5.39 gives:

$$N_{or} = \frac{U_o}{A_{or} \times U_{or}} \quad \ldots\ldots 5.40$$

Substitution of the appropriate values in equation 5.40 gives:

$$N_{or} = \frac{U_o}{A_{or}\times U_{or}} = \frac{1.52}{7.067\times10^{-6}\times43.7} \approx 4922\ /m^2$$

Hence, the distributor should be constructed with 4922 orifices per square meter. Since an even distribution of gas has to be ensured all over the cross-sectional area of the bed, distributors are designed with the same cross-sectional area as the bed. The cross sectional area of the bed A_b under consideration is:

$$A_b = \frac{\pi \times 2.35^2}{4} = 4.357\ m^2$$

The actual number of orifices can be determined by equation 5.41

$$N_{or.d} = N_{or} \times A_b \ldots\ldots 5.41$$

Where $N_{or.d}$ is the actual number of orifices on the distributor. Thus,

$$N_{or.d} = 4922 \times 4.357 = 21{,}446\ orifices$$

However, this number of orifices was determined for the minimum flowrate of air. Thus, it is necessary to determine the pressure drop over the distributor of the maximum air flowrate as well, to ensure that it would be acceptable in terms of power consumption for the blower. The pressure drop and gas velocity are related according to equation 5.42 [8]:

$$\Delta P \propto U^2 \ldots\ldots 5.42$$

For two different gas velocities under identical flow conditions equation 5.42 becomes:

$$\frac{\Delta P_1}{\Delta P_2} = \frac{(U_1)^2}{(U_2)^2} \ldots\ldots 5.43$$

Or $\Delta P_2 = \Delta P_1 \times \frac{(U_1)^2}{(U_2)^2}$ where $U_1 = U_{max} = \frac{Q_{air,o}}{A_r} = \frac{7.734}{4.365} = 1.78\frac{m}{s}$

Substituting the appropriate values in equation 5.43 with subscript 1 denoting minimum air flowrate and 2 maximum air flowrate, the following result is obtained:

$$\Delta P_{max} = \Delta P_{min} \times \frac{(U_{max})^2}{(U_{min})^2} = 35 \times \frac{(1.78)^2}{(1.52)^2} = 47.56\ cm\ H_2O = 4.76kpa$$

Since the size of the reactor is large the above pressure drop is acceptable to ensure a good distribution over the cross-sectional are of the bed.

5.9Pressure drop for the air compressor

The total pressure drop over the reactor is given by equation 5.44:

$$\Delta P = \Delta P_d + \Delta P_b \ldots\ldots 5.44$$

$$\Delta P = 4.76 + 12.74 = 17.5\ kpa$$

Considering a safety margin of 15%, then the compressor must supply the air at 20.1kpa more than the atmospheric pressure used as the working pressure. Therefore the pressure in the freeboard and the cyclone will be 2.6kpa.

6. CONSTRUCTION AND DETAIL GEOMETRY OF THE REACTOR

6.1 Introduction

Since the reactor was a process development unit, it would be operated under different - even extreme conditions - in order to identify its limitations. These would help define the range of operating parameters which could ensure trouble free operation. The construction had to provide for: [8]

a) Versatility in operation,
b) Measurement of all parameters of importance,
c) Operating with different feedstocks,
d) Easy removal of inerts from the bed,
e) Inspection of distributor and walls of reactor and
f) Easy access to the internals for repairs and maintenance.

In this section the construction of the distributor is first discussed and then the shell of the fluidized bed and its various provisions.

Although the scope of the thesis is limited to the design of the reactor only here an effort has been made to give an idea on how the reactor should be constructed and the construction materials that should be used are discussed. A detail design for manufacturing of the reactor couldn't be found on the literatures hence only a theoretical approach has been used for the construction of the reactor.

6.2 Construction of the distributor

As stated above in section 5.8.1 the quality of fluidization is strongly influenced by the type of gas distributor used. Operating problems (such as bed sintering and accumulation of inerts in the bed) arising from the utilization of feedstocks with high ash/inerts content (above 5 wt %), had to be considered and provisions also made for the removal of the foreign bed material. In studies investigating the segregation of particles in a fluidized bed [8], it has been concluded that in a bed of similarly shaped particles, the heavy (larger density) and big (larger size) congregate at the bottom of the bed (Jetsam), while the light and small particles congregate at the top of the bed (Flotsam). Since the inerts in some feedstocks include stones bulky solids and sometimes pieces of iron as well as ash (e.g. the ash content of bagasse is about 11 wt %), these would accumulate at the bottom of the bed.

There are several types of distributors; some of them are applicable to standard fluidized beds, while others have been especially designed for special applications. The most commonly used types of distributor are shown in Figure 6.1. [8]

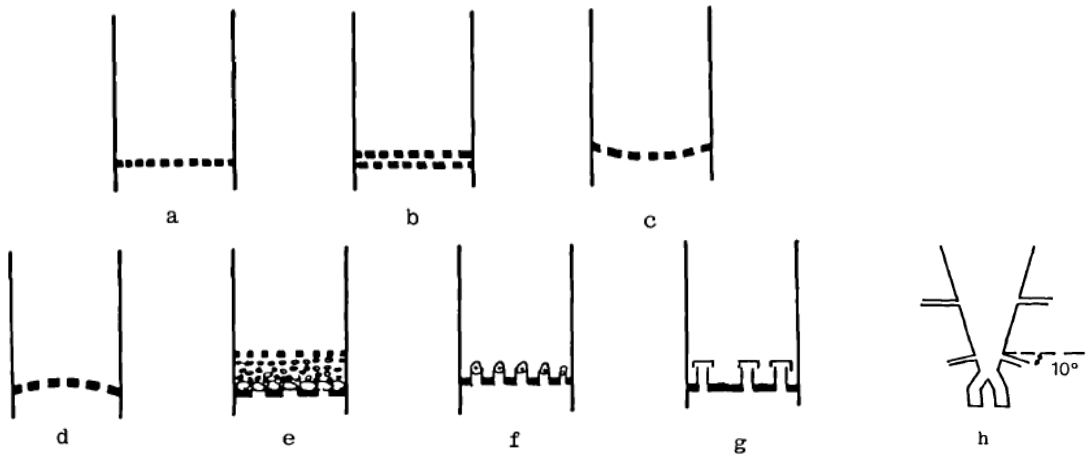

Figure 6.1 Schematic examples of various distributors for fluidized beds

Type (a), a flat perforated plate or wire mesh, is usually applied for laboratory-scale units; it has the disadvantage that fine solids can fall through the orifices when the gas flow is stopped. This, however, can be countered by using two staggered perforated pates, (b). This can also be applied for industrial applications, since it is easy to design and construct and offers good gas distribution. With the heavy load in large diameter beds, flat plates deflect appreciably and hence curved plates (c and d) which withstand heavy loads and thermal stresses are used. However, in order to ensure good gas distribution non uniform orifice spacing is required, which is a disadvantage from the point of view of fabrication. When the inlet gas is free of solids, then a packed bed of granular material sandwiched by two perforated plates (e): is a good distributor and an excellent thermal insulator protecting low temperature gases from a hot bed. In addition, the packing can be used to mix feed gases. Thus injecting a second gas in the packed bed, where the first gas is flowing, results in good design for explosive reactant gas mixtures. Nozzles (f).and bubble caps (g) have also been used to prevent solids from falling through the distributor. In spite of their complicated construction they do not offer better gas distribution than (b) and (e), while solids tend to settle on the distributor. However, none of these distributor types shown in Figure 5.1 permit easy removal of inerts from the bed. This can be overcome by using a distributor of type (h), which was used in a modified design of the Winkler generator. No plate or distributor is used, but the gas is introduced through six side mixing nozzles into a teetered bed. However, the hydrodynamics of such a bed are difficult to describe and predict, since there is no uniform distribution of gas. The only type of distributor that allows for a classic fluidized bed as well

as for easy removal of bed material is the type shown in Figure 6.2. It was therefore decided to use the "pipe grid" concept as a gas distributor. This configuration permits efficient distribution of gas and the simultaneous passage of Jetsam in between the pipes of the grid.

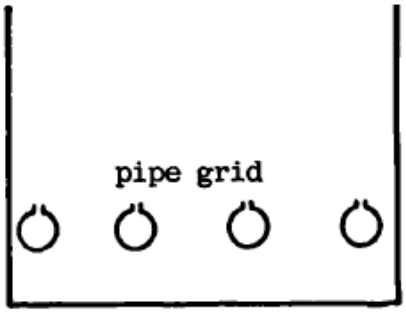

Figure 6.2 Configuration of pipe grid distributor

6.2.1 Configuration of the Distributor

For simplicity in inspection and maintenance the pipe grid was composed of two identical parts. The incoming gas was split into two flows, each of which passed through a gas collector pipe of 0.125 m diameter and parallel around the reactor. The gas flow from each collector was then introduced into the bed through seven pipes with a total of 10,723 orifices of 3 mm for each side (total design number of orifices21,446).

The number of orifices per pipe was: 500 orifices in pipes 1 and 7, 1000 orifices in pipes 2 and 6, 2000 orifices in pipes 3 and 5 and 4000 orifices in pipe 4 respectively. The distance between the pipes is 0.4 m. To avoid blockage of the orifices by sand particles or other foreign material, the orifices should be drilled in pairs on the pipes, facing downwards at 90° of each other, in a modified version of pipe grid than the one shown in Figure 5.2. The pipes were 25 mm inside diameter and were introduced into tile bed through a pipe of 0.05 m. Flingerit rings were used between the flanges to prevent gas leaks.

6.2.2 Material of Construction

Both metallic and ceramic materials can be used for distributors and have certain advantages. Ceramics are more resistant to corrosive gasses and to high temperatures, but they have a low strength against thermal shock or expansion stresses [8]. Ceramics are also eroded relatively easily, resulting in a gradual widening in the orifice openings. Metallic distributors are very good for expansion stresses or thermal shocks and in the case of a solids free gas have a high resistance to erosion. However unless special alloys (such as inconel) are used, metallic distributors are susceptible to corrosive gases. It was therefore decided to use refractory steel

pipes. This type of pipe is very good for high temperature applications and is difficult to erode.

6.3 Construction of the fluidized Bed

The reactor is 4.2 m diameter cylinder tube of 11.3 m height, outside dimensions. The shell is composed of carbon steel having a thickness of 6.4 mm. The freeboard region is of great importance in a fluidized bed gasifier it is not only serves as a solids disengagement zone, but it is in this part of the reactor that the tar is believed to be cracked and the water gas shift reactor attains equilibrium at higher temperatures [8].

In order to allow for a good disengagement of solids due to a relatively large diameter of bubbles at the surface of the bed the reactor was constructed with an expanded freeboard. The bed diameter was set at 2.357 m as described in section 5.3 as a basic parameter. Some of the parameters had to be set arbitrarily. Thus the diameter of the freeboard was chosen arbitrarily as 150 % of the bed diameter, or 3.536 m. Emphasis was given in ensuring stable fluidization and providing a relatively large freeboard for the cracking of tars. A detail drawing is attached in the Appendix showing detail geometry of the reactor and the distributor.

6.3.1 Insulation

A layer of refractory bricks forms the inner lining of the shell to give a finished diameter of 2.35 m bed and 5.3 m freeboard. This layer is 0.25 m at the freeboard and 0.5m at the bed. At the top of the reactor, the horizontal surface is protected inside by a layer of 0.25 m of steel mix (refractory material). Sandwiched between the carbon steel outer shell and the refractory is a 0.05 m layer of rock wool, which acts as a further insulating medium. The conical reduction between the freeboard and the bed was constructed by refractory cement. Details about the fluidized bed insulation are given in Figure 6.3

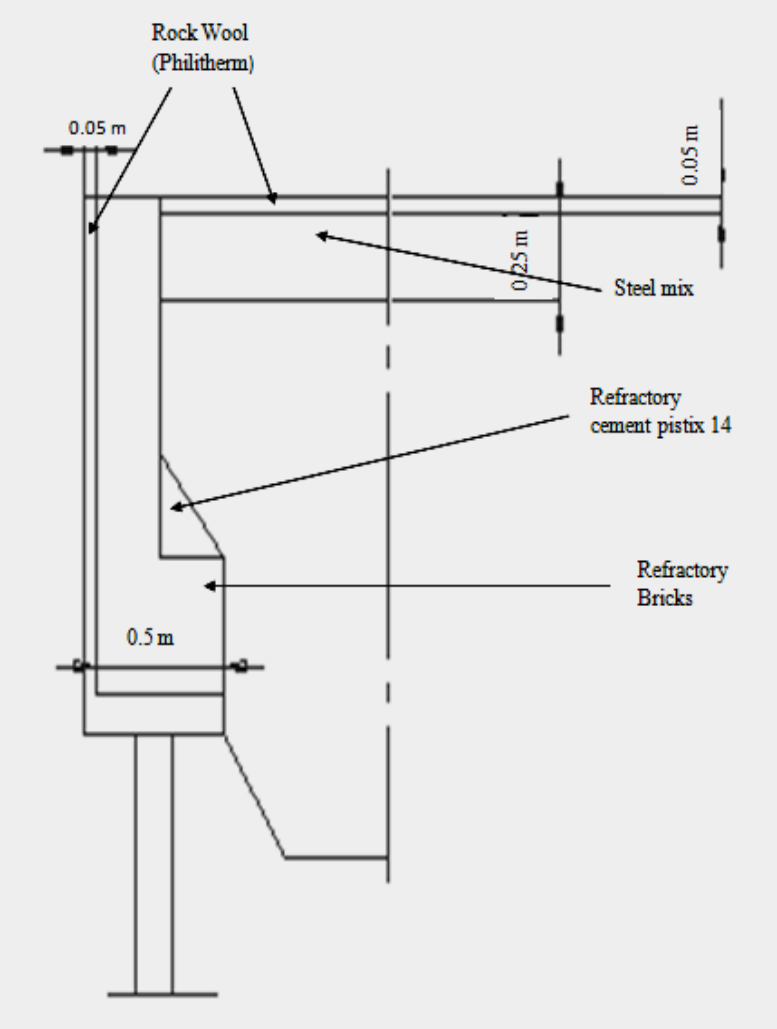

Figure 6.3 Insulation of the fluidized Bed

6.3.2 Details of Construction

These are shown in Figures in the Appendix. The fluidized bed is supported on four legs of 1.5m height. A square cone forms the bottom of the reactor. The cone ends in a square opening 2.4 m above and 0P1, below the distributor level, on which a manual gate valve was installed. The Jetsam is collected in this part of the reactor which otherwise contained sand. The gases are introduced from the pipe grid, PG, and exit from a side opening, 0P2, at the top of the reactor of 0.6 m diameter. Two wells, 0P3, 0P4, for over bed preheating burners of 0.22 diameters are foreseen. Since some feedstocks with a high content of fines (e.g. wood shavings) might be used in future, two horizontal feeding ports FP_1, FP_2, of 0.8 m diameters are provided. An observation well, 0W, is constructed at the top of the bed. In total there are 5 ports for thermocouple TP and pressure drop measurements. It is possible to enter the reactor vessel by removing the conical square bottom of the reactor and one side of the pipe grid distributor which helps as a cooling medium for the bed or for inspection of the distributor orifices.

7. ENERGY BALANCE AND EQUIPMENT SPECIFICATIONS

7.1 Energy Balance

7.1.1 Introduction

In this section an energy balance between the input and output components is going to be evaluated because it is another way of evaluating how effective the design of the fluidized bed reactor is. The energy input to the reactor consists of two parameters: the sensible heat of air and the energy of the feedstock [8]:

$$Energy\ \ in\ feedstock = G_{feedstock} \times HHV_{feedstock} \ldots\ldots\ldots\ldots\ldots\ldots\ldots\ldots\ldots\ldots\ldots\ldots\ldots 7.1$$

Where: $G_{feedstock} = mass\ flowrate\ of\ the\ feedstock, on\ as\ received\ basis\ kg/h$

$HHV_{feedstock} = higher\ heating\ value\ of\ the\ feedstock, KJ/kg$

The energy output consists of six parameters:

a. The sensible heat of the product gas.
b. The sensible and latent heat of steam
c. The sensible heat of the fly ash and tars
d. The heat loss from the reactor walls
e. The chemical energy in the product gas
f. The energy in flay ash, tars and carbon in the condensate.

The general balance over the reactor is given by equation 7.2:

$$Cp_{air} \times G_{air}(T_r - 20) + HHV_{feedstock} \times G_{feedstock}$$
$$= \sum Cp_{i,out} \times G_{i,out}(T_E - 20) + L_{H_2O} \times G_{H_2O} + HHV_{gas} \times G_{gas} + H_w + H_F$$
$$+ H_c \ldots\ldots\ldots\ldots\ldots\ldots\ldots\ldots\ldots\ldots\ldots\ldots\ldots\ldots\ldots\ldots\ldots\ldots\ldots\ldots\ldots\ldots\ldots\ldots\ldots\ldots\ldots\ldots\ldots\ldots\ldots\ldots\ldots\ldots\ldots\ldots\ldots\ldots\ldots 7.2$$

Where: $Cp_{i,out} = specific\ heat\ capacity\ of\ gas\ componenet$

$G_{i,out} = mass\ flowrate\ of\ gas\ component\ i$

$HHV = Higher\ heating\ value$

$L_{H_2O} = latent\ heat\ in\ the\ steam\ leaving$

$T_r = temperature\ of\ reactor$

$T_E = Temperature\ of\ gases\ at\ exit\ of\ reactor$

$H_w = heat\ losses\ from\ reactor\ walls$

$H_F = higher\ heating\ value\ of\ fly\ ash$

$H_c = energy\ in\ the\ condensate$

A detail analysis of the energy balance is discussed step by step in the following sections. All the above variables used in the equation of energy balance have been calculated either in one way or another in previous sections except the energy loss through reactor walls which had to wait until the geometry of the insulation to be determined.

7.1.2 Heat Loss from Reactor walls

In the energy balance the heat losses through the reactor walls were considered. These were calculated using equation 7.3 [29]:

$$Heat\ loss\ reactor\ walls = \frac{K \times S \times \Delta T}{X} \quad \ldots \quad 7.3$$

Where: K = *thermal conductivity of insulation*

S = *surface area*

X = *thickness of insulation*

ΔT = *temperature difference between inside and outside walls.*

The thermal resistances of the insulating materials have been obtained from supplier and manufacturer of the insulating material through different literatures [8]. The following values were given:

Table 7.1: Thermal resistance of the insulating materials [8]

Position in reactor	representation	values	units	values	units
For the bed wall	K_b	0.3125	$\frac{Kcal}{m^2 h°C}$	0.3634375	$\frac{W}{m^2 K}$
For the freeboard wall	K_f	0.6313	$\frac{Kcal}{m^2 h°C}$	0.7342019	$\frac{W}{m^2 K}$
For the ceiling of reactor (thermal resistance)	$Rc = \frac{X}{k}$	1.0144	$\frac{m^2 h°C}{Kcal}$	1.1797472	$\frac{m^2 K}{W}$

To account for the heat losses through all measuring ports and openings, the manufacturer of the insulating material and Vyncke Warmtetechniek recommended that the calculated heat losses through the reactor walls be increased by a factor of 2. Also to account for the heat losses to the nonfluidized sand bed below the distributor and through the non-insulated conical wall at the bottom of the reactor, it was recommended to further increase the heat losses by a factor of 2 [8].

7.1.2.1 Surface Area calculations

While calculating the heat loss through reactor walls its evident that the use of the thickness or the surface area of the insulated walls are important. This section gives the surface area calculation for the bed wall, freeboard wall and the ceiling of the reactor respectively.

I. The bed plus the bottom cone surface area: see Figure 7.1

For the conical frustum part

$$S_{bc} = \pi \times (r_1 + r_2) \times \sqrt{(r_1 - r_2)^2 + {h_2}^2}$$

$$S_{bc} = \pi \times (1.1875 + 0.075) \times \sqrt{(1.1875 - 0.075)^2 +$$

$$S_{bc} = 5.14\ m^2$$

For the cylindrical part

$$S_{bcy} = \pi \times d_1 \times h_1$$

$$S_{bcy} = \pi \times 2.357 \times 1.0$$

$$S_{bcy} = 7.404\ m^2$$

Totally the bed part surface area:

$$S_b = S_{bc} + S_{bcy} = 5.14 + 7.404$$

$$S_b = 12.54\ m^2$$

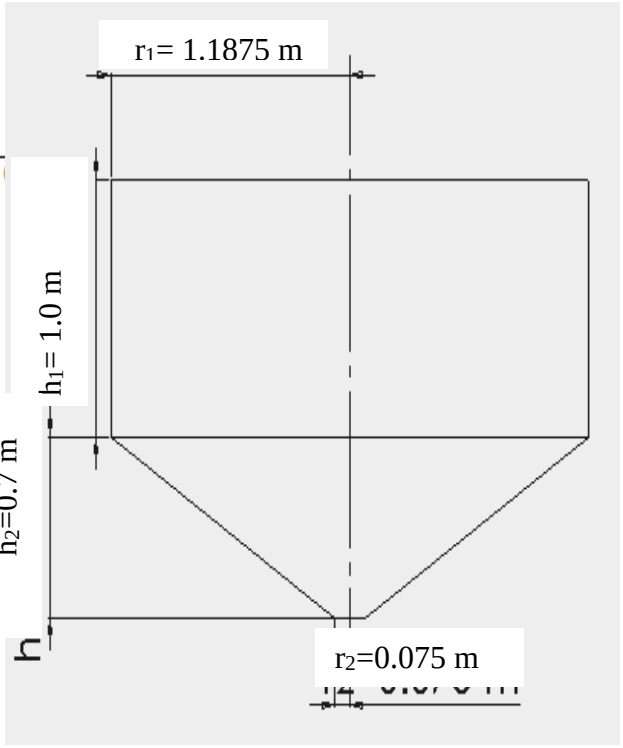

Figure 7.1: Surface area of reactor bed

II. Surface area of the free board Figure 7.2

For the conical frustum part

$$S_{fc} = \pi \times (r_1 + r_2) \times \sqrt{(r_1 - r_2)^2 + {h_2}^2}$$

$$S_{fc} = \pi \times (1.768 + 1.1875) \times \sqrt{(1.768 - 1.1875)^2 + 3.0^2}$$

$$S_{fc} = 28.37\ m^2$$

For the cylindrical part of the freeboard

$$S_{fcy} = \pi \times d_1 \times h_1$$

$$S_{fcy} = \pi \times 3.536 \times 7.3$$

$$S_{fcy} = 81.1\ m^2$$

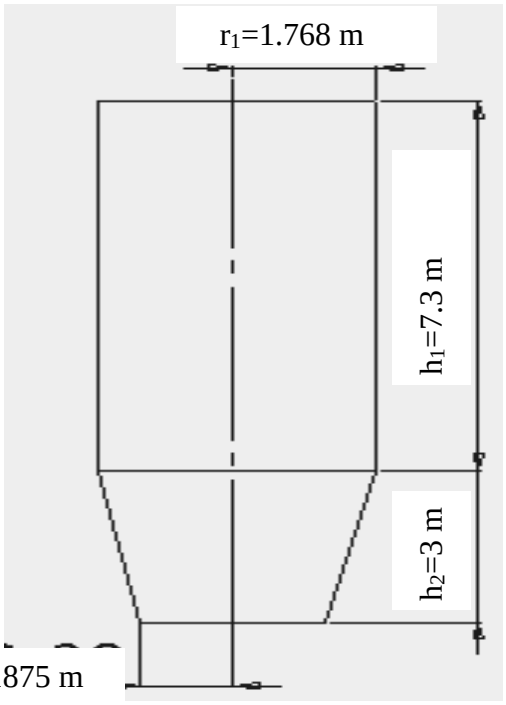

Totally the freeboard part surface area:

$S_f = S_{fc} + S_{fcy} = 28.37 + 81.1$

$S_f = 109.46\, m^2$

Figure 7.2: Surface area of the freeboard

III. Surface are of the reactor ceiling (S_c)

$$S_c = 2\pi \times \left(\frac{d_1}{2}\right)^2$$

$$S_c = 2\pi \times \left(\frac{3.536}{2}\right)^2 = 19.64 m^2$$

7.1.3 Energy Balance calculations

a. Input Energy :

i. $Sensible\ heat\ in\ air = G_{air} \times Cp_{air} \times (T_{inlet} - 20)$

Where: $Cp = mean\ specific\ heat\ capacity, \frac{KJ}{Kg^{\circ}C}$

$$H_{s,air} = \frac{(7180.06 \times 1.05 \times (25 - 20))}{1000} = 37.7\, \frac{MJ}{h}$$

$$Energy\ in\ feed\ stock = G_{feed\ MAF} \times HHV_{feed}$$

$$= 3788.2 \times 9.794$$

ii. $Energy\ in\ feed\ stock = 37{,}101.63 \frac{MJ}{h}$

$Total\ Input = Energy\ in\ feed\ stock + sensible\ heat\ in\ air$

$$Total\ input = 37{,}101.63 + 37.7 = 37{,}139.33 \frac{MJ}{h}$$

b. Output Energy:

i. $sensible\ heat\ in\ gas = \sum G_i \times \frac{Cp_i \times (T_E - 20)}{1000}$

$$S_g = \left[\left(G_{H_2} \times CP_{H_2}\right) + \left(G_{N_2} \times CP_{N_2}\right) + \left(G_{CH_4} \times CP_{CH_4}\right) + \left(G_{CO} \times CP_{CO}\right) + \left(G_{CO_2} \times CP_{CO_2}\right)\right] \times \frac{(T_g - 20)}{1000}$$

$$S_g = [(68.54 \times 14.86) + (5507.1 \times 1.11) + (43.727 \times 3.74) + (1332.45 \times 1.12) + (1713.453 \times 1.11)] \times \frac{(750 - 20)}{1000}$$

$$sensible\ heat\ in\ gas(S_g) = 7803.12\frac{MJ}{h}$$

ii. sensible and latent heat in steam

$$= G_{con} \times CP_{H_2O,l} \times (100 - 20) + G_{con} \times CP_{H_2O,g} \times (T_s - 100) + G_{con} \times L_{H_2O}$$

$$= \frac{[(867.50 \times 4.19 \times 80) + (867.50 \times 2.09 \times (750 - 100))]}{1000} + 867.50 \times 2.26$$

$$sensible\ and\ latent\ heat\ in\ steam = 3429.83\frac{MJ}{h}$$

iii. Sensible heat in Fly ash.

$$= G_{fa} \times Cp_{fa} \times \frac{T_g - 20}{1000}$$

$$= 0$$

Since the model we have been using is an equilibrium model which states that the carbon in the biomass is totally burned hence no tar and ash is predicted as an exit gas.

iv. Heat Loss reactor walls

$$H_l = \frac{(T_f - 20) \times S_f \times K_f}{d_o} + \frac{(T_b - 20) \times S_b \times K_b}{d_o} + \frac{(T_o - 20) \times S_c}{K_c}$$

Where: $T_i = temperature$

$S_i = surface\ area$

$K_i = heat\ transfer\ coefficient$

$d_o = outside\ diameter$

$i = f\ (freeboard), b\ (bed), O\ (outlet), C(cieling\ of\ reactor)$

$R = thermal\ resistance$

$$H_l{}^* = \frac{\left(\frac{(800 + 750)}{2} - 20\right) \times 109.46 \times 0.6313}{4.2} + \frac{(900 - 20) \times 12.54 \times 0.3125}{4.2} + \frac{(750 - 20) \times 19.64}{1.0144}$$

$$H_l^* = 27{,}376.66\ \frac{Kcal}{h}$$

Since to account for different losses that have been mentioned in section 7.1.2 the heat loss should be multiplied by a factor of 4.

$$H_l = H_l^* \times 4 = 27{,}376.66 \times 4 = 109{,}506.64 \frac{kcal}{h}$$

Or $H_l = 458.72 \frac{MJ}{h}$

Heat losses correspond to 1.236 % of the energy in the feedstock which is generally considered an acceptable value.

v. Energy in Gas (E_g)

$$E_g = G_{gas} \times HHV_{gas} = 9{,}505.98 \times 2.687$$

$$E_g = 25{,}542.57 \frac{MJ}{h}$$

vi. Energy in tar and fly ash

Since the model we have been using is an equilibrium model which states that the carbon in the biomass is totally burned hence no tar and ash is predicted as an exit gas.

$$energy\ in\ tar\ and\ fly\ ash = 0$$

$$Total\ output\ energy = S_g + sensible\ and\ latent\ heat\ in\ steam + S_{fa} + H_l + E_g + E_{fa}$$

$$Total\ output\ energy = 7803.12 + 3429.83 + 0 + 458.72 + 25{,}542.57 + 0$$

$$E_{OUT} = 37{,}234.5 \frac{MJ}{h}$$

$$Unaccounted\ heat\ loss = Total\ input - Total\ output$$

$$Unaccounted\ heat\ loss = 37{,}139.33 - 37{,}234.5 = 94.91 \frac{MJ}{kg}$$

This is about 0.25 % which is very low and in very good acceptance margin.

$$Balance = \frac{Total\ output}{Total\ input} \times 100$$

$$Balance = \frac{37234.50}{37139.33} \times 100 = 100.25\%$$

7.2 Equipment Specifications

7.2.1 Introduction

Even though the scope of this thesis is limited in the design of the reactor; in this section some of the equipments and auxiliary parts are discussed. Some standard specifications are also discussed based on the output values of the reactor design.

7.2.2 The feeding system

The feeding system consists of two parts: the feeder and the hopper.

I. The feeder system

In this section only the recommendation for the design of the feeder system is suggested in other works one might focus on the design of the feeder system.

The design is based on different properties. One of the properties is the feedstock. Since the feedstock contains relatively large amounts of inerts, it is expected to be abrasive. Thus, a slow moving feeder with minimum of moving components must be selected. It can be envisaged that the feedstock could be screened to reduce sand and dirt content [8].

The feeding ports are selected to be two from previous design of the reactor geometry. Anyone who is engaged to do the design of the feeder system should conceder the amount of ports available.

II. Hopper

The hopper is not the prime focus of the reactor design though when designing the hopper one must conceder the following specifications [8]:

- The angle of repose of the feedstock
- Volume
- Angle at outlet
- Diameter of cylinder
- Height of cylinder
- Volume of cylinder
- Diameter of outlet

7.2.3 Determination of the distance between feeding ports

In the literature on biomass gasification no information could be found concerning this problem. However, from the coal gasification literature [8] the following simplified

procedure can be applied. If S is the distance between two feeding ports, then the time required for complete mixing of the feedstock is [8]:

$$M_t = \frac{S^2}{U_l} \quad \ldots\ldots 7.4$$

Where: $M_t = mixing\ time$

$U_l = lateral\ mixing\ velocity$

In general, for sand-char mixtures fluidized beds $U_l = 0.1\ \frac{m^2}{s}$ [28]. Also it can be assumed that for single, fine biomass char particles, the burn out time is 30 seconds. Thus, solving for S and substituting these data in equation 7.4 gives:

$$S = \sqrt{M_t \times U_l} \quad \ldots\ldots 7.5$$

$$S = 1.7\ m.$$

It can therefore be concluded that in general feeding ports should be placed at about 1.7 m from each other.

7.2.4 Openings on the shell of the reactor

The openings (ports) necessary for the operation of the reactor are listed below:

1. Feeding port diameter = 0.8 m
2. Outlet of gas diameter = 0.6 m
3. Removal of bed diameter = 0.15 m
4. Observation port diameter = 0.3 m

The bed feeding port is placed above the surface of the bed. Assuming that the maximum expansion of bed under all conditions is 50%, and then the feeding port is placed at 1.5 m above the distributor.

The removal of the bed is accomplished through the grid distributor. The base of the reactor is square conical and is not insulated in order to accelerate cooling of the bed material. The exit has a diameter of 0.15 m. The height of the conical base is 0.7 m.

The base cone is detachable, so that the orifices and the pipes of the distributor can be inspected easily. The observation port is placed at the ceiling of the reactor, in order to have a complete view of the reactor.

Two thermocouples, one in the centre of the bed (0.5 m above distributor) and the other above the bed (1.6 m above distributor), are foreseen in the bed section. A third one is placed close to the outlet of the gases, at the freeboard. Provisions for pressure measurement (ΔP over bed and operating pressure at the freeboard) are also foreseen.

7.2.5 Auxiliary equipment for the fluidized bed

7.2.5.1 Compressor

A compressor of the centrifugal type has to be selected which deliver 1.54 m3/s air at 20.1 Kpa. The compressor power consumption and its Rpm can be supplied by the manufacturer [22].

7.2.5.2 Heater

The heater is a direct fired, atomizing oil burner. The exit temperature of the gas is specified at 750 °C. Thus, the energy required to heat up the air from 25 oC to 750 oC is:

E = 5465.8 MJ/h

Assuming the oil has a higher heating value of 43 MJ/kg, and then 127.11 kg/h of oil is required. Its power consumption is the major selection criteria. The fuel oil and power are only consumed during start up.

7.2.5.3 Bed screw

As far as this design is concerned the removal of the bed ash is done at the bottom cone of the reactor where there is a 0.15 m opening. But for future work as a recommendation a bed screw having specifications like length, pitch diameter, inclination angle etc. is required to remove the waste. The screw empties the bed material in containers, to facilitate transportation to the dump site [22].

7.2.5.4 Gas cleaning Cyclone

The cyclone is also auxiliary equipment used as an attachment on the reactor. It is used to clean the output gas from fly ashes and tars. The design of the cyclone depends on the output values of the reactor design. One can pursue the design of a cyclone based on the output of this thesis work.

After the cyclone an ash collecting bin and a fly ash feeder design is also required to re-use the fly ash in the reactor for a secondary gasification.

7.3 Utilities

The utilities required for the operation of the gasification are electrical power, water for cooling the reactor and compressed air for the control instruments. Since these utilities are readily available at Fincha Sugar it can be directly supplied to the reactor.

8. Economic Analysis of the FBG

8.1 Introduction

Gasifier reactor manufacturers could not provide any information on the capital cost of the fluidized bed gasifier and related equipment. It is therefore necessary to use data from the literature for the economic analysis. On the basis of the information provided by several gasifier fabricators Bridgewater [30] proposed a method by which the costs of the gasification plant can be determined. It is so hard to determine the exact quantity and cost of each component and materials to be used in the manufacturing cost of the fluidized bed gasifier a rough estimate of the economic analysis of the reactor is discussed in the following sections.

8.2 Costs

8.2.1 Total Capital cost

For relatively simple gasifier systems the total plant cost - from the gasifier feeding system to clean gas - is estimated by equation 8.1 [30].

$$\text{Capital Cost}_{birr} = (£_{1985}260{,}000(Capacity\ MAF\ t/h)^{0.65}) \times 22.50 \ldots\ldots\ldots\ldots\ldots\ldots\ldots\ldots\ldots\ldots\ldots\ldots 8.1$$

Where the capital cost is expressed in 1985 pounds sterling and the capacity in MAF basis. Literature [31] shows that from the year 1985 through 2012 the British Pound has lost about 12 % of its buying power. So there would be a 12% inflation increment on the total capital cost when the economic analysis is done this year. And 22.50 is the exchange rate in to the local currency (Birr).

8.2.2 Utilities

The average electricity cost of gasifiers was found equal to Birr 3.24/GJ product gas. Since this value does not include the other utilities costs, it was proposed to use a value of Birr 5.4/GJ. However, for the gasification plant of this case study the only utility consumed is electricity (the plant also needs oil for start up and cooling water for shut down which is available at the site); therefore a value of Birr 3.24/GJ product gas will be used.

The product gas energy was calculated in the energy balance in section 6.1.3 excluding the heat loss to be $36{,}775.52\frac{\text{MJ}}{\text{h}}$ this value should be multiplied in yearly working hours of (23

hours/day x 260 days/year = 6000 hours/year). So the product gas energy is $36{,}775.52\frac{\text{MJ}}{\text{h}} \times 6000 = 220{,}653.12\ GJ/year$

8.2.3 Maintenance

Yearly maintenance cost is usually estimated as a proportion of the gasifier capital cost. The mean maintenance cost was found to be 2.5% on the total plant cost basis. However, if only fluidized bed gasifiers are considered, then the yearly maintenance cost reduces to 1.9%. Therefore, this value will be used in the economic analysis.

8.2.4 Overheads

A fraction of 0.08 of the total plant cost is proposed to cover annual overheads (local tax, insurance) and all head office expenses. Payroll overheads have been included in the labor cost.

8.2.5 Labor cost

Supervision is provided by the technical manager of Fincha Sugar factory free of charge. The cost per shift is Birr 90,000/y. This includes the cost of three operators per shift per day. Three shift per day run the plant (plant runs only on week days and 23 hours per day).

8.2.6 Feedstock

Fincha sugar was using about half of the bagasse produced for a boiler, while the other half had to be discharged. It is assumed that the cost of discharging these residues was equal to the cost of the feedstock. Thus, the cost of the feedstock for the gasification plant is zero since the bagasse could be found for free from the sugar company.

The results of the above discussed costs are summarized in the following table 8.1.

Table 8.1 Cost of fluidized bed Gasifier

Item	Recommendation	Cost Birr
Total Capital Cost	Birr $(£_{1985} 260{,}000(Capacity\ MAF\ t/h)^{0.65}) \times 22.50$ With 12% inflation from 1985-2012	18,988,920
Utilities	3.24 /GJ	714,915
Maintenance	1.9% CC	360,787.5
Overheads	8% CC	1,519,110
Labour	Birr 90000/y ,shift	270,000

8.3 Product Costs

In order to determine the product cost, the annual capital charges (ACC) has to be estimated [22]. The annual capital charges are the initial plant cost (C) annualized over the lifetime of the plant (t) at the interest rate (i). Thus, ACC is given by equation 8.2.

$$ACC = \frac{CC \times i}{1-(1+i)^{-t}} \quad \ldots\ldots 8.2$$

The expected lifetime of the plant is 10 years, while the interest rate is 10%.

The results are summarized in table 8.2

Table 8.2 Product Cost

Item	Cost in Birr
ACC	3,090,352.5
Utilities	714,915
Overhead	1,519,110
Labour	270,000
Total Annual cost	5,729,377.5

$$Total\ gas\ output\ gasifier = 36.785\frac{GJ}{h} \times 6000 = 220{,}710\ GJ/year$$

$$Product\ Cost = \frac{Total\ Annual\ cost}{Total\ gas\ output\ energy} = \frac{5{,}729{,}377.5}{220{,}710} = Birr\ 25.875/GJ$$

This value has to be compared to energy costs from natural gas at around Birr 112.5/GJ. It has been recommended to consider a discount of about 25% as compensation for lower quality [32]. Therefore the savings made by the installation of the gasification plant are:

$$savings = 112.5 \times 0.75 - 25.875 = Birr\ 58.5/\ GJ$$

$$or\ on\ Annual\ bases\ (savings) = 58.5 \times 220{,}710 = Birr\ 12{,}911{,}535$$

8.4 Pay Back Period

The payback period (P) is calculated by equation 8.3 [56].

$$P = \frac{CC}{RE} \quad \ldots\ldots 8.3$$

Where: $CC = the\ total\ capital\ Cost$

$RE = the\ reveunes\ (or\ savings)\ minus\ the\ expenses.$

$$P = \frac{CC}{RE} = \frac{18{,}988{,}920}{12{,}911{,}535 - 5{,}729{,}377.5} = 2.6\ years$$

Based on the current situation of the world industrial economy this payback period is acceptable. However, this method of estimating the economic feasibility of a project neglects the potential income after the costs have been regained.

8.5 Internal Rate of Return

This method of project economic feasibility is carried out on the basis of the actual value of the proceeds given by the following equation [22].

$$V = \left[\sum_{t=1}^{t=n} \frac{RE}{(1+i)^t}\right] - CC \quad \ldots\ldots 8.4$$

Where: $V = The\ actual\ value\ of\ the\ proceeds$

$t = The\ number\ of\ years$

$RE = The\ revenues\ minus\ expenses$

$CC = Total\ Capital\ cost$

$n = The\ number\ of\ years\ the\ plant\ will\ be\ Amortized$

$i = interest\ rate$

For gasification plants, it can be assumed that RE is constant, so that equation 8.4 becomes:

$$V = RE\left[\frac{1-(1+i)^{-t}}{i}\right] - CC \quad \ldots\ldots 8.5$$

When V = 0, the project yields an interest of i per year. This interest rate is the internal rate of return. To obtain the correct value of i, an assumed value for i is taken and by iteration the best fitting for V = 0 is sought. If the rate of interest on the bank is lower than the internal rate of return, the project can be evaluated positive.

Substituting the appropriate values in equation 8.5, the iteration gives:

$V = 0\ for\ i = 36.0865\ \%$

Thus the internal rate of return, IRR is 36.08 % which is very higher than the rate of interest in banks which is around 10 %.

8.6 Benefits- Costs Ratio

The benefits-costs ratio (BCR) is a third method of evaluating the economic feasibility of a project. It is calculated by equation 8.6. [8]

$$BCR = \frac{RE}{CC\left[\frac{i}{1-(1+i)^{-t}}\right]} \quad \ldots\ldots 8.6$$

The more the BCR of a project is bigger than 1 or smaller than 1, the more the project is respectively appreciated or depreciated concerning the financial aspects. The benefits-costs ratio equals 1 when the value of i is equal to the internal rate of return [8].

For the case study BCR = 2.32 hence the project is appreciated.

8.7 Discussion

The results of the economic analysis indicate that the economics of the proposed gasification plant are very robust. Since the exact cost of a product gas found from gasification is not known from literatures or experiments the cost of a natural gas used in diesel generator is used with a product cost of Birr 112.5/GJ.

The strongest effect on the result of the economic analysis is the cost of feed stock. Since the cost of the feedstock is found directly from the waste of the sugar factory its cost is zero. The length of the annual operating period also has a fairly large effect on the product cost and economics. Nevertheless, if it drops to below 2000 h/y the gasification plant becomes uneconomic.

9. CONCLUSIONS AND RECCOMENDATION

9.1 Conclusions

9.1.1 Gas composition

An equilibrium model with a MATLAB code as an instrument used to determine the product gas composition. Five gas components were identified with concentrations higher than 0.1 Vol. %, namely hydrogen, nitrogen, carbon monoxide, carbon dioxide and methane. The last component, although only produced in small amounts, had a significant influence on the higher heating value of the gas, the composition found using the equilibrium model strongly agree with various literature and experimental values. The higher heating value (HHV) found is 2.69 MJ/kg that is very attractive with the moisture content of 15%.

The equilibrium composition of the water gas shift reaction was approached only at bed temperatures higher than 900 °C.

9.1.2 Air factor

Since the design work is done for maximum output efficiency; an Air factor that could result in a maximum output efficiency is selected from the range of (0.2-0.6). An air factor value of 0.233 is selected because most of the fluidized bed gasifiers operate efficiently at this value of air factor. Different literatures show that if the air factor is changed it has a strong influence on the HHV of the product gas.

9.1.3 Efficiency and gas yield

By comparison of the product gas chemical energy and the maximum flow rate of (5.14 tone/h) feedstock energy the efficiency of the gasifier is found to be 50.74% is obtained. Many literatures show a value of thermal efficiency 40-55 % has been observed hence this value is fairly acceptable. If the sensible heat of the product gas is also incorporated the thermal efficiency would have reached about 80%.

The gas yield was also found to be very satisfactory , In general a gas yield between 2 and 3.5 kg gas/kg MAF feedstock for specified air factor is acceptable, hence the value of gas yield Y= 2.56 kg of gas/ kg feed stock (MAF) is adequate.

9.1.4 Operational stability

The fluidized bed best operates at 900^{o}C since it is necessity equilibrium should be attained. But the freeboard temperature and the exit gas temperature must be regulated to be 800 ^{o}C and 750^{o}C respectively in order to gain efficient operation of the fluidize bed.

9.1.5 Retention time of product gas

For industrial applications, acceptable retention times of 10 to 20 seconds are to be expected. In this case a retention time of 12.5 seconds is selected to give the volume of the reactor as Vr = 96.675 m^3 this value of reactor volume is one of the basis for designing the geometry of the reactor.

9.1.6 Mass Balance and Energy Balance

The mass and energy balance closures were within acceptable experimental limits. A typical value of total mass balance was 92.85%. The elemental mass balance was also satisfactory with values in the range of 89-112%.

The total energy balance is about 100.14% giving rise to a 0.14% of unaccounted heat loss. The reactor wall heat loss was found to be 1.12% which is acceptable value for this size of reactor.

9.1.7 Modelling and Design

It appeared that a comprehensive design procedure incorporating all the following aspects was missing from the literature:

a) A model to predict the product gas composition of a fluidized bed reactor
b) A method of determining the fluidization parameters and characteristics for designing the fluidized bed, as well as,
c) A conceptual design of fluidized bed reactor geometry and its economic analysis.

By using the procedure in Appendix III an extensive calculations and design work has been done in previous sections which are verified with different empirical relations and also compared with available literatures.

As far as this thesis is concerned a fluidized bed working with bubbling fluidized bed is selected because of its vigorous advantages. The fluidized bed works with a bagasse found from a waste by-product of Fincha sugar factory; however the design is multipurpose one can use other biomass types for obtaining a different quantity and quality of product gasses. As far as the reagents or catalysts are concerned the design work doesn't incorporate a reagent

material because it is out of the scope of this thesis. The operating condition of the reactor is at an atmospheric pressure and at a room temperature around 20^{o}C. But the bed operates at slightly higher pressure than atmospheric pressure because of the pressure drop in the bed material.

The maximum capacity (feedstock flow rate) is 5140kg/h which is the base independent variable used in the design. With the selected equivalency ratio (s) of 0.233 the air flow rate has been determined to be 7180 kg/h. By the use of the equilibrium model about 9505.98 kg/h of product gas is obtained of which an amount of 867.5 kg/h is steam. The output of the equilibrium model balance shows there is an accounted flyash and condensate flow rates.

The design of the distributor is done using empirical correlations and later verified with its pressure drop value with standard values from literatures. The minimum pressure drop of the distributor is found to be 350mm H_2O. With certain empirical relation of Reynolds number of the approaching flow of air the flow was found to be turbulent. This gives a specific value of drag coefficient of 0.6 which enabled us to calculate the velocity of the gas through the orifices to be 47.3 m/s. The diameter of the orifices has been selected to be slightly higher than the size of the sand particles which is about 3mm and finally the number of orifices has been calculated from the total distributor area and the diameter of orifices and about 21,446 orifices are required for the perfect fluidization.

The pressure drop of the compressor is also calculated since it is going to be used later in equipment specification of the gasification plant. The pressure drop of the compressor must inculcate both the bed pressure drop and the distributor pressure and its value is 17.5 kpa which is very attractive value.

From different size of sand particle obtained from libratory measurement of literature a mean sand particle diameter of 0.414mm is obtained.

The first step done in the fluidization parameter calculation is determining the minimum fluidization velocity. The minimum fluidization velocity is 0.1766 m/s; from which the internal reactor diameter or the bed diameter is calculated to be 2.35m. The Reynolds number at minimum fluidization condition was calculated and it was as low as 1.73 which intern give rise to a drag coefficient of 13.7 from which the maximum fluidization velocity was calculated and a value of 1.14 m/s was obtained. The particle terminal velocity was also calculated to be 12.36 m/s above which the particles will elutriate or entrain and the reactor type would be a circulating bed type. While calculating the maximum size of the bubbles the restriction of equation 4.22 is satisfied indicating there won't be any slugging of the bubbles or there won't be excessive carryover of particles.

A method of verifying the fluidization parameters was performed with different criteria and all of them came positive.

The bed diameter was a base for determining the bed height since the value calculated was slightly above the recommended value a bed height of 1m has been taken. Next the geometry of the freeboard is calculated with an appreciated safety margin so that the gasification process could have a sufficient resident time.

All the insulation and the construction materials are selected from literatures so that they can fit the design of the reactor and the values obtained in there verification came out impressive.

Since the working pressure and temperature of the reactor is required a sufficient amount of gauge ports has been specified for temperature and pressure measurements. Finally the above empirical calculations gave the reactor a 4.2 m external diameter and a height of 11.3 m.

Even though the scope of the thesis is limited to the reactor designs the equipments and auxiliary component specifications of the fluidized bed reactor have been also dealt with. This includes the cyclone, the burners, compressors, bed screw, the feed stock feeding system etc.

Finally the economic analysis of the reactor gave economically feasible output. Three methods of calculating the feasibility of the design work has been (the payback period 2.6 years, the internal rate of return36.0856% and the benefit cost ratio 2.32) dealt with and all of the methods show that the project is appreciated.

9.2 Recommendations

The research results of this work provide a better understanding of fluidized bed air gasification of biomass and provide a frame work for future research in the system design and optimization of this subject. The following recommendations are made for extending and developing this work.

9.2.1 Moisture content of the Feedstock

In this work a moisture content of 15% was selected arbitrarily for maximum output without any pre- treatment of the feedstock while it was obvious that the moisture content of the feed stock form the sugar factory is 50%. A Mechanism design work should be done for drying the feedstock to desired moisture content and also other moisture content values below or above 15% should be investigated for efficient usage of the feedstock.

Also other than just bagasse other feedstock types having bigger or smaller feedstock size should be inculcated in the design work for future work; because literatures show using multi biomass types at the same time has better efficiency and could give a larger higher heating value of the product gas.

9.2.2 Feeding point

In this reactor configuration the feeding was above the bed surface. To minimize carryover of light feedstock particles (e.g. bagasse), feeding below the surface of the bed should be tested. However, this is not possible with the present feeding system, since the gas leaks through it would be significant. Indeed with the feeding port in the bed, higher pressure at that point would exist, which would result in gas leaks.

9.2.3 Full and detail design of the auxiliary components

By widening the scope of the project one can add the detail design of auxiliary components of the reactor like the cyclone, the ash bin, the feeding system, the bed and ash removal system etc.

9.2.4 Problems associated with equilibrium modelling

The equilibrium model used in this work has a draw back in efficiently determining the exact gas composition. It couldn't also provide the exact amount of fly ash and tar content of the product gas. If it is possible in the future there should be a more effective way of determining

exactly all the components of the reaction so that the mass and energy balance of the design work would have a better efficiency closure.

9.2.5 Gas composition and Temperature profile in the reactor

In this work only the gas composition at the out let of the reactor and at some specific points of the reactor that the temperature profiles are discussed. In the future works one can apply a CFD model to determine the exact gas composition and temperature profiles within the reactor.

9.2.6 Sampling of bed, construction and insulations material

Most of the materials used in the design work are either product of previous libratory outputs or from literatures. A more efficient way of determining the properties of the materials used for contraction and insulation should be dealt with to minimize the heat loss through the reactor walls. Bed material locally available should also be investigated and a personal sampling method should be considered for efficient design of the fluidized bed.

9.2.7 Construction and experimentation

The design work should continue on either in constructing a prototype or a pilot plant in the near future and an experimental procedure should also be used to further increase the efficiency of the gasification plant.

9.2.8 Economic Data

The economic analysis is done based on a rough estimation of previously constructed gasifiers; but a detail cost analysis of each material and utilities to be used in the construction should be obtained for better economic analysis. Detailed economic data are necessary for a more accurate economic analysis. It is recommended that information about the cost of all components of the plant for different capacities be collected.

REFERENCES

1. Yohannes Shiferaw, 2011, Design and performance evaluation of biomass gasifier stove, Addis Ababa University, department of chemical engineering, master's thesis.
2. P.K. Senapati, 2008 Advanced Biomass Gasification Technology for Rural Industrialization, Institute of Minerals and Materials Technology Council of Scientific & Industrial Research, (CSIR) Bhubaneswar–751013, Orissa, India.
3. World Bank, August 1990 Energy in the developing countries. world bank home page
4. Fincha sugar industry, 2008/9, Input Data for Fincha F.S.F energy Audit , fincha, Ethiopia
5. J. j. Ramírez; J.d. Martínez and S.i. petro, 2007, Basic design of a fluidized bed gasifier for rice husk, Universidad Pontificia Bolivariana. Medellín, Colombia. .
6. D.A. Tillman, 1970, Wood as an energy resource, Acad. Press, N. Y.
7. Ethiopian Electric Agency, 2002, Symposium Proceedings of Rural Electrification, Addis Ababa, Ethiopia.
8. Kyriakos Maniatis, October 1986, Fluidized bed gasification of biomass, Doctoral thesis, university of Austin, Birmingham, UK.
9. Lim Mook Tzeng, 2007, Characterization of a bubbling fluidized bed biomass gasifier, university Sains, Malaysia.
10. S.M.Kohan, 1981, Basic principles of thermochemical conversion, eds. S.S. Sofer, O.R. Zaborsky, Plenum Publishing Corporation.
11. T.B. Reed, April 1900, Types of gasifiers and gasifier design considerations. Vo1.3. Seri.
12. R.N. Shand, A.V. Bridgwater, 1984, Fuel from biomass: Status and new modelling approaches in Thermochemical processing of biomass, ed. A.V. Bridgwater, Butterworths
13. TB. Reed, M. Markson, 1985, Biomass gasification reaction velocities, in Fundamentals of thermochemical biomass conversion, ed. R.P. Overend, T.D. Milne, K.K. Mudge and Elsevier applied science publishers.
14. W.P.M. van Swaaij, 1980, Gasification - The process and the technology, Resources and Cons., 7: 337-349.

15. L.K. Mudge and C.A. Rohrmann, Sept. 1979, Gasification of solid waste fuels in a fixed bed gasifier, Div. Env. Chem. Am. Chem. Soc. Washington D.C.
16. J.F. Davidson, D. Harrison, 1963, Fluidized particles Cambridge University-Press.
17. D. Kunii, 0. Levenspiel, 1977, Fluidization engineering, R.E. Krieger Publsihing Co., Huntington Nev' York.
18. J.G. Yates, 1983, "Fundamentals of fluidized bed chemical processes, Butterworths.
19. J. Werther, 1980, Mathematical modelling of fluidized bed reactors, International chemical engineering, Vol. 20, No. 4.
20. Wen –ching yang, 2003, Hand book of fluidization, Siemens Westinghouse Power Corporation Pittsburgh, Pennsylvania, U.S.A., Taylor & Francis Group LLC, New York, Base.
21. E. Smith, 1984, Reactors: Some Design Perspectives, Chapter 15. Thermochemical Processing of Biomass, ed. kV. Bridgwater, Butterworths, London.
22. P.H. Perry, C. Chilton, 1973, Chemical Engineers Handbook, McGraw Hill Kogakusha, 5th ed.
23. A.Mountouris, E. Voutsas, D. Tassios, December 2005, Solid waste plasma gasification: Equilibrium model development and exergy analysis, School of Chemical Engineering, Technical University of Athens, Greece.
24. F.C. Schaffer and Associates, Inc.; July, 1997, Fincha Sugar factory Operations manual, Volume II, Fincha valley, Eastern Wollega province, Ethiopia
25. Gopal Gautam, December 2010, Parametric Study of a Commercial-Scale Biomass Downdraft Gasifier: Experiments and Equilibrium Modelling, A Master of Science thesis submitted to Graduate faculty of Auburn University, Alabama, USA.
26. B. Fakhim and B. Farhanieh, 2008, Second Law Analysis of Bubbling Fluidized Bed Gasifier for Biomass Gasification, School of Mechanical Engineering, Division of Energy Conversion, Sharif University of Technology, Tehran, Iran
27. Yunus A. Cengel, Michael A. Boles, August 1997, Thermodynamics: An Engineering Approach, 5th ed. Thermodynamics textbook, Mc. Grawhill, USA.
28. Venkata Ramayya A, Eyerusalem M, Endalew M, Melaku M., 2006, Design and Simulation of Fluidized Bed Power Gasifier for a Coffee Hulling Centre, Advances in Energy Research, Jimma University, Department of mechanical Engineering; Ethiopia.
29. D.Q. Kern, 1965, Process heat transfer, Int. Student ed. McCraw Hill International.
30. A.V. Bridgwater, J.M. Double, D.M. Earp, Technical and market assessment of biomass gasification in the UK, Vol. 1, Report to energy technology support unit, agreement no. E/5A/CON/1167/1338F.

31. http://en.wikipedia.org/wiki/Pound_sterling.
32. A.V. Bridgwater, 1986, Worldwide markets for biomass gasification systems, Private communication.

APPENDIX

I. MAT LAB CODE FOR DETERMINGING EQUILIBRIUM CONSTANTS K1 AND K2

This code requires the reaction temperature only as a dependent variable.

```
%Program for finding equilibrium constant for various reactions
%Rxn-1: CO+H_2O=CO_2+H_2
%Rxn-2: C+2H_2=CH4
function[k]=Delta_G(T)
%%%%%%%%%%%%%%%%%%%%%%%%%%%%%%%%%%%%%%%%%%%%%%%%%%%%%%%%%%%%%%%%%%%%%%%%
%
%    finding general equations for calculating k1 and k2
%
%%%%%%%%%%%%%%%%%%%%%%%%%%%%%%%%%%%%%%%%%%%%%%%%%%%%%%%%%%%%%%%%%%%%%%%%
%
G_CO=[3.376 0.557e-3 0 -0.031e5 -110525 -137169];
G_CO2=[5.457 1.045e-3 0 -1.157e5 -393509 -394359];
G_H2O=[3.470 1.450e-3 0 0.121e5 -241818 -228572];
G_H2=[3.249 0.422e-3 0 0.083e5 0 0];
G_C=[1.771 0.771e-3 0 -0.867e5 0 0];
G_CH4=[1.702 9.081e-3 -2.164e-6 0 -74520 -50460];
delta_ws_final=[];
delta_meth_final=[];
for iii=1:6
delta_ws=G_H2(iii)+G_CO2(iii)-G_CO(iii)-G_H2O(iii);
delta_meth=G_CH4(iii)-G_C(iii)-2*G_H2(iii);
delta_ws_final=[delta_ws_final delta_ws];
delta_meth_final=[delta_meth_final delta_meth];
end
T_0=298;
k1=exp(-((delta_meth_final(6)-
delta_meth_final(5))/(8.314*298.15)+(delta_meth_final(5)/(8.314*T))...
+(int_eq_sp2(delta_meth_final,T)/T)-int_eq_sp1(delta_meth_final,T)))
k2=exp(-((delta_ws_final(6)-
delta_ws_final(5))/(8.314*298.15)+(delta_ws_final(5)/(8.314*T))...
+(int_eq_sp2(delta_ws_final,T)/T)-int_eq_sp1(delta_ws_final,T)))
k=[k1,k2];
%%%%%%%%%%%%%%%%%%%%%%%%%%%%%%%%%%%%%%%%%%%%%%%%%%%%%%%%%%%%%%%%%%%%%%%%
%
%function for calculating int_eq_sp
function int_for_gibbs_difff1= int_eq_sp1(difff,T)
tau=T/298.15;
int_for_gibbs_difff1=difff(1).*log(tau)+((difff(2).*T_0+...
((difff(3)*T_0^2+(difff(4)/(tau^2.*T_0^2)))*((tau+1)/2)))*(tau-1));
end
```

```
function int_for_gibbs_difff2= int_eq_sp2(var_sp,T)
tau=T/298.15;
int_for_gibbs_difff2=var_sp(1).*T_0*(tau-1)+...
var_sp(2)*0.5*T_0^2*(tau^2-1)+var_sp(3)*T_0^3*(tau^3-1)/3+...
var_sp(4)*(tau-1)/(tau*T_0);
end
end
%%%%%%%%%%%%%%%%%%%%%%%%%%%%%%%%%%%%%%%%%%%%%%%%%%%%%%%%%%%%%%%%%%%%%%%%%%%%%%
%
```

II. MAT LAB CODE FOR DETERMINING OUTPUT GAS COMPOSITION

```
%This program is set to give syn gas composition in dry or wet syn gas basis
function[final_frac_comp]=eq_comp_model_gen(g_temp,ele_comp)
format short
tol=0.0001;
maxit=100;
%disp('elemental composition should be of the form [C, H, O, N, Ash]');
ele_comp=input('Enter elemental composition of biomass: ');
%disp('Initial guess is of the form [H2 CO CO2 H2O CH4 3.76N2] ')
xx0=[0.1,0.1,0.1,0.1,0.1,0.1]';
%%%%%%%%%%%%%%%%%%%%%%%%%%%%%%%%%%%%%%%%%%%%%%%%%%%%%%%%%%%%%%%%%%%%%%%%%%%%%%
%
% Heat of formation of different compounds at 25 C, kJ/kmol
H_f_H2O_g=-241818;H_f_H2O_l=-285830;H_f_CO2=-393509;H_f_CO=-110525;
H_f_CH4=-74520;H_f_H2=0;H_f_O2=0;H_f_N2=0;
%%%%%%%%%%%%%%%%%%%%%%%%%%%%%%%%%%%%%%%%%%%%%%%%%%%%%%%%%%%%%%%%%%%%%%%%%%%%%%
%%Function for finding sensible heat for various gases constants
C_p_H2O=[32.24 0.1923e-2 1.055e-5 -3.595e-9];
C_p_H2=[29.11 -0.1916e-2 0.4003e-5 -0.8704e-9];
C_p_CO=[28.16 0.1675e-2 0.5372e-5 -2.222e-9];
C_p_CO2=[22.26 5.981e-2 -3.501e-5 -7.469e-9];
C_p_CH4=[19.89 5.204e-2 1.269e-5 -11.01e-9];
C_p_N2=[28.90 -0.1571e-2 0.8081e-5 -2.873e-9];
%%%%%%%%%%%%%%%%%%%%%%%%%%%%%%%%%%%%%%%%%%%%%%%%%%%%%%%%%%%%%%%%%%%%%%%%%%%%%%
%
%finding general equations for calculating k1 and k2
G_CO=[3.376 0.557e-3 0 -0.031e5 -110525 -137169];
G_CO2=[5.457 1.045e-3 0 -1.157e5 -393509 -394359];
G_H2O=[3.470 1.450e-3 0 0.121e5 -241818 -228572];
G_H2=[3.249 0.422e-3 0 0.083e5 0 0];
G_C=[1.771 0.771e-3 0 -0.867e5 0 0];
G_CH4=[1.702 9.081e-3 -2.164e-6 0 -74520 -50460];
delta_ws_final=[];
delta_meth_final=[];
```

```
for iii=1:6
delta_ws=G_H2(iii)+G_CO2(iii)-G_CO(iii)-G_H2O(iii);
delta_meth=G_CH4(iii)-G_C(iii)-2*G_H2(iii);
delta_ws_final=[delta_ws_final delta_ws];
delta_meth_final=[delta_meth_final delta_meth];
end
T_0=298;
k1=exp(-((delta_meth_final(6)-
delta_meth_final(5))/(8.314*298.15)+(delta_meth_final(5)/(8.314*g_temp))...
+(int_eq_sp2(delta_meth_final,g_temp)/g_temp)-int_eq_sp1(delta_meth_final,g_temp)));
k2=exp(-((delta_ws_final(6)
delta_ws_final(5))/(8.314*298.15)+(delta_ws_final(5)/(8.314*g_temp))...
+(int_eq_sp2(delta_ws_final,g_temp)/g_temp)-int_eq_sp1(delta_ws_final,g_temp)));
%%%%%%%%%%%%%%%%%%%%%%%%%%%%%%%%%%%%%%%%%%%%%%%
%
%function for calculating int_eq_sp
function int_for_gibbs_difff1= int_eq_sp1(difff,g_temp)
tau=g_temp/298.15;
int_for_gibbs_difff1=difff(1).*log(tau)+((difff(2).*T_0+...
((difff(3)*T_0^2+(difff(4)/(tau^2.*T_0^2)))*((tau+1)/2)))*(tau-1));
end
function int_for_gibbs_difff2= int_eq_sp2(var_sp,g_temp)
tau=g_temp/298.15;
int_for_gibbs_difff2=var_sp(1).*T_0*(tau-1)+...
var_sp(2)*0.5*T_0^2*(tau^2-1)+var_sp(3)*T_0^3*(tau^3-1)/3+...
var_sp(4)*(tau-1)/(tau*T_0);
end
%finding lambda and gamma for below calculation%%%%%%%%%%%%%%%%%
norm_1_C=ele_comp(1)/(12);
norm_1_H=ele_comp(2)/(1.008);
norm_1_O=ele_comp(3)/(16);
norm_1_N=ele_comp(4)/(14.007);
lambda=norm_1_H/norm_1_C;
gamma=norm_1_O/norm_1_C;
beta=norm_1_N/norm_1_C;
%%%%%%%%%%%%%%%%%%%%%%%%%%%%%%%%%%%%%%%%%%%%%%%
%
x0=xx0;
iter=1;
iter_m=1;
sol_final=[];
%w=M_fs*Moisture_Content/(18*(1-Moisture_Content));
w=linspace(0,1,15);
%w=0;
```

```
Moisture_Content=[];
M_fs=12+lambda*1.008+gamma*16;
for N=1:length(w)
Moisture_Content=[Moisture_Content 18*100*w(N)/(M_fs+18*w(N))];
end
Moisture_Content
%%%%%%%%%%%%%%%%%%%%%%%%%%%%%%%%%%%%%%%%%%%%%%%
%
%Main Loop for solving the equations of interests
for iter_m=1:length(w)
while(iter<=maxit)
y=-df1(x0)\f1(x0);
xn=x0+y;
err=max(abs(xn-x0));
if(err<=tol)
x=xn;
else
x0=xn;
end
iter=iter+1;
end
iter=1;
sol_temp=x;
%%%%%%%%%%%%%%%%%%%%%Continued
below%%%%%%%%%%%%%%%%%%%%
sol_final=[sol_final sol_temp];
iter_m=iter_m+1;
end
%Multiplying m with 3.76 to get correct N2 mols
p=length(w);
frac_N2=[];
for l=1:p
frac_N2=[frac_N2 sol_final(6,l)*3.76];
end
final_comp=[sol_final(1:5,1:p);frac_N2]
%%%%%%%%%%%%%%%%%%%%%%%%%%%%%%%%%%%%%%%%%%%%%%%
%
%fin_rep=input('Do you want to find syngas composition in dry syngas
basis(y/n): ','s');
fin_rep='y';
if fin_rep=='n';
%%%%%%%%%%%%%%%%%%%%%%%%%%%%%%%%%%%%%%%%%%%%%%%
%
%finding total amount of product gas for each moisture content
```

```
total_frac_m=[];
for n=1:p
total_frac_m=[total_frac_m sum(final_comp(1:6,n))];
end
total_frac_m; %sum of all product gases
else
%%%%%%%%%%%%%%%%%%%%%%%%%%%%%%%%%%%%%%%%%%%%%%%%%%%%%%%%
%
%finding total amount of product gas on dry basis for each moisture content
dry_final_comp=final_comp;
dry_final_comp(4,:)=[];
total_frac_m=[];
for n=1:p
total_frac_m=[total_frac_m sum(dry_final_comp(1:5,n))];
end
total_frac_m;
final_comp=dry_final_comp;
end
%%%%%%%%%%%%%%%%%%%%%%%%%%%%%%%%%%%%%%%%%%%%%%%%%%%%%%%%
%
%expressing all the components in molar fraction or volumetric fraction
final_frac_comp=[];
for MM=1:length(total_frac_m)
final_frac_m=[];
if fin_rep=='y'
l_in=length(xx0)-1;
else
l_in=length(xx0);
end
for NN=1:l_in
final_frac_m=[final_frac_m;final_comp(NN,MM)/total_frac_m(MM)];
end
final_frac_comp=[final_frac_comp final_frac_m];
end
```

III. General Procedure in Designing a Fluidized Bed Reactor

The overall approach used is summarized as follows.

1. Set specifications
   a) Type of gasifier
   b) Feedstock
   c) Reagents
   d) Operating conditions
2. Calculation of throughputs
   a) air input
   b) feedstock input
   c) dry gas output
   d) steam output
3. Design of distributor
   Calculate:
   a) minimum Pressure drop of distributor
   b) Reynolds number for flow approaching distributor
   c) velocity of gases through orifice
   d) number of orifices
   e) diameter of orifices
4. Pressure drop for the compressor
5. Size of sand
   Calculate the mean particle size of the sand
6. Fluidization parameters
   Calculate:
   -minimum fluidization velocity
   -Reynolds number at conditions of minimum fluidization
   -particles terminal falling velocity
   -size of bubbles at max and min conditions
7. Verification of design
   Calculate:
   -amount of gas flowing interstitially
   -residence time of gas flowing interstitially
   -bubble velocities at max and min conditions
   -the ratio of bubble velocity to interstitial gas velocity
   - the fraction of bubbles in contact with particles
8. Geometry of the reactor
   -Bed geometry
   -Distributor geometry
   -Freeboard geometry
   -Insulation and construction materials
   -Openings, temperature and pressure measurements
9. Auxiliary equipments specifications
10. Economic Analysis of the fluidized bed reactor

IV. ANNEX

1. Gasifier Reactor Drawings

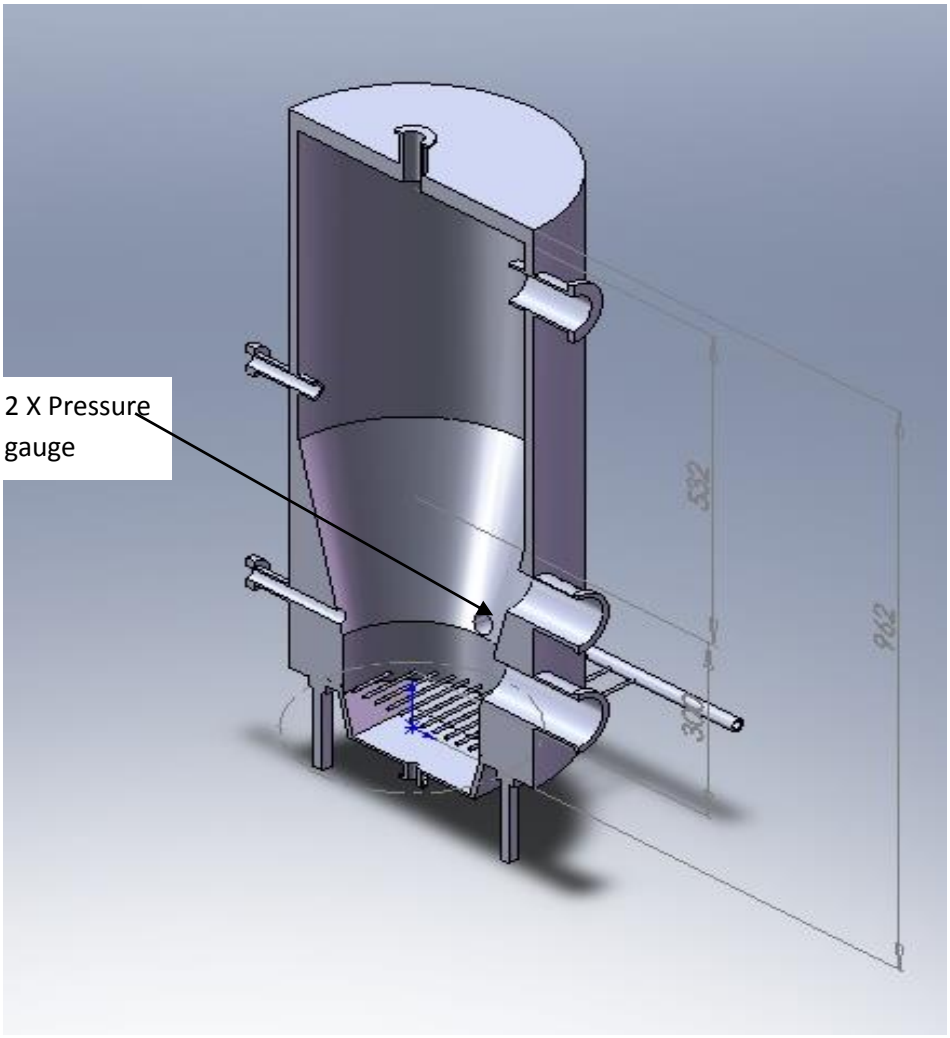

Figure1. Sectional view of the reactor in 3D solid work model

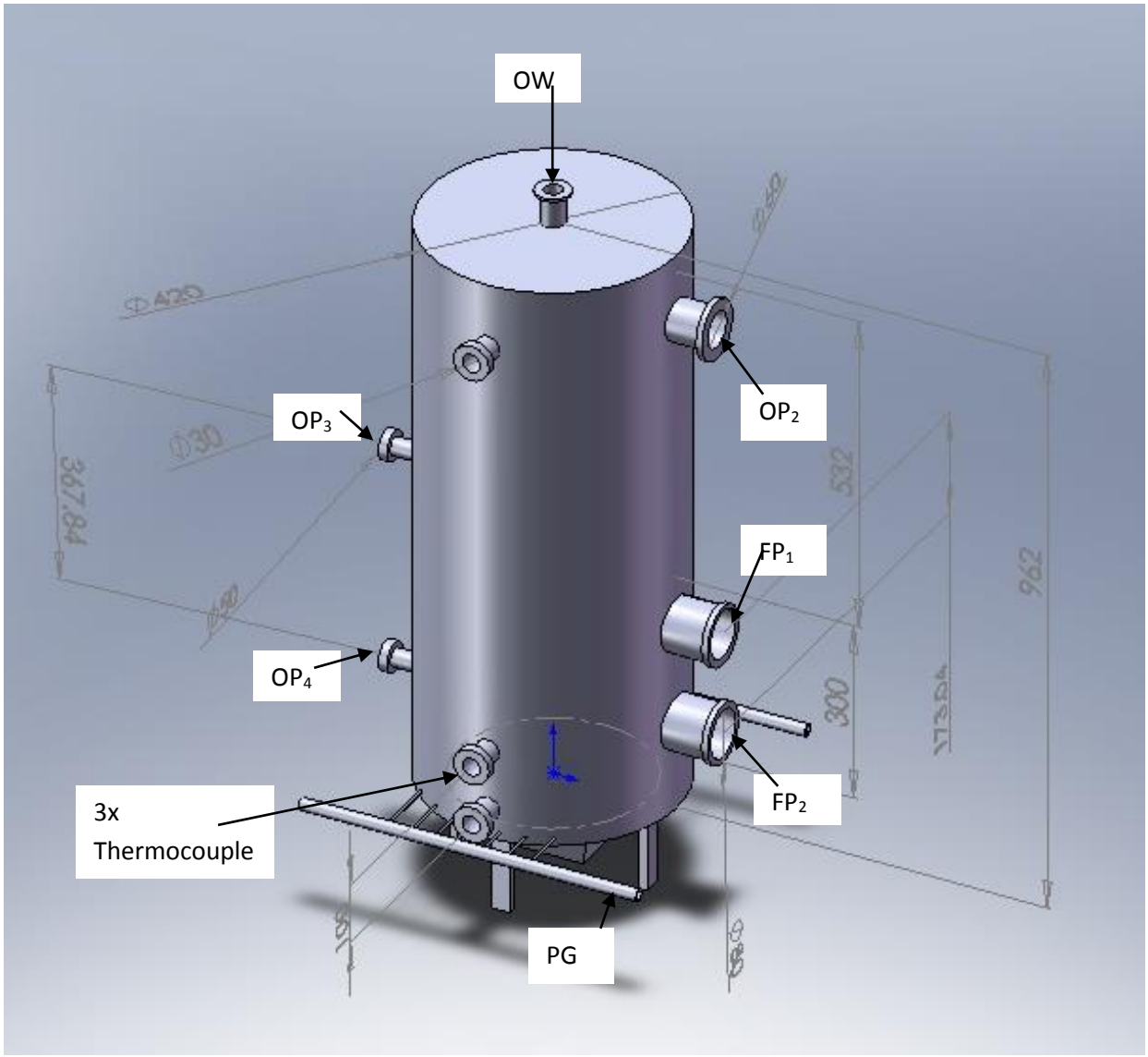

Figure 2: 3D solid work model of the reactor and its openings.

Key:

OP1= Opening for bed and ash removal

OP2= Opening for product gas out let

OP3= Over head burner opening on the freeboard region

OP4= over head burner opening near the distributor

PG= Pipe grid opening for Air inlet to the distributor

Fp1= Biomass Feeding port 1

FP2= Biomass feeding port 2

Ow= Observation well

Figure 3: Reactor Detail Drawing

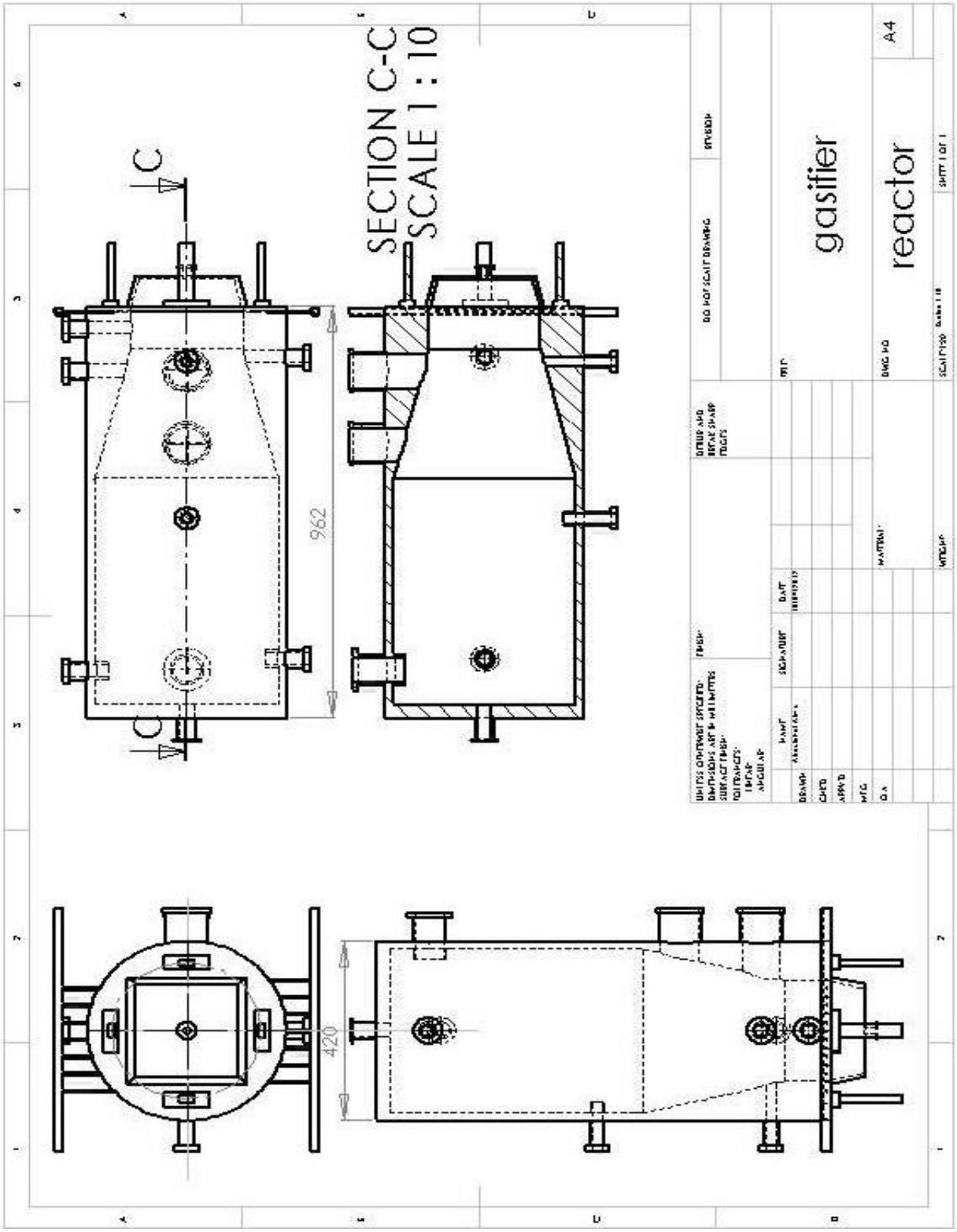

2. Distributor Detail Drawing

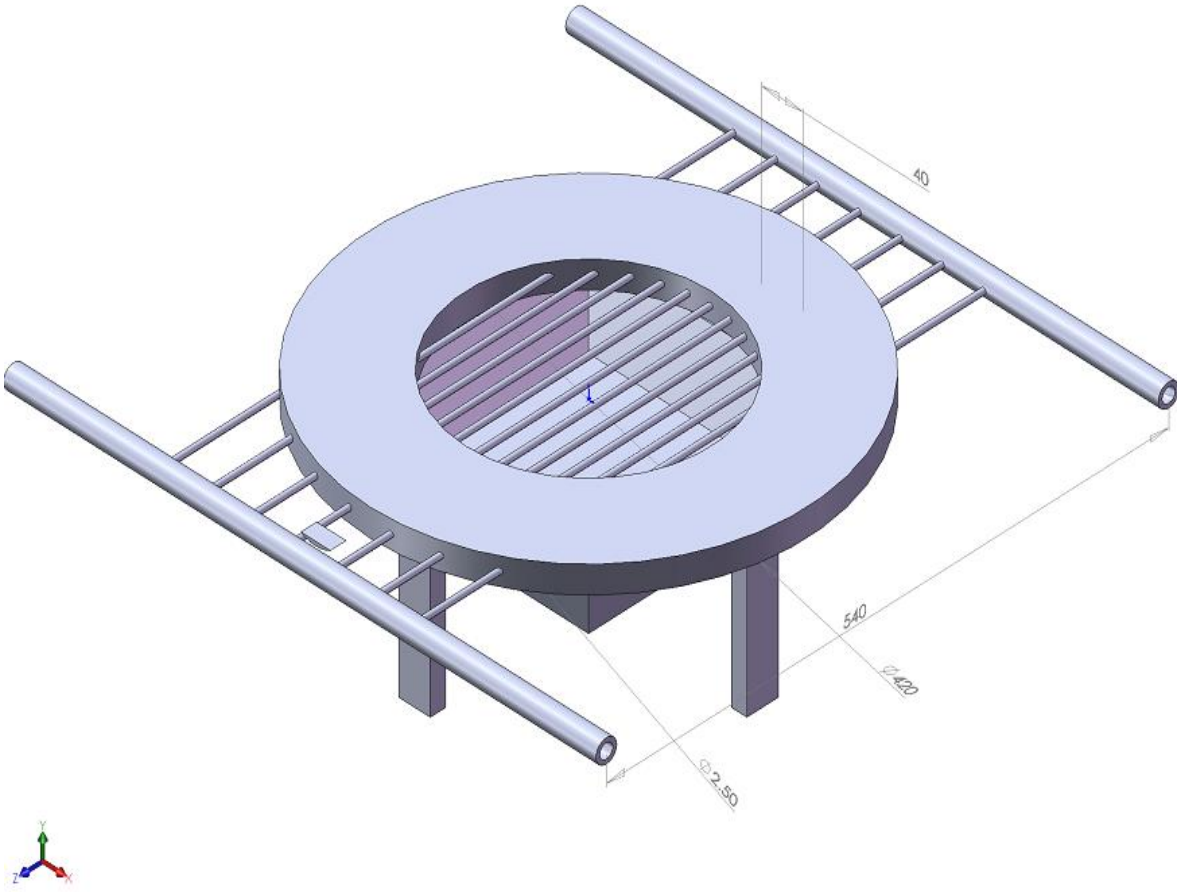

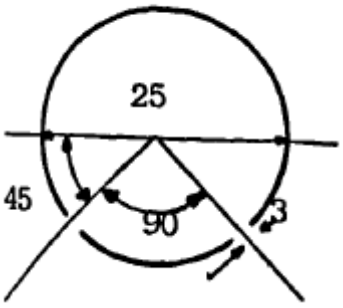

The orifices are drilled in pairs, facing dawn wards to avoid blockage by sand, at 90°. The pipes are introduced through larger pipes of 50 mm supported by flanges. They are held in place by wells in the reactor wall.

Figure 4: 3D model of the distributor section and detail of the orifice

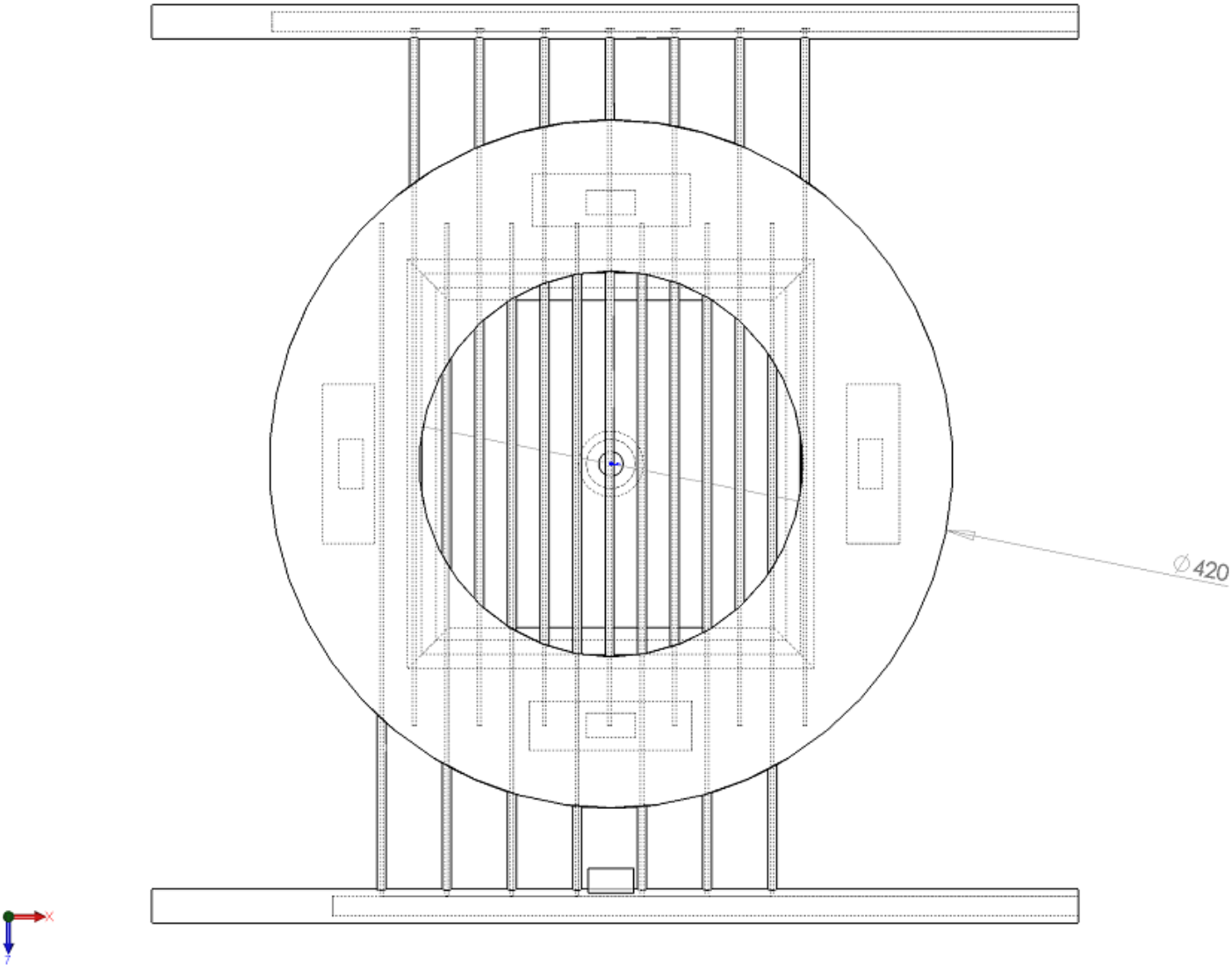

Figure 5: Top view of the distributor blow the bed

Declaration

I, the undersigned, declare that this is my original work, has not been presented for a degree in this or any other University, and that all sources of materials used for the thesis have been duly acknowledged.

Name**: Abdulehak Alemu Asfaw**

Signature: _____

Place: **Addis Ababa, Ethiopia**

Date of submission: _____